



3 1293 01801 7412

LIBRARY
Michigan State
University

This is to certify that the

thesis entitled

synthesis of group IV metal dichlorides
stabilized by β -ketiminato ligands

presented by

Hellen Kakaliou

has been accepted towards fulfillment
of the requirements for

MS degree in Chemistry

Milton R. Smith, Jr.

Major professor

Date 12/17/98

PLACE IN RETURN BOX to remove this checkout from your record.
TO AVOID FINES return on or before date due.
MAY BE RECALLED with earlier due date if requested.

DATE DUE	DATE DUE	DATE DUE

SYNTHESIS OF GROUP IV METAL DICHLORIDES STABILIZED BY
 β -KETIMINATO LIGANDS

By

Lena Kakaliou

A THESIS

Submitted to

Michigan State University

in partial fulfillment of the requirements

for the degree of

MASTER OF SCIENCE

Department of Chemistry

1998

ABSTRACT

SYNTHESIS OF GROUP IV METAL DICHLORIDES STABILIZED BY β -KETIMINATO LIGANDS

By

Lena Kakaliou

A Ziegler–Natta catalyst may broadly be defined as a material which consists of a Group III–VIII transition metal together with a group I, II, or XIII organometallic, the combination of which is capable of polymerizing olefins and dienes under relatively mild conditions of temperature and pressure. Our work targets Ziegler–Natta type catalysts based on Group IV metal centers in non–Cp₂ ligand environments. We have utilized β -ketimines as chelating ligands since they can be readily synthesized from 2,4-pentanedione and anilines, while at the same time enable facile stereochemical and electronic tuning by using various substituted anilines. Reaction of the free ligands with the proper Group IV metal starting materials afforded the corresponding non–chelated organometallic complexes. By employing the ligand's lithium or sodium salts on the other hand, the desired chelated metal dichlorides were obtained in excellent yields. Single crystal X–ray studies along with ¹H and ¹³C NMR spectroscopy were the methods of choice for the characterization of the complexes, indicating that halide sites adopt *cis* geometry. In addition, these are positioned inside a well–shielded environment, created by the substitution pattern of the β -ketiminato ligand. In principle, this could enable stereochemical control over catalytic reactions.

To my husband who inspired me to start this work
and
to my son who showed me the way in a hard moment.

ACKNOWLEDGMENTS

I would like to thank my advisor Mitch Smith for giving me the chance to work on this project. His advice and knowledge helped me get into the scientific world in which I really enjoyed being a part. Besides science I appreciated his help and support in a difficult situation I've been through.

The environment in the lab created by my coworkers was excellent and promoted productivity and creativity in an efficient way. For providing this to me I wish to thank all of them: Douglas, Scott, Carl, Dean, Baixin, Bill, Aimee, Suzi, Sung, and Autumn. Working with them was more than enjoyable and opened not only my scientific horizons but also improved me as a person by understanding the differences between cultures and backgrounds. My appreciation along with my thankful feelings to Douglas, Carl, Dean, and Baixin who taught me the experimental techniques and were willing to answer my questions and discuss with me about my science.

Also I would like to express my gratitude to Professor G. Karabatsos for his substantial help and support during my hard moments.

I really cannot forget officer Collins and his sensitive and kind treatment to me during our fatal encounter.

My friends Spiros, Nikos, Zoe, Markos, Lykourgos, Jen, Babis, Vicki, Filippos, and Fabiana made my years as a graduate student to pass quickly and smoothly. I would like to thank them for being there for me whenever I needed them and for sharing with me my good and bad unforgettable moments.

Words are not enough to express my thankfulness to my husband who inspired me to start this work and continuously expanded my knowledge through our infinite discussions about science. His contribution was not limited only to helping me on practical but at the same time substantial parts of this work. He

sentimentally supported me from my first day in the lab until the last one and furthers more during my pregnancy and after the birth of our precious little one.

My parents deserve my thanks for giving me the chance to accomplish my studies to the degree I did. Also their essential presence during my son's birth and the nursing months was more than helpful for the completion of the writing process.

At last I would like to thank my handsome little son for being such a nice and well-behaved baby when I had to share my time between nursing, writing, and teaching.

TABLE OF CONTENTS

TABLE OF CONTENTS	vi
LIST OF TABLES	viii
LIST OF FIGURES	x
CHAPTER 1	1
INTRODUCTION	1
A. Polymerization Processes; General Considerations	2
1. Condensation polymerization	6
2. Addition polymerization	8
3. Ring opening polymerization	8
4. Living Polymerization	8
B. Ziegler–Natta polymerization	12
1. Cp ₂ ligand Systems	17
2. Non–Cp ₂ ligand Systems	26
C. Thesis Outline	29
LIST OF REFERENCES	30
CHAPTER 2	36
EXPERIMENTAL METHODS	36
A. Instrument Setups	36
1. Nuclear Magnetic Resonance	36
2. Mass Spectroscopy	36
3. Single Crystal X–ray Structure Determination	37
B. Materials and Synthesis	41

1.	Synthesis of Ketimine–Type Free Ligands	41
2.	Synthesis of Ketimine–Type Ligand Salts	43
3.	Synthesis of 2–(dimethylamino)–4–(arylimino)–pent–2–ene Compounds	45
4.	Synthesis of Titanium and Zirconium Starting Materials	46
5.	Synthesis of Non–chelated Titanium Complexes	48
6.	Synthesis of Chelated Titanium and Zirconium Complexes by Reaction with the β –Ketimine Lithium Salts	49
	LIST OF REFERENCES	53
	CHAPTER 3	54
	SYNTHESIS AND CHARACTERIZATION OF METAL DICHLORIDES STABILIZED BY β–KETIMINE LIGANDS	54
A.	Introduction	54
B.	Results and Discussion	57
1.	Synthesis and Characterization of β –ketimine Free Ligands	57
2.	Reactivity of Free Ligands towards Titanium Complexes	68
3.	Synthesis of Group IV Chelate Complexes	78
	CONCLUSIONS	98
	LIST OF REFERENCES	100
	APPENDIX	101

LIST OF TABLES

CHAPTER 3

Table 1. Crystallographic Data for <i>N</i> -(4-tolyl)-acetamide, and (TMPPOH) ₂ TiCl ₄ .	61
Table 2. Selected Bond Distances and Angles of Compound <i>N</i> -(4-tolyl)-acetamide.	62
Table 3. ¹ H NMR Data of the β-Ketimine Free Ligands.	66
Table 4. ¹³ C NMR Data of the β-Ketimine Free Ligands.	67
Table 5. Selected Bond Distances and Angles of (TMPPOH) ₂ TiCl ₄ .	74
Table 6. ¹ H ^a and ¹³ C ^b NMR Data for the Non-chelate (β-ketimine) ₂ TiCl ₄ Complexes.	76
Table 7. ¹ H ^a and ¹³ C ^b NMR Data for the Lithium Salts of β-Ketimine Ligands.	80
Table 8. Crystallographic Data of (MPPO) ₂ TiCl ₂ , (TMPPO) ₂ TiCl ₂ , and (MPPO) ₂ ZrCl ₂ .	84
Table 9. Selected Bond Distances and Angles of Compound (MPPO) ₂ TiCl ₂ and (TMPPO) ₂ TiCl ₂ .	86
Table 10. Selected Bond Distances and Angles of (MPPO) ₂ ZrCl ₂ .	92
Table 11. ¹ H ^a and ¹³ C ^b NMR Data (MPPO) ₂ TiCl ₂ and (TMPPO) ₂ TiCl ₂ .	94
Table 12. ¹ H ^a and ¹³ C ^b NMR Data (MPPO) ₂ ZrCl ₂ and (TMPPO) ₂ ZrCl ₂ .	95

APPENDIX A

Table 1. Atomic Coordinates ($\times 10^4$) and Equivalent Isotropic Thermal Parameters ($\text{\AA}^2 \times 10^2$) for <i>N</i> -(4-tolyl)-acetamide.	101
--	-----

Table 2. Anisotropic Thermal Parameters ($\text{\AA}^2 \times 10^3$) for <i>N</i> -tolylmethanamide.	102
Table 3. Atomic Coordinates ($\times 10^4$) and Equivalent Isotropic Thermal Parameters ($\text{\AA}^2 \times 10^2$) for $\{\mu\text{-O-[2-(2,4,6-trimethylphenylimino)-pentane-4-one]}\}_2\text{TiCl}_4 \cdot 0.5\text{C}_4\text{H}_8\text{O}$.	103
Table 4. Anisotropic Thermal Parameters ($\text{\AA}^2 \times 10^3$) for $\{\mu\text{-O-[2-(2,4,6-trimethylphenylimino)-pentane-4-one]}\}_2\text{TiCl}_4 \cdot 0.5\text{C}_4\text{H}_8\text{O}$.	105
Table 5. Atomic Coordinates ($\times 10^4$) and Equivalent Isotropic Thermal Parameters ($\text{\AA}^2 \times 10^2$) for $\{\mu^2\text{-O,N-[2-(4-methylphenylimino)-pentane-4-one]}\}_2\text{TiCl}_2$.	107
Table 6. Anisotropic Thermal Parameters ($\text{\AA}^2 \times 10^3$) for $\{\mu^2\text{-O,N-[2-(4-methylphenylimino)-pentane-4-one]}\}_2\text{TiCl}_2$.	108
Table 7. Atomic Coordinates ($\times 10^4$) and Equivalent Isotropic Thermal Parameters ($\text{\AA}^2 \times 10^2$) for $\{\mu^2\text{-O,N-[2-(2,4,6-trimethylphenylimino)-pentane-4-one]}\}_2\text{TiCl}_2 \cdot \text{CH}_2\text{Cl}_2$.	109
Table 8. Anisotropic Thermal Parameters ($\text{\AA}^2 \times 10^3$) for $\{\mu^2\text{-O,N-[2-(2,4,6-trimethylphenylimino)-pentane-4-one]}\}_2\text{TiCl}_2 \cdot \text{CH}_2\text{Cl}_2$.	111
Table 9. Atomic Coordinates ($\times 10^4$) and Equivalent Isotropic Thermal Parameters ($\text{\AA}^2 \times 10^2$) for $\{\mu^2\text{-O,N-[2-(4-methylphenylimino)-pentane-4-one]}\}_2\text{ZrCl}_2$.	113
Table 10. Anisotropic Thermal Parameters ($\text{\AA}^2 \times 10^3$) for $\{\mu^2\text{-O,N-[2-(4-methylphenylimino)-pentane-4-one]}\}_2\text{ZrCl}_2$.	114

LIST OF FIGURES

CHAPTER 1

- Figure 1.* Molecular weight distributions for various polymerization schemes. As the PDI values approaches one (curve A), more narrow distributions are obtained. 5
- Figure 2.* Condensation (A), addition (B) and ring opening polymerization (C) general reaction schemes. 7
- Figure 3.* Anionic (A), cationic (B), and covalent (C) living polymerization reaction schemes. 10
- Figure 4.* Monometallic (A) and bimetallic mechanisms of olefin polymerization by a Ziegler–Natta catalyst. 14
- Figure 5.* Propene approach to a TiCl_3 catalytic surface. 16
- Figure 6.* Mechanism of olefin polymerization with $\text{Cp}_2\text{Cl} / \text{Et}_2\text{AlCl}$ (P = polymer chain). 18
- Figure 7.* Protolysis approach to the synthesis of zwitterionic metallocene catalysts (A) and the various adducts of the electron deficient intermediate present in solution under the reaction conditions (B). 22
- Figure 8.* Alkyl group abstraction (A and B) and alkyl group coordination (C) synthetic approaches for metallocene based catalysts. 24
- Figure 9.* Non– Cp_2 transition metal (group IV metals) complexes for Ziegler–Natta polymerization catalysts. 28

CHAPTER 3

- Figure 1.* General synthetic scheme of β –ketimine ligands. 58
- Figure 2.* ORTEP representation (at 50% probability) of N –(4–

tolyl)-acetamide.	60
<i>Figure 3.</i> Fragmentation mechanism and assignment of the main MS peaks of the allene.	63
<i>Figure 4.</i> Proposed mechanism accounting for the formation of the amide and β -ketimine products, in the condensation reaction of substituted anillines with 2,4-pentanedione.	64
<i>Figure 5.</i> Fragmentation mechanism and assignment of the main MS peaks of the 2-(dimethylamino)-4-(4-methylphenylimino)-pent-2-ene.	70
<i>Figure 6.</i> ORTEP diagram (at 50% probability) of the non-chelate $\{\mu\text{-O-[2-(2,4,6-trimethylphenylimino)-pentane-4-one]}\}_2\text{TiCl}_4 \cdot 0.5\text{C}_4\text{H}_8\text{O}$, displaying one of the two crystallographically independent organometallic complexes.	73
<i>Figure 7.</i> General synthetic scheme for the synthesis of Titanium chelate complexes.	79
<i>Figure 8.</i> ORTEP representation (50% probability) of $\{\mu^2\text{-O,N-[2-(4-methylphenylimino)-pentane-4-one]}\}_2\text{TiCl}_2$.	87
<i>Figure 9.</i> ORTEP representation (50% probability) of $\{\mu^2\text{-O,N-[2-(2,4,6-trimethylphenylimino)-pentane-4-one]}\}_2\text{TiCl}_2 \cdot \text{CH}_2\text{Cl}_2$.	89
<i>Figure 10.</i> ORTEP representation (50% probability) of $\{\mu^2\text{-O,N-[2-(4-methylphenylimino)-pentane-4-one]}\}_2\text{ZrCl}_2$. Only half of the molecule is crystallographically unique.	91
<i>Figure 11.</i> Synthesis of Zirconium and Titanium chelates by <i>in situ</i> generation of the β -ketoimine salt with triethylamine (top), and from the corresponding non-chelate complex by action of triethylamine (bottom).	96

CHAPTER 1

INTRODUCTION

Transition metal catalyzed polymerizations comprise some of the most important metal-mediated industrial processes. Of these processes, Ziegler-Natta catalysts for α -olefin polymerization are particularly prominent. First generation catalysts were derived from metal-alkyl complexes and main-group initiators. Over the past few decades, considerable effort has been directed toward catalyst design. Among early transition metal systems, cyclopentadienyl complexed catalysts have been studied extensively in attempts to prepare catalysts where polymer tacticity is dictated by the ligand environment. While significant progress has been achieved in these systems, some problems have

proven to be particularly difficult. These catalysts are generally active only in their cationic form and require initiators that are often ill-defined. A second and more fundamental problem is the termination of the polymerization sequence via β -alkyl elimination¹, chain transfer to a co-catalyst², and β -hydrogen elimination³. For these reasons truly "living" Ziegler-Natta processes were not known before 1996. Recently however the first such examples appeared in the literature, based on early transition metal systems in non-Cp₂ ligand environments⁴.

It is the goal of this thesis to describe the synthesis and characterization of potentially promising complexes for "living" Ziegler-Natta polymerizations. In the following sections a general background on polymerization processes will be given, followed by past and recent advances in Cp₂-based Ziegler-Natta catalysts.

A. Polymerization Processes; General Considerations

Natural polymers such as starch, cellulose and proteins have been known to humanity since the ancient times, although their structure, even in elementary terms, was not understood until the late nineteenth century. In early investigations the macromolecular composition of these materials was not recognized by the majority of the scientific community. In addition, limitations in technology resulted in poor experimental data to ascertain the true character of the polymers. Hence, the macromolecular hypothesis was not accepted until 1930, although, surprisingly, some important polymeric materials (PVC, Rayon, rubber) were synthesized prior to this proposal.

In the early years of the twentieth century the industrial needs for starting materials were mainly satisfied by steel, glass, wood, stone, brick, cotton, and

wool. However these demands changed rapidly in the beginning of World War II. The extended research efforts during and after this period resulted in a series of key scientific discoveries, which were further accelerated by the availability of starting materials and monomers from the petrochemical industry. The renaissance of polymer chemistry, triggered by these events, had a marked impact in science and society. The subsequent increase in the range of manufactured products following World War II, is the direct outcome of the development of a broad range of new polymeric materials, such as fibers, plastics, elastomers, adhesives, and resins. In our days, products made from polymers are all around us. Therefore, it is not surprising that more than 50% of all chemists and chemical engineers, and nearly all materials scientists, are involved with research and development work in polymer science.

The study of polymers is a uniquely broad discipline that encompasses the whole of chemistry and several other fields as well. These macromolecular entities, are defined as long-chain molecules possessing uniform repeat units. Although the nature of their physical properties is imposed by the geometrical and electronic attributes of the monomer, these are unique for the polymeric material and clearly distinct from those of the building blocks. Within a given material however, not all the chains have the same length in antithesis to molecular species. As a consequence, new types of molecular weight averages need to be introduced in order to describe and characterize these composite compounds⁵.

Two main molecular weight averages have been introduced. The former is the number average molecular weight M_n defined in equation 1.1

$$M_n = \frac{\sum N_i M_i}{\sum N_i} \quad (1.1)$$

where N_i is the number of molecules that have molecular weight M_i and represents the mean value of the molecular weight. In a distribution curve its caliber accounts for the highest value of the distribution.

The latter is the weight average molecular weight M_w defined in equation 1.2

$$M_w = \frac{\sum N_i M_i^2}{\sum N_i M_i} \quad (1.2)$$

where N_i has been replaced by $N_i M_i$, which is proportional to the weight of polymer that has a specified M_i value; M_w is seen to be always greater than the number average molecular weight.

The experimental determination of a polymer's molecular weight is not an easy task, but this knowledge is vital for the understanding of the relationship between structure and properties. Generally two approaches, based on absolute and secondary methods, are utilized in order to measure it. The absolute methods are the outcome of direct measurements using the "colligative" properties of the polymer (boiling point elevation, melting point depression, osmotic pressure, vapor pressure lowering). The secondary methods (viscosity, gel permeation chromatography) yield comparisons between the molecular weights of different polymers, and must be calibrated by reference to a system that has been studied by one of the absolute approaches. Unfortunately, none of the two methodologies can offer an accurate determination of the molecular weight, due to unavoidable errors associated with solubility problems and unsuccessful calibration, to name a few. To overcome these obstacles, the molecular weight of a polymer is usually measured by more than one technique.

An alternative approach does not seek absolute values of molecular weights, but rather a molecular weight distribution (*Figure 1*) termed as polydispersity index (PDI)

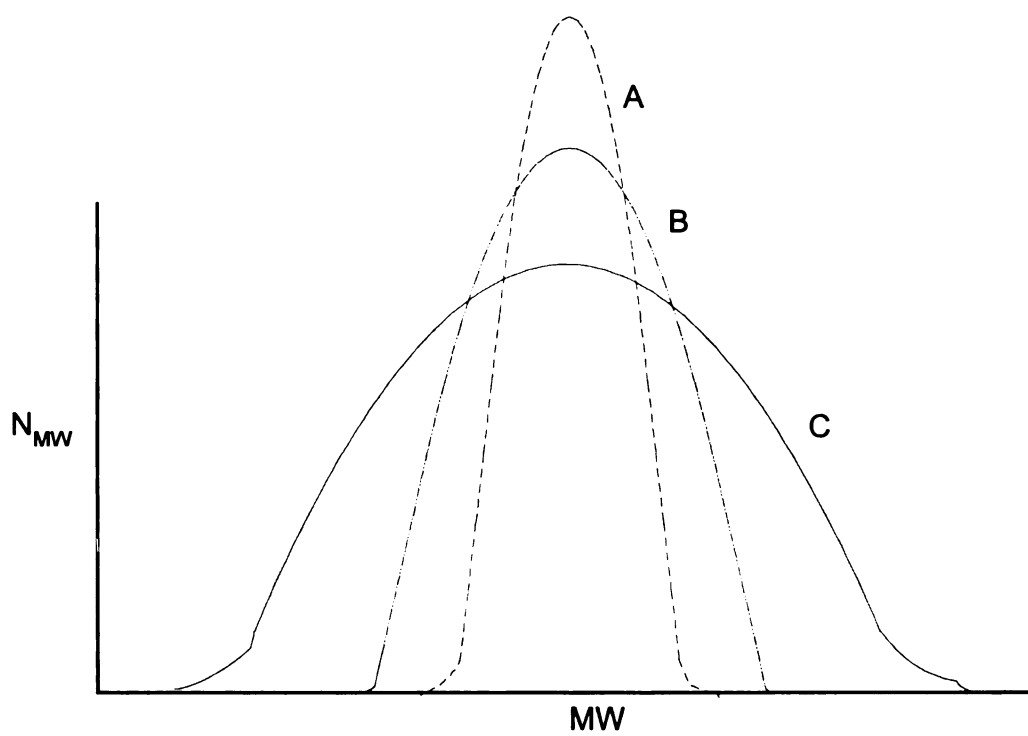


Figure 1. Molecular weight distributions for various polymerization schemes. As the PDI values approaches one (curve A), more narrow distributions are obtained.

$$\text{PDI} = \frac{M_w}{M_n} = 1 + \frac{1}{dp} \quad (1.3)$$

where dp is the degree of polymerization, or the number of monomer units per chain. The PDI parameter provides valuable clues to the polymerization reaction mechanism, along with indications regarding the degree of homogeneity of a given material. It is the latter that is greatly influenced by the chemical process and the synthetic methodology utilized. As a consequence, general synthetic schemes have been devised that categorize the large number of chemical reactions for the generation of polymeric species. There are three main groups of polymerization events, with the classification based on the structure of the monomeric precursors: condensation, addition and ring opening polymerization (*Figure 2*). Each category is briefly discussed below, along with the main characteristics that distinguish each one from the others.

1. Condensation polymerization

This stepwise process involves initial reaction of the monomeric species to form dimers with the simultaneous release of a small molecule such as water or ammonia. Subsequent chain growth is accomplished by further condensation of the monomers with the generated entities (*Figure 2(A)*). Any molecular species in the system (monomers, dimers etc.) can be the active species for the polymerization resulting in a slow increase of the molecular weight throughout the reaction. As a consequence of the slow, stepwise manner of the chain growth, the monomer disappears at early stages of the polymerization resulting in polymeric products of broad molecular weight distributions (*Figure 1, curve C*).

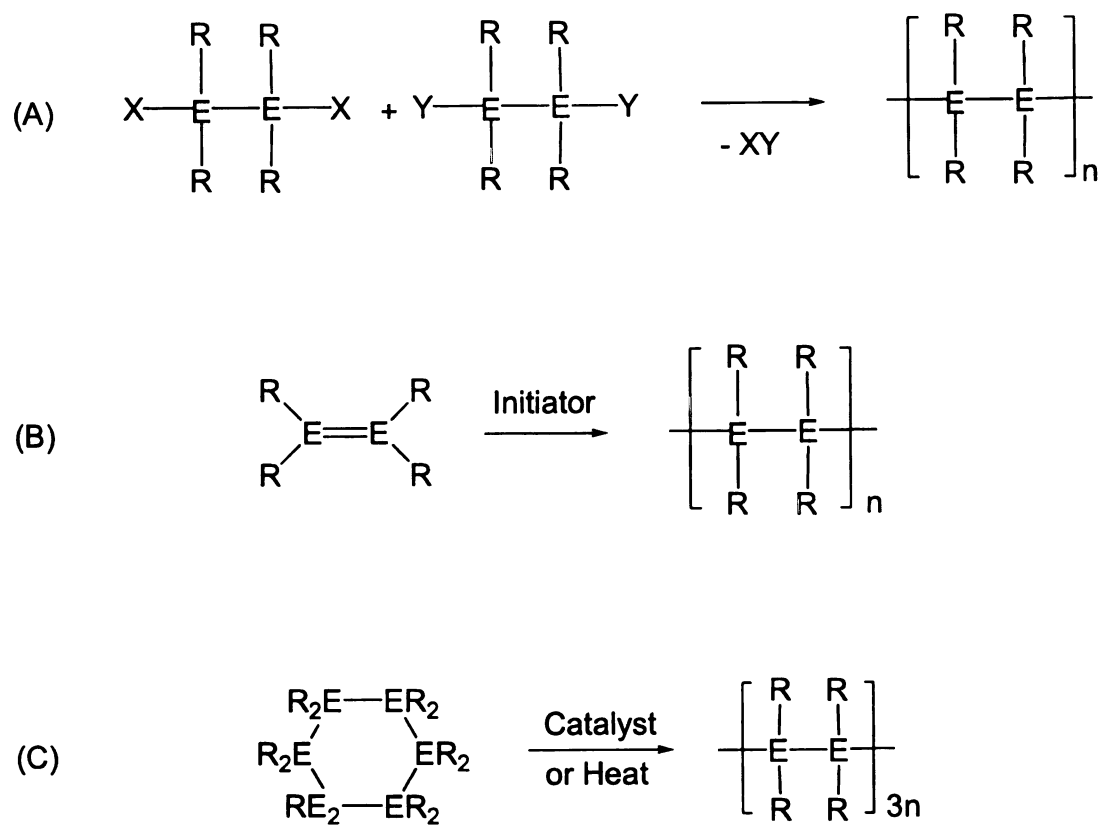


Figure 2. Condensation (A), addition (B) and ring opening polymerization (C) general reaction schemes.

2. Addition polymerization

In this chain type reaction, the building blocks are unsaturated molecules, such as alkenes or alkynes. An initiator is necessary to activate the monomers producing a small population of few radical or charged activated species, which undergo polymerization by attacking the unsaturated substrates. Chain growth takes place only at the end of those initiated chains (*Figure 2(B)*). The monomer concentration decreases steadily during the reaction and ideally — on account of the rapid initiation — the system contains only unreacted monomer and high molecular weight polymeric species throughout the reaction. Narrow molecular weight distributions is the final outcome of the rapid initiation (*Figure 1, curve B*).

3. Ring opening polymerization

Treatment of cyclic monomers with a catalyst or heat induces cleavage of the ring followed by polymerization to yield high molecular weight polymers (*Figure 2(C)*). Mechanistically this process is a chain type reaction, and its characteristics are expected to be similar to those of the addition polymerization.

4. Living Polymerization

In contrast to the previously described polymerizations in which initiation, propagation and termination steps roughly compose the overall reaction sequence, a new type of process termed "living polymerization" has been developed. It confines itself only to initiation and propagation steps. The term "living" was initially coined by Swarz⁶ as early as the 1950's, and was used to describe those systems in which the polymeric chain ends remain active until "killed". In such an ideal system, each chain should retain its ability to react with



of
of
po
ap
se
m
ca
3
a
d
fo
re
s
s
c
o
s
i
n
o
f

monomer species infinitely, since their complete consumption does not bring about the end of the polymerization. Hence, addition of fresh monomer resumes the reaction process.

The living polymerization systems can be classified⁷ into three groups depending on the nature of the active chain end and the type of the initiator species. In the first group, termed *anionic* living polymerization, initiation occurs by the addition of the initiator across an unsaturated bond of the monomer (*Figure 3(A)*). Alkali metal suspensions, alkyl or aryl lithium reagents, Grignard reagents, aluminum alkyls and organic radical anions are utilized as common initiators, while typical substrates include substituted styrenes with non-base sensitive groups⁸, methacrylates and acrylates⁹, as well as lactones¹⁰. Anionic chains – further stabilized by the presence of electron withdrawing groups on the monomers – are the active polymerization sites. The subsequent propagation step involves the insertion of a monomer into the terminal "ionic bond"; a sequence that lasts until the complete consumption of the monomer or until the reaction is intentionally terminated.

The second type of living polymerization, termed *cationic*, involves the formation of cationic chain ends instead of anionic. The combination of electron donating groups at the substrates and suitable strong Lewis acids as initiators are thought to be the optimum conditions for a successful polymerization (*Figure 3(B)*). Rival reaction pathways, however, such as transfer of β -hydrogen from the cationic species to the monomer⁷, result in dead chain ends and accordingly to mixtures of low molecular weight products. Although these cationic systems seem not to be very "living", specific combinations of monomers with the appropriate initiators have circumvented this problem. More specifically, the polymerization of vinyl ethers¹¹ with hydrogen iodide and iodine as initiators and of isobutylene,¹² initiated by tertiary esters or ethers with an excess of BCl_3 , are

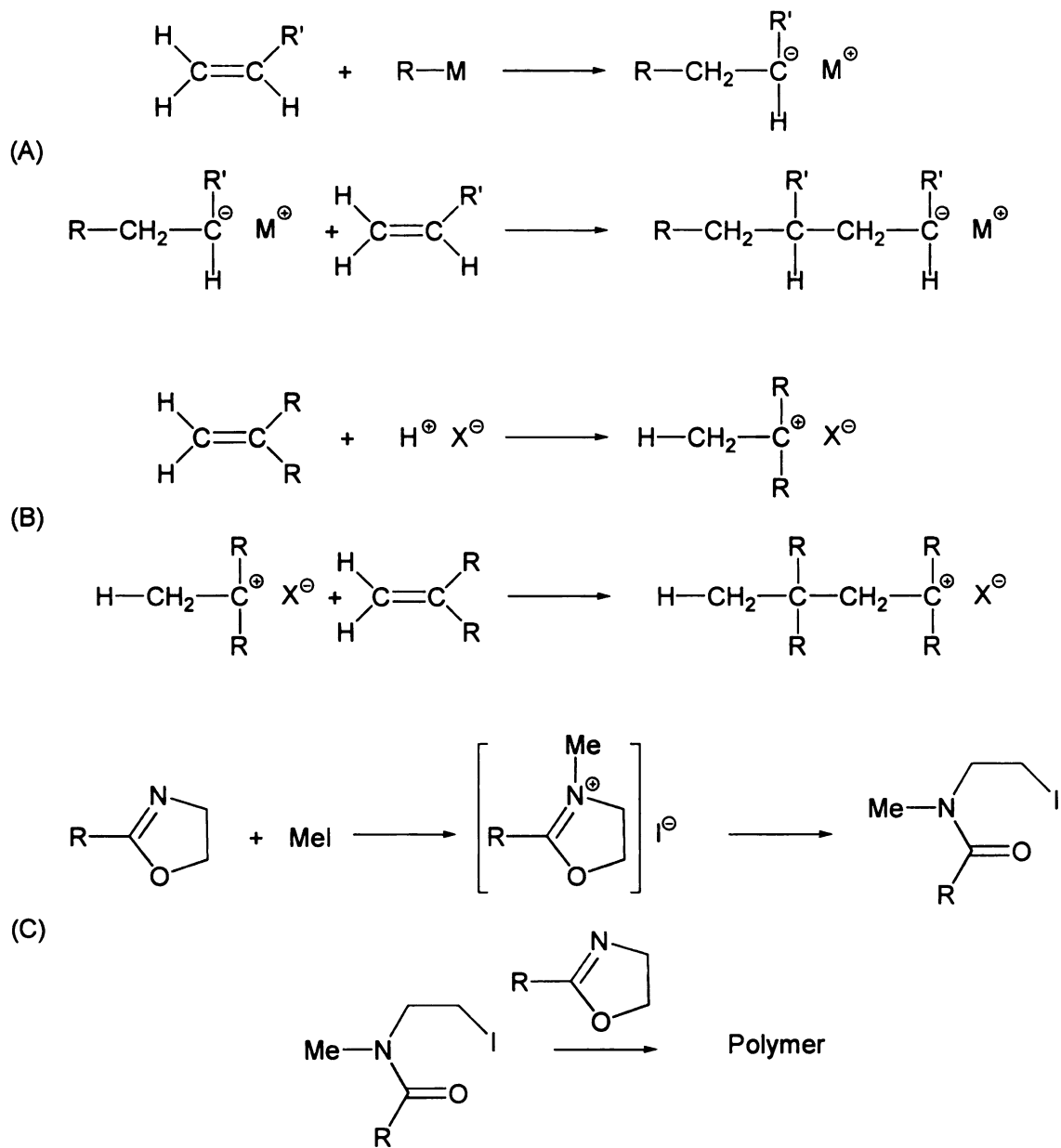
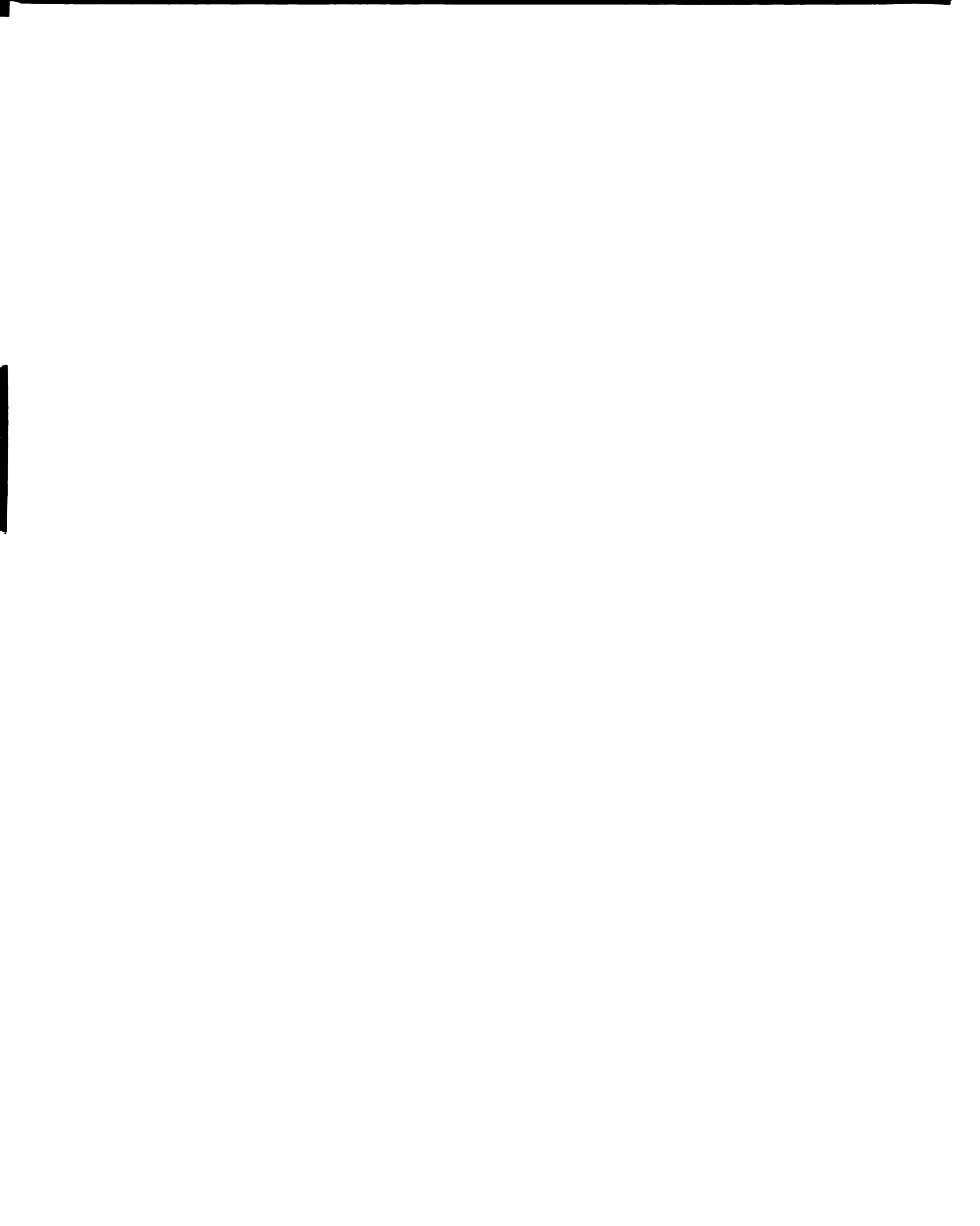


Figure 3. Anionic (A), cationic (B), and covalent (C) living polymerization reaction schemes.



successful examples where the problems of β -hydrogen transfer are overcome, affording true living systems.

Finally a number of living polymerizations, although nucleophilic or electrophilic in character, initiate and propagate by reaction of a reactive covalent end group with the monomer. This type is termed *covalent* living polymerization, since although a charged intermediate is involved, the propagation step proceeds by two neutral species. In *Figure 3(C)* one such example, the polymerization of oxazolines by methyl iodide¹³, is demonstrated, with the iodide ion possessing the dual role of the nucleophile and leaving group.

Well-behaved living systems advance by a rapid initiation¹⁴ step, where all the chains are initiated at the same time followed by their simultaneous growth until the complete consumption of the monomer. As a consequence, very narrow (in most of the cases, close to unity) molecular weight distributions are obtained (*Figure 1*, curve A) in contrast to those from the classical methods of polymerization (*Figure 1*, curves B and C). Each initiator molecule, in principle, generates only one polymer chain, providing the means for controlling the polymer's molecular weight; the more initiator is added the lower the molecular weight will be. It can actually be determined by the relative ratio of the initiator to the monomer as shown by equation 1.4

$$\text{Degree of polymerization} = [\text{monomer}] / [\text{initiator}] \quad (1.4)$$

Living polymerization methods offer new advantages in comparison with the other polymerization processes. The existence of unterminated living end chains when the monomer is consumed can lead to either further polymerization if new monomer is supplemented or to selective termination of the reaction. The latter enables the synthesis of functional-ended polymers where, for example, a polar end and a lipophilic chain core are both incorporated into the

polymerization product. If continuing the reaction sequence is the desirable choice, addition of a different substrate than the one already composing the polymer backbone provides a facile method for the synthesis of block copolymers. Such processes are of extreme importance since composite materials with unique properties become readily available.

B. Ziegler–Natta polymerization

In early 1950's Karl Ziegler reported the polymerization of ethylene¹⁵ with TiCl_4 / Et_2AlCl catalysts under the mild conditions of atmospheric pressure and room temperature. This great scientific discovery was shortly reinforced by Natta's findings that similar catalysts could also polymerize propene producing a crystalline, stereoregular product¹⁶. Those two events triggered an enormous amount of subsequent research on α -olefin polymerization, soon finding industrial application. It is worth mentioning, that the world production of polyolefins in 1995 was estimated to be 53.6 million tons, and is expected to grow by 50% over the next 10 years¹⁷.

The classical Ziegler–Natta catalysts consist of two components. Firstly, a transition metal compound, which is usually a halide or oxyhalide of titanium, vanadium, chromium, molybdenum, or zirconium (groups IVB to VIII B of the periodic table). The second component, an organometallic co-catalyst, often consists of an alkyl, aryl, or hydride of aluminum, lithium, magnesium, or zinc (groups IA to IIIA of the periodic table). Such catalytic systems can be either heterogeneous (some titanium–based) or homogeneous (most vanadium-based).

In Ziegler–Natta catalysis, coordination of an olefin to an empty site of a low valent transition metal is the primary step, followed by subsequent insertion

of the activated monomer into a metal carbon bond. During the first step, a stable π -complex between the olefin and the low-valent transition metal is formed by an effective overlap between the d-orbitals of the transition metal and the π or π^* orbitals of the olefin. π -Complexation however, is plausible only when at least one of the ligands is weakly bound to the metal center¹⁸.

Although the exact details of the coordination and the olefin addition process are still the subject of debate, two general mechanistic schemes have been devised attempting to describe the catalytic sequence in solution. These are monometallic and bimetallic mechanisms, the latter assuming that both the transition metal and the aluminum (or a metal from groups IA to IIIA) atom play an active role in the catalytic process. In the context of the monometallic mechanism (*Figure 4(A)*), the olefin is initially coordinated to an empty site on the transition metal and subsequently is inserted into the metal-carbon bond. Incoming monomers are then positioned on the new vacant site, and the catalytic cycle resumes its activity. The monometallic mechanism allows a partial understanding of the reasons for stereospecific addition. The side groups on the olefin and the metal substituents sterically determine the coordination and insertion geometries. Approach of the monomer to the reactive metal-carbon bond occurs preferentially from the least hindered site, favoring a trans-arrangement of the bulky groups (Scheme 1 A vs B), and/or from the most available face of the metal octahedron (Scheme 1C, where S stands for small and L for large substituents).

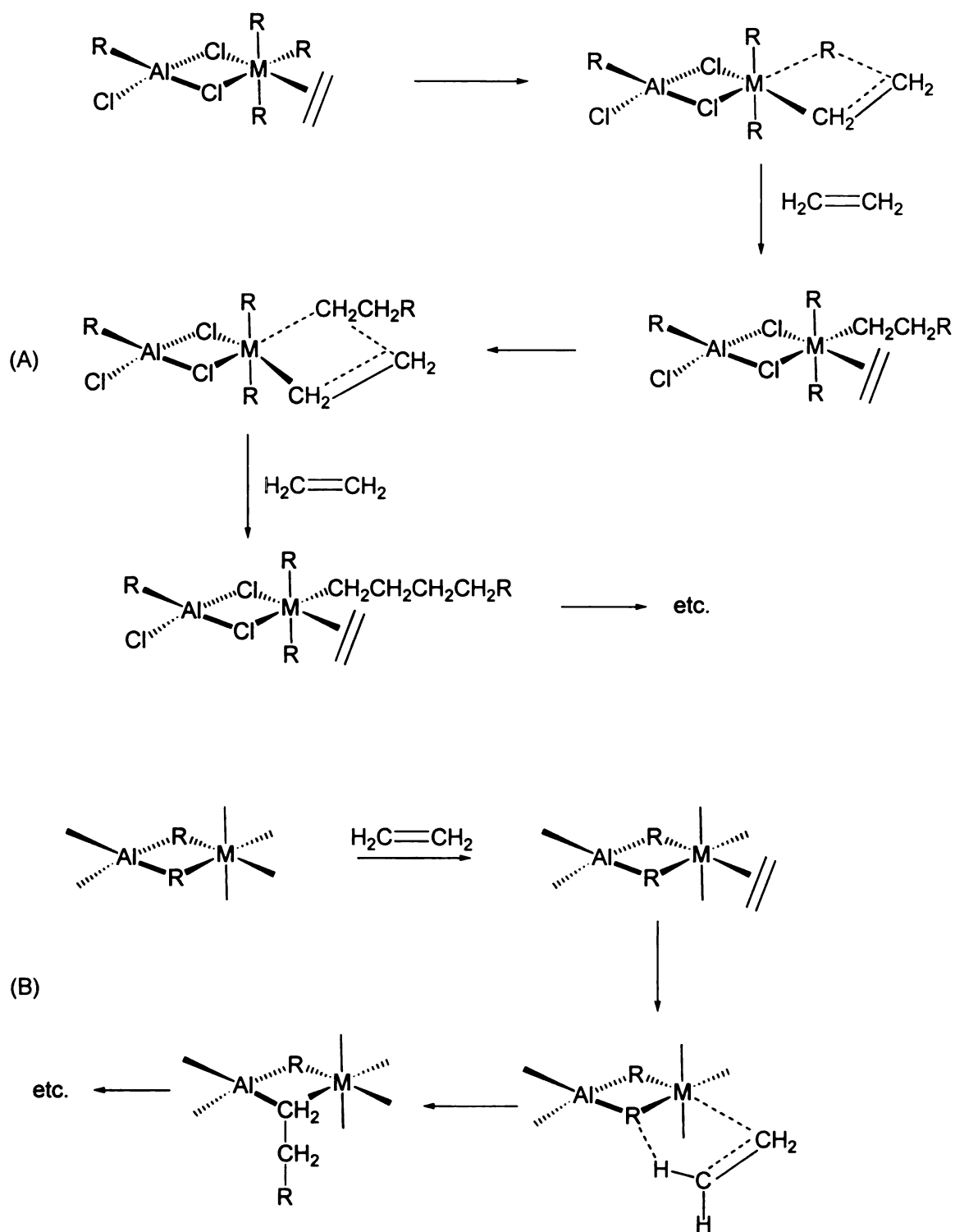
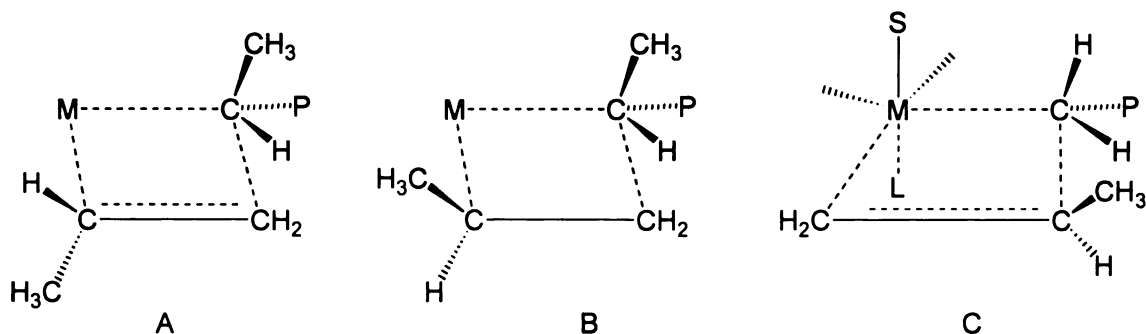


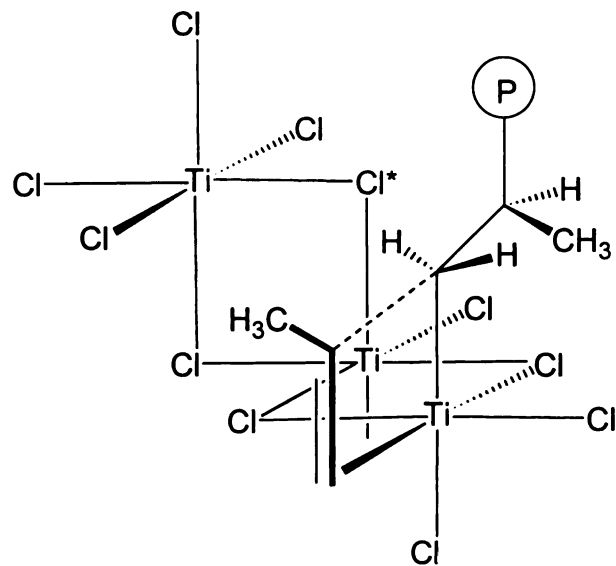
Figure 4. Monometallic (A) and bimetallic (B) mechanisms of olefin polymerization by a Ziegler-Natta catalyst.



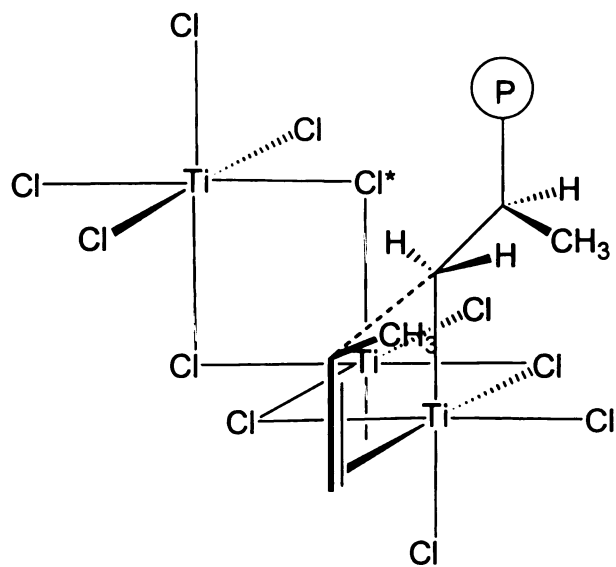
Scheme 1

In the context of the bimetallic mechanism, the alkyl groups of the catalyst are presumed to function as bridging units between the metal centers (*Figure 4(B)*). Again, π -complexation of the substrate is the initial step, followed by formation of a new bridged species after olefin insertion to the transition metal — carbon bond. Coordination and insertion of additional monomers takes place by the same pathway.

Heterogeneous Ziegler–Natta catalysts, function in a different manner than their solution counterparts; defects in the crystal surface are thought to be the primary sites of catalysis. Natta's early ideas about the role of chiral surface sites in the formation of isotactic polyolefin¹⁹ inspired the proposal of adequate models^{20,21} which explained the induction of stereoregular polymer growth by the environment of the catalytic centers. One of those models, reported by Corradini and coworkers²², describes the stereospecific polymerization of propene at a chiral octahedral Ti center on the edge of a TiCl_3 crystal (*Figure 5*). The growing polymer chain is bound to the metal center, with free rotation around the Ti — C bond restricted by the steric bulk of a neighboring chlorine atom (indicated as Cl^* in *Figure 5*). The incoming monomer coordinates to the metal through the *si* face to minimize steric interactions with the chiral β -carbon of the polymer's alkyl



si



re

Figure 5. Propene approach to a TiCl₃ catalytic surface.

chain. Conversely, coordination with the other π -face is disfavored (re coordination).

Consequently in heterogeneous systems, many different types of active catalytic sites exist, resulting in polymeric products with typically broad molecular weight distributions²³. An uneven degree of co-monomer incorporation, with a large and small incorporation rate in short and long chains respectively, is the outcome of the diversity in the catalyst's surface. Although traditional Ziegler–Natta systems still find industrial application, these drawbacks have prompted research efforts to design alternative homogeneous catalysts incorporated within various ligand environments.

1. Cp₂ ligand Systems

In 1953 Wilkinson²⁴ and coworkers reported the synthesis of the first Group IV metallocenes. Shortly after this great discovery, Breslow and Newburg²⁵ and independently Natta²⁶, discovered that Cp₂TiCl₂, a very soluble organometallic complex in aromatic hydrocarbons, along with aluminum dialkyl chlorides (R₂AlCl^{27,28}) could replace traditional Ziegler–Natta catalysts in the polymerization of olefins. Spectroscopic investigations²⁹ identified the presence of a cationic species as the active center of the polymerization process³⁰. This is generated by initial alkylation of the organometallic complex by the aluminum co-catalyst, followed by Lewis acid complexation or complete removal of the chloride from the Cp₂TiRCl (*Figure 6*)³¹. Olefin coordination to titanium and σ -bond metathesis produce the polymeric chains, which either resume the catalytic cycle or reductively disproportionate³² by a bimolecular process forming polymer chains with saturated and vinyl end-groups.

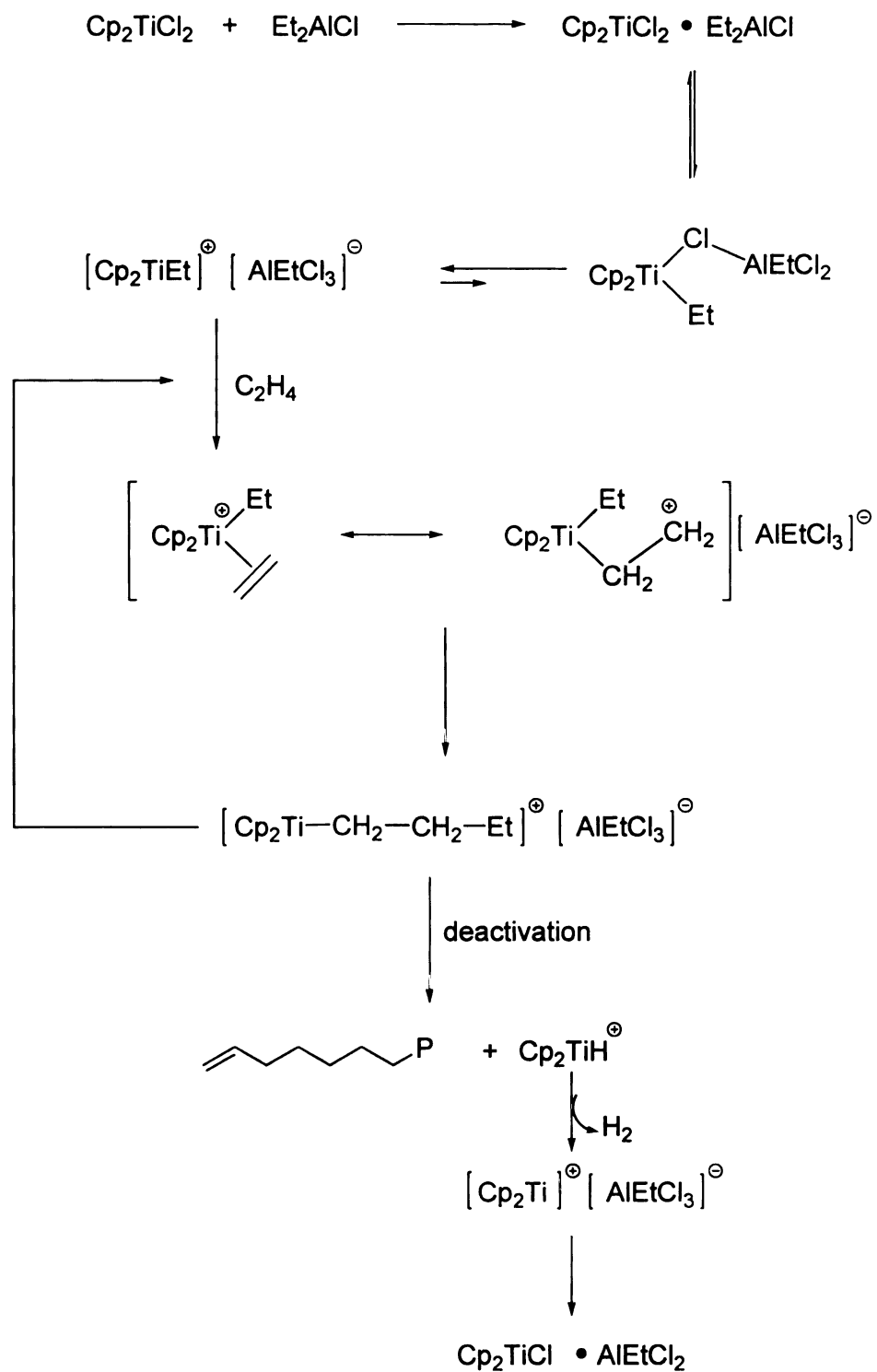
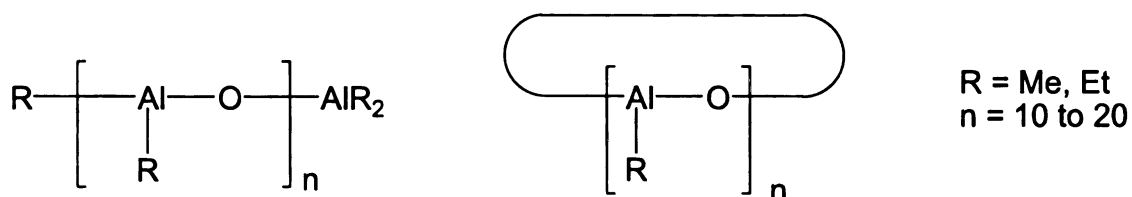


Figure 6. Mechanism of olefin polymerization with $\text{Cp}_2\text{Cl} / \text{Et}_2\text{AlCl}$ (P = polymer chain).

Traces of water were found to enhance the rate of polymerization in titanocene based catalysts, in antithesis to early Ziegler–Natta systems, such as $\text{TiCl}_3 / \text{AlEt}_3$ ³³, where water was poisonous. This effect, also seen in the polymerization of olefins by $\text{Cp}_2\text{ZrMe}_2 / \text{AlMe}_3$ ³⁴, was attributed to the formation of aluminoxanes (MAO), which are linear or cyclic oligomers^{35,36} (Scheme 2) produced by partial hydrolysis of the aluminum alkyl components³⁷.



Scheme 2

Characterization of aluminoxanes is a difficult task on account of their high reactivity towards oxygen and moisture, and their incomplete solubility in hydrocarbon and aromatic solvents³⁸. Consequently, the understanding of their structure and function as co-catalysts is inadequate. It is believed however, that they are responsible for alkylation of the catalyst^{39,40}, stabilization of the cationic metallocene alkyl by acting as counterion⁴⁰, and finally prevention of the bimolecular reduction of the catalyst⁴¹. In addition they scavenge impurities such as water and oxygen from the reaction medium prolonging the catalyst's life.

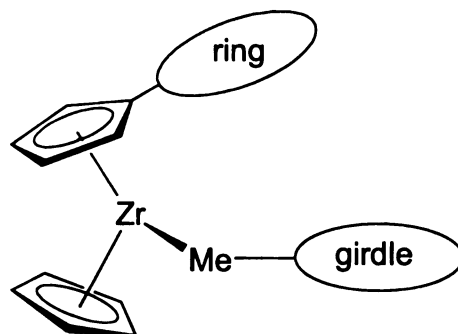
In comparison with the aluminum dialkyl halides, MAO is a much more effective activator for metallocene halides. Nevertheless, in order to achieve high activity, MAO has to be employed in a large excess over the metallocene component (typical Al : M ratios of 10^3 to 10^4 : 1), far surpassing the cost of the metal complex. Despite this disadvantage, MAO is the most widely used co-

catalyst for metallocene-based systems, including large-scale industrial processes.

Although the metallocene active species using either MAO or aluminum alkyls have been identified by various spectroscopic methods, including UV-visible spectroscopy^{29(a)}, electro dialysis experiments⁴², chemical trapping⁴³, XPS⁴⁴, solution⁴⁵ and solid state⁴⁶ NMR studies, it has not been possible to isolate them. Since the most important function of the co-catalyst is to facilitate the formation of the electron-deficient and coordinatively unsaturated "cationic" metallocene alkyl species (e.g. $[\text{Cp}_2\text{MR}]^+$), any potent Lewis acid could be suitable and effective, providing at the same time stable enough reactive intermediates. In addition the ideal co-catalyst should possess minimum ion-ion contacts with the cationic metallocene, since such forces reduce the catalytic activity. A strategy for controlling ion pairing was developed in the last few years by chemically incorporating the counterion in some spatial region of the molecule physically removed from the reaction center. Such systems possess a zwitterionic character, which offers at least two other foreseeable advantages. First, higher solubilities are anticipated in hydrocarbon media, where olefin polymerizations are performed. Second, unlike the traditional two component systems, stable zwitterions are preactivated, well-defined single-component catalysts. In other words an activation step is not required, offering advantages from a process engineering perspective.

Such co-catalysts were found to be boron-based compounds⁴⁷, with their strong molecular Lewis acidity and good solubility in nonpolar solvents. There are two distinct classes of zwitterionic catalysts as shown in Scheme 3. Girdle-type, where the Lewis acid is attached to the alkyl group and they do not remain zwitterionic for long under typical polymerization conditions, and the ring-type

where the Lewis acid is introduced through chemically modified cyclopentadienyl rings.



Scheme 3

The first metallocene catalytic system of the girdle-type was discovered by Hlatky and Turner.⁴⁸ The synthesis was accomplished via protolysis of $\text{Cp}^*_2\text{ZrMe}_2$ by $[\text{Bu}_3\text{NH}][\text{B}(\text{C}_6\text{H}_4\text{R})_4]$ ($\text{R} = \text{H}, \text{Me}, \text{Et}$) as shown in *Figure 7(A)*. The initially formed nonzwitterionic monomethyl cation is prone to σ -bond metathesis with a C — H bond of the tetraphenylborate counterion producing the stable girdle zwitterion capable of rapidly polymerizing ethylene under mild conditions. Utilizing the same synthetic approach Bochmann⁴⁹ and coworkers reported the synthesis of the cationic titanium and zirconium complexes $[\text{Cp}_2\text{MMe}][\text{BPh}_4]$, which were effective catalysts in the polymerization of ethylene, and propene. However, the protolysis synthetic approach had important disadvantages, since all the species in solution – namely the liberated amine, the tetraphenylborate counterion, and the solvent – were capable of binding to the cationic intermediate $[\text{MCp}_2\text{R}]^+$. Under polymerization conditions this means that all adducts depicted in *Figure 7(B)* are in competition⁵⁰ with the only productive species, the olefin complex.

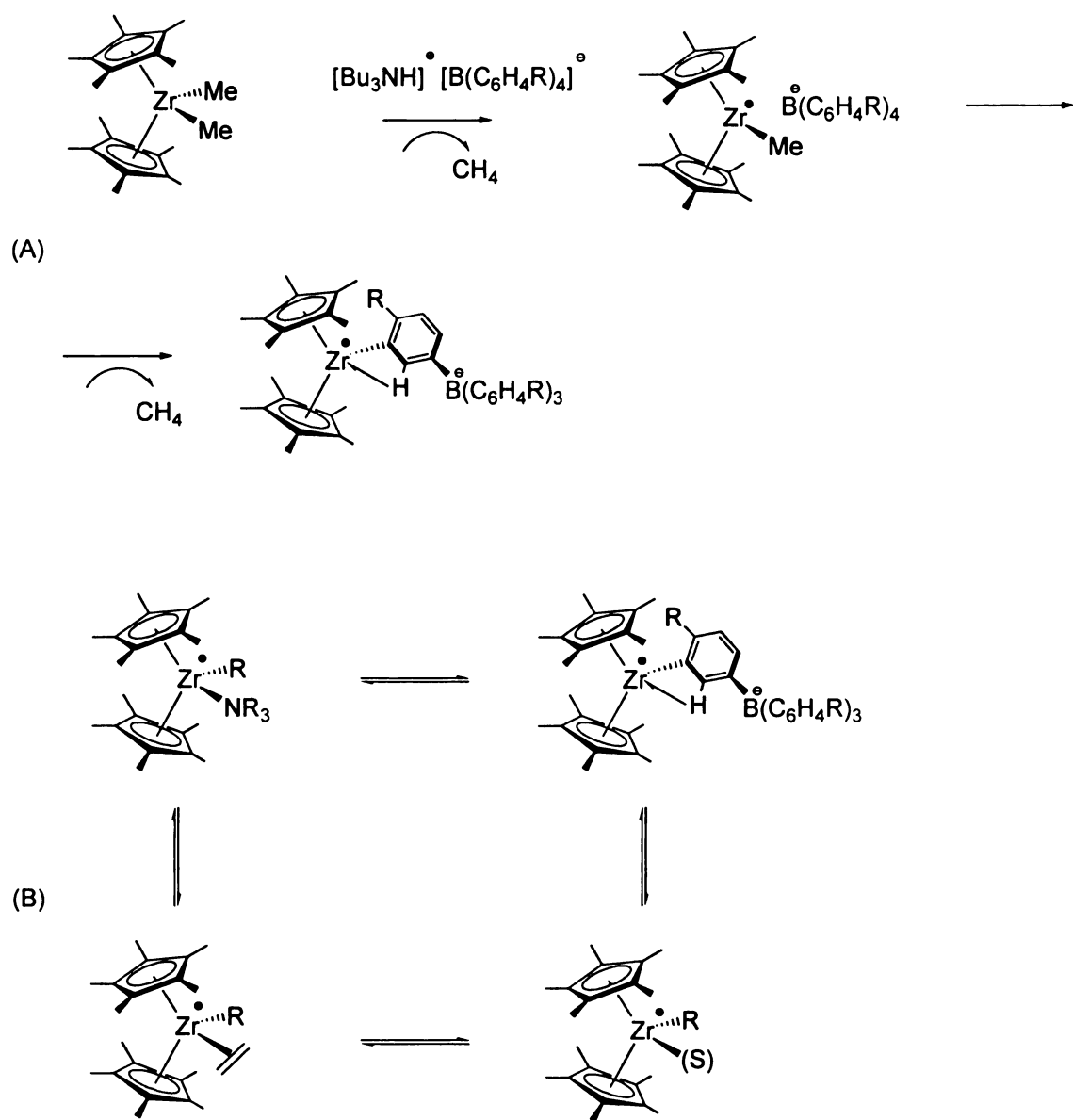


Figure 7. Protolysis approach to the synthesis of zwitterionic metallocene catalysts (A) and the various adducts of the electron deficient intermediate present in solution under the reaction conditions (B).

The initial success of metallocene zwitterions towards olefin polymerization stimulated other researchers to begin exploring this area. Alternative synthetic methodologies were pursued, targeting rigorously base-free conditions in low polarity, weakly coordinating solvents (e.g. benzene or toluene) in an effort to overcome the problems associated with the protolysis approach. Chien⁵¹ and Bochmann⁵² developed a general route⁵³ which involved alkyl abstraction from a neutral Cp₂MR₂ complexes by a strong Lewis acid, such as the trityl cation ([CPh₃]⁺). Utilization of perfluorotetraphenylborate⁵⁴, which is considerably less basic and less prone to phenyl transfer reactions than its unsubstituted counterpart, as a counterion also reduces the cation-anion interaction further facilitating olefin complexation to the metal center (*Figure 8*, path A). Marks⁵⁵ and coworkers on the other hand utilized the neutral perfluorotrisborate as a Lewis acid, resulting in either alkyl abstraction (*Figure 8*, path B for R = benzyl) or coordination to the alkyl group (*Figure 8*, path C for R = methyl). The latter route offers the advantage that the product is stabilized by methyl coordination, being at the same time less polar and thus significantly more soluble in nonpolar solvents. X-ray diffraction studies^{54,56} on several such complexes reveal rather long Zr — C bond distances with Zr — CH₃ — B bridges. The Zr — C distance appears to be sensitive to the steric requirements of the cyclopentadienyl ligands and with two of the methyl hydrogens agostically interacting with the metal center. Under the catalytic conditions the methyl-bridged zwitterionic complex partially dissociates to the nonzwitterionic ion pair complex [ZrCp₂Me]⁺[BMe(C₆F₅)₃]⁻ which is found to be a good ethylene polymerization catalyst.

In addition to the previously discussed girdle-type catalysts, which do not remain zwitterionic under typical polymerization conditions⁵⁷, a lot of research has been focused on ring-type catalytic systems. Their zwitterionic character, in

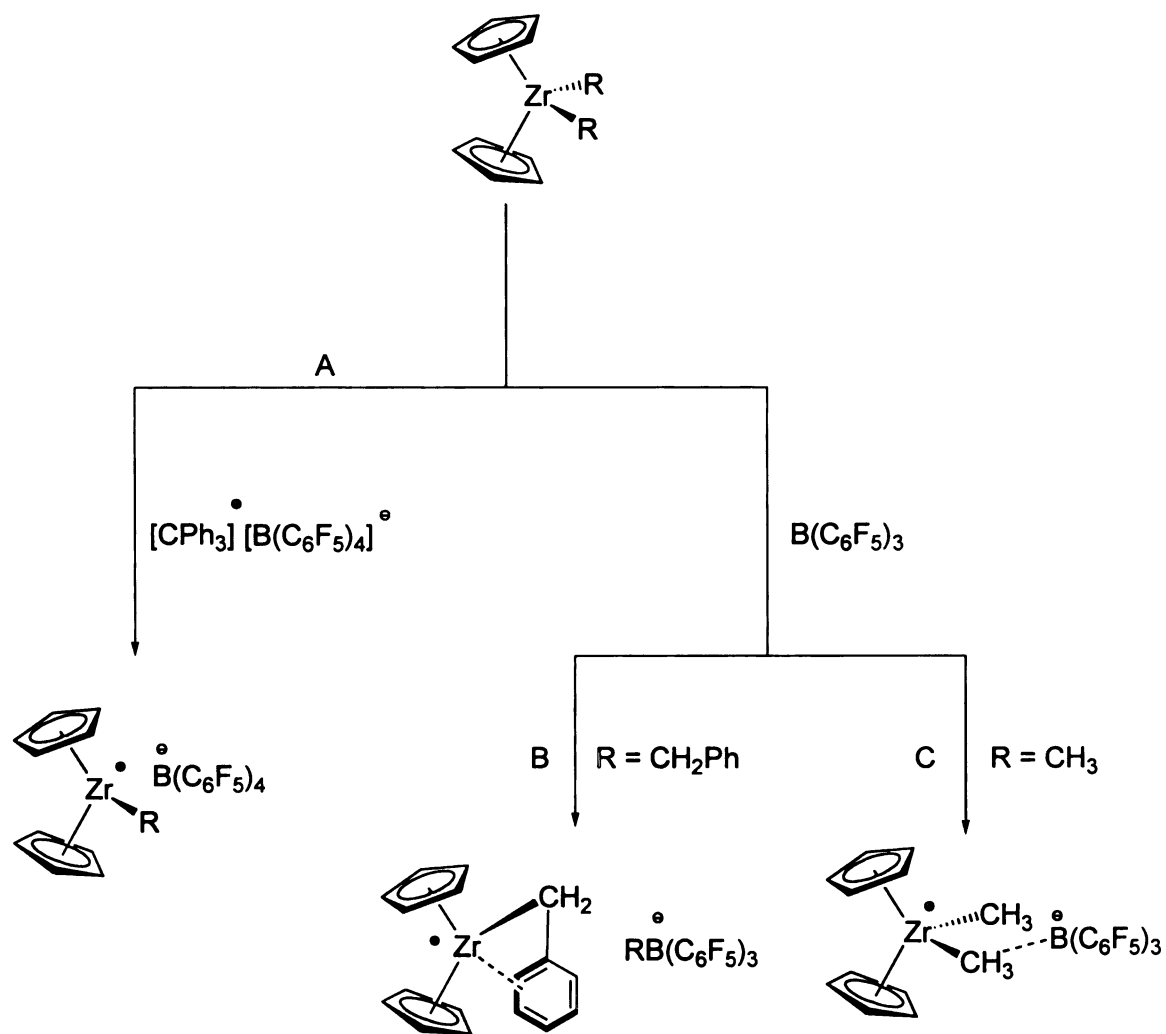


Figure 8. Alkyl group abstraction (A and B) and alkyl group coordination (C) synthetic approaches for metallocene based catalysts.

principle, should be maintained throughout the enchainment process since the counterion is attached on the cyclopentadienyl rings. It is interesting and also clear from the examples known that the means by which the borate is tethered to the ring has a significant impact on the catalytic properties of these zwitterions. In particular, the length of the tether connecting the ring with the borate is crucial in determining both the stability of the compound as a zwitterion and the nature of intramolecular ion–ion contacts. Thus the initial approach to ring–type zwitterions involved the hydroboration⁵⁸ of allyl groups attached to the cyclopentadienyl ring using the reagent $\text{HB}(\text{C}_6\text{F}_5)_2$. This three–carbon tether system is not a successful one, since the borate often gives side reactions with the transition metal⁵⁹ carbon bonds, and even in cases where the hydroboration is clean, the final complex resulting from a rearrangement reaction is a nonzwitterionic one. When shorter linkers of only one carbon⁶⁰, or with none⁶¹ between the ring and the borate were used the resulting complexes were found to be effective catalysts for olefin polymerization⁶².

The bulk of the research today is carried out by using the cationic group IV metallocene complexes as polymerization catalysts. They are still receiving considerable attention because they display the best performance of all Ziegler–Natta type catalysts and they are the ones most often utilized in industrial applications. These species retain a high catalytic activity possessing a series of advantages, which can be summarized as: 1) the electrophilic nature of the cationic d^0 metal center, 2) the large degree of polarizability attained by the $\text{M} - \text{C}$ bonds making them inherently reactive, 3) the bent metallocene structure, which restricts coordination of substrates to sites *cis-* to the $\text{M} - \text{R}$ group, and finally 4) the steric, electronic and chirality properties of the metal centers, which in principle may be tailored by modifying the Cp ligands with substituents and linking groups.

Research efforts towards the latter began as early as 1971 when Henrici-Olivié and Olivé⁶³ pointed out that modification of the electronic and steric properties of the catalyst's ligand system could lead to specific changes in catalytic activity and product stereochemistry⁶⁴. The tuning of the electronic environment, for example, could have a marked impact on the metal-olefin coordination interactions. In addition, the electron donor ability of the involved species – namely olefin, co-catalysts, cyclopentadienyl rings and their substituents – could reduce the positive charge on the metal, thereby weakening the M — R bond, which is directly involved to the polymerization process. Their marked effect is also seen when the group IV metal is replaced by a lanthanide producing isoelectronic neutral metallocene complexes, LnCp₂R. These systems are poorer catalysts due to their predominantly trigonal planar geometry⁶⁵, which is not suitable for olefin approach. In addition, the lanthanide complexes tend to form stable dimers upon reaction with an olefin, a feature that distinguishes them from the Group IV cations, leading to deactivated catalysts.

2. Non-Cp₂ ligand Systems

Increasing efforts are being made towards olefin polymerization systems that possess new, non-Cp₂ ligand environments. The ideal systems should be coordinatively unsaturated⁶⁶, and initial synthetic approaches have targeted the use of both neutral and anionic ancillary ligands that sterically "saturate" a metal center but at the same time remain coordinatively and electronically unsaturated. The aim of using such catalytic systems is twofold ; first, to find a ligand that can rival the extensively patented cyclopentadienyls, and second, to eliminate the complications of a counterion by developing neutral analogues of the cationic active species. In addition such ligand environments are more easily modified

enabling the fine electronic tuning of the metal's frontier orbitals. The latter condition is highly desirable since olefin coordination is feasible only when appropriate electronic matching exists between its orbitals and the corresponding ones of the metal.

Some of the new ligand environments⁶⁷ that have been tested as catalysts toward olefin polymerization are shown in Figure 9. In all these cases, the common feature shared with the well established Cp₂M (M = group IV metal) systems, is that the polymerization sites are constrained to be *cis*- to each other. Therefore the insertion and σ -bond metathesis steps are strongly facilitated.

Although these non-Cp₂M catalytic systems have a geometry closely related to that of the cyclopentadienyl complexes, and their cationic alkyl derivatives can be readily made, their catalytic activity is at best modest. Their distinct advantage however, is the facile tuning of their electronic and steric properties, as it has been demonstrated nicely by the work of Jacobsen and coworkers, who used an electronically tuned Mn(III) catalyst for enantioselective olefin epoxidation⁶⁸. By utilizing electron withdrawing-donating substituents on the Schiff base type, salen ligand environment of the Mn(III) catalyst, they were able to favor one enantiomer over the other. Similar expectations are anticipated by the use of such tunable catalysts in olefin polymerization.

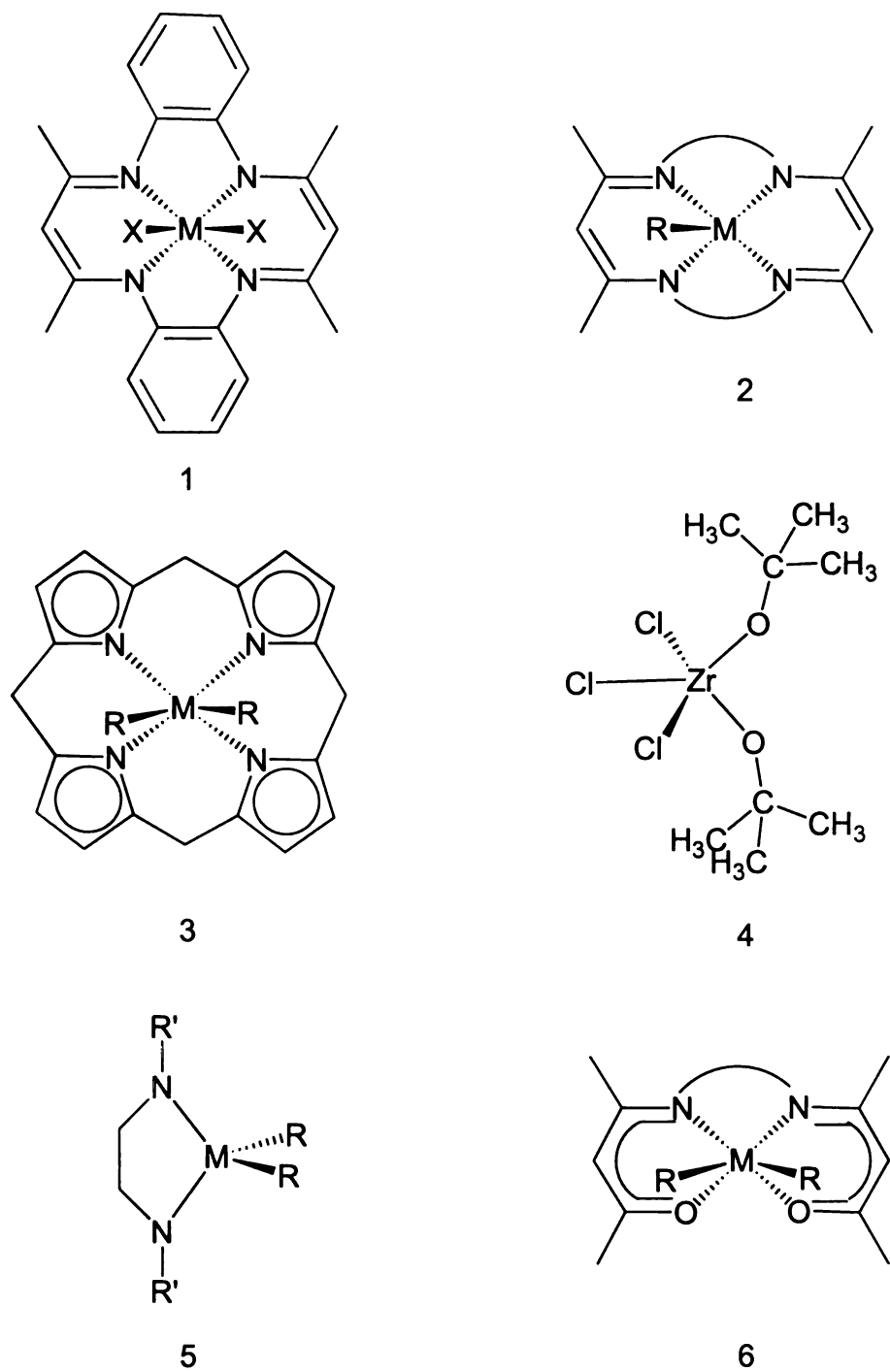


Figure 9. Non- Cp_2 transition metal (group IV metals) complexes for Ziegler-Natta polymerization catalysts.

C. Thesis Outline

The goal of the present thesis is the development of non-Cp₂ type ligand environments that will efficiently accomplish the polymerization of olefins and other catalytic transformations. Specifically, we have developed the synthesis of β-keto-imine ligands, which can be easily modified both sterically and electronically by varying the substituents on the nitrogen site of the ligand, stabilizing at the same time Group IV metal centers.

Chapter two describes the experimental procedures followed for the synthesis of the free ligands and their salts, and for their complexation with group IV metals, in both a chelate and a non-chelate manner. Additionally, all the general methods used for the characterization and purification of the synthesized compounds are given, as well as the purification of the solvents and the starting materials.

Chapter three elaborates the synthetic details and structural characterization of such complexes. Their geometric aspects, which might have a prominent role to their catalytic activity, are described, emphasizing their versatility towards stereochemical and electronic modification.

LIST OF REFERENCES

- (1) Eshuis, J.; Tan, Y.; Teuben, J.; Renkema, J. *J. Mol. Catal.* **1990**, *62*, 277.
- (2) Chien, J.; Wang, B. *J. Polym. Sci. Polym. Chem. Educ.* **1990**, *28*, 15.
- (3) Cross, R. J. in *The Chemistry of the Metal–Carbon Bond*; John Wiley and Sons: New York, 1985; Vol 2, Chapter 8.
- (4) (a) Schollard, J. D.; McConville, D. H. *J. Am. Chem. Soc.* **1996**, *118*, 10008. (b) Horton, A. D.; de With J.; van der Linden, A. J.; van de Weg, H. *Organometallics* **1996**, *15*, 2672. (c) Schollard, J. D.; McConville, D. H. *Organometallics* **1997**, *16*, 1810. (d) Baumann, R.; Davis, W. M.; Schrock, R. R. *J. Am. Chem. Soc.* **1997**, *119*, 3830.
- (5) Sperling, L. H. in *Introduction to Physical Polymer Science*; John Wiley and Sons: New York, 1992.
- (6) (a) Szwarc, M. *Nature* **1956**, *178*, 1168. (b) Szwarc, M.; Levy M.; Milkovich, R. *J. Am. Chem. Soc.* **1956**, *78*, 2656. (c) Szwarc, M. Carbanions, *Living Polymers and Electron Transfer Processes*; Wiley: New York, NY, 1968. (d) Szwarc, M. *J. Polym. Sci. : Part A* **1998**, *36*, ix-xv.
- (7) Webster, O. W. *Science* **1991**, *251*, 887.
- (8) Morton, M. *Anionic Polymerization: Principles and Practise*; Academic Press: New York, 1983.
- (9) (a) Schulz, G.O.; Milkovich, R. *J. Appl. Polym. Sci.* **1982**, *27*, 4773. (b) Schulz, G.O.; Milkovich, R. *J. Polym. Sci. Polym. Chem. Ed.* **1984**, *22*, 1633. (c) Reetz, M. T.; Knauf, T.; Minet, U.; Bingel, C. *Angew. Chem. Int. Ed. Engl.* **1988**, *27*, 1373.
- (10) Bigdelli, E.; Lenz, R. W. *Macromolecules* **1978**, *11*, 493.
- (11) (a) Miyamoto, M.; Sawamoto, M.; Higashimura, T. *Macromolecules* **1984**, *18*, 265. (b) Higashimura, T.; Aoshima, S.; Sawamoto, M. *Makromol. Chem. Macromol. Symp.* **1988**, *13/14*, 457.
- (12) (a) Faust, R.; Kennedy, J. P. *Polym. Bull.* **1986**, *15*, 317. (b) Mishra, M. K.; Kennedy, J. P. *J. Macromol. Sci. Chem.* **1987**, *24A*, 933. (c) Kaszas, G.; Puskas, J. E.; Chen, C. C.; Kennedy, J. P. *Macromolecules* **1990**, *23*, 3909.

-
- (13) Saegusa, T.; Ikeda, H.; Fujii, H. *Macromolecules* **1973**, *6*, 315.
- (14) Matyjaszewski, K. *J. Phys. Org. Chem.* **1995**, *8*, 197.
- (15) (a) Ziegler, K.; Holzkamp E.; Breil H.; Martin, H. *Angew. Chem.* **1955**, *67*, 541. (b) Ziegler, K. *Angew. Chem.* **1964**, *76*, 545.
- (16) (a) Natta, G.; Pino, P.; Corradini, P.; Danusso, F.; Mantica, G., Mazzanti, G; Moraglio, G. *J. Am. Chem. Soc.* **1955**, *77*, 1708. (b) Natta, G. *Angew. Chem.* **1956**, *68*, 393. (c) Natta, G. *Angew. Chem.* **1964**, *76*, 553.
- (17) Thayer, A. N. *Chem. Eng. News* **1995**, *73*, 15.
- (18) Allock, H. R.; Lampe, F. W. in *Contemporary Polymer Chemistry*; Prentice Hall: New Jersey, 1990.
- (19) Natta, G.; Pino, P.; Manzanti, G.; Lanzo, R. *Chim. Ind. (Paris)* **1957**, *39*, 1032.
- (20) (a) Zambelli, A.; Gatti, G.; Sacchi, C.; Crain, W. O. Jr.; Roberts, J. D. *Macromolecules*, **1971**, *4*, 475. (b) Crain, W. O. Jr.; Zambelli, A.; Roberts, J. D. *Macromolecules*, **1971**, *4*, 330. (c) Zambelli, A.; Tosi, C. *Adv. Polym. Sci.* **1974**, *15*, 31. (d) Zambelli, A.; Tosi, C. *Adv. Polym. Sci.* **1974**, *25*, 32.
- (21) (a) Cosse, P. *Tetrahedron Lett.* **1960**, *17*, 12. (b) Cosse, P. *J. Catal.* **1964**, *3*, 80. (c) Arlman, E.J. *J. Catal.* **1964**, *3*, 89. (d) Arlman, E. J.; Cosse, P. *J. Catal.* **1964**, *3*, 99. (e) Natta, G.; Farina, M.; Peraldo, M. *Chim. Ind. (Paris)* **1960**, *42*, 255. (f) Miyazawa, T.; Idegushi, Y. *J. Polym. Sci. Part B* **1963**, *1*, 389. (j) Zambelli, A.; Giongo, M.G.; Natta, G. *Makromol. Chem.* **1968**, *112*, 183.
- (22) (a) Corradini, P.; Barone, V.; Fusco, R.; Guerra, G. *Eur. Polym. J.* **1979**, *15*, 1133. (b) Corradini, P.; Guerra, G.; Fusco, R.; Barone, V. *Eur. Polym. J.* **1980**, *16*, 835. (c) Corradini, P.; Barone, V.; Fusco, R.; Guerra, G. *J. Catal.* **1982**, *77*, 32. (d) Corradini, P.; Barone, Guerra, G. *Macromolecules* **1982**, *15*, 1242.
- (23) Gavens, P. D.; Bottril, M.; Kelland, J. W.; McMeeking, J. in *Comprehensive Organometallic Chemistry*; Wilkinson, G., Stone, F. G. A., Abel, E. W., Ed.; Pergamon: Oxford, 1982; Vol. 3, p. 475.
- (24) Wilkinson, G.; Pauson, P. L.; Birmingham, J. M.; Cotton, F. A. *J. Am. Chem. Soc.* **1953**, *75*, 1011.
- (25) (a) Breslow, D. S.; Newburg, N. R.; *J. Am. Chem. Soc.* **1957**, *79*, 5072. (b) Breslow, D. S.; Newburg, N. R.; *J. Am. Chem. Soc.* **1959**, *81*, 81.

-
- (26) (a) Natta, G.; Pino, P.; Mazzanti, G; Giannini, U. *J. Am. Chem. Soc.* **1957**, *79*, 2975. (b) Natta, G.; Pino, P.; Mazzanti, G; Giannini, U.; Mantica, E.; Peraldo, M. *Chim. Ind. (Paris)* **1957**, *39*, 19.
- (27) Chien, J. C. W.; Rieger, B.; Sugimoto, R. Mallin, D. T.; Raush, M. D. in *Catalytic Olefin Polymerization*, Keii, T., Soga, K., Ed.: Proc. Int. Symp.: Tokyo, 1989; p. 535.
- (28) Chien, J. C. W.; Bres, P. *J. Polym. Sci. A, Polym. Chem. Ed.* **1986**, *24*, 1967.
- (29) (a) Long, W. P.; Breslow, D. S. *J. Am. Chem. Soc.* **1960**, *81*, 1953. (b) Fink, G.; Zoller, W. *Makromol. Chem.* **1981**, *182*, 3265.
- (30) Taube, R.; Krukowka, L. *J. Organomet. Chem.* **1988**, *347*, C9. (b) Bochmann, M.; Jaggar, A. J. *J. Organomet. Chem.* **1992**, *424*, C5.
- (31) Bochmann, M.; Wilson, L.M.; Hursthouse M. B.; Motevalli, M. *Organometallics* **1988**, *7*, 1148.
- (32) Bueschges, U.; Chien, J. C. W. *J. Polym. Sci., Polym. Chem. Ed.* **1989**, *27*, 1525.
- (33) Kaminsky, W.; Kopf, J.; Sinn, H.; Vollmer, J. *Angew. Chem. Int. Ed. Engl.* **1976**, *15*, 629.
- (34) Andersen A. A.; Cordes, H.G.; Herwing, J.; Kaminsky, W.; Merck, A.; Mottweiler, R.; Pein, J.; Sinn, H.; Vollmer, H. *J. Angew. Chem. Int. Ed. Engl.* **1976**, *15*, 630.
- (35) (a) Miya, S.; Hasata, M.; Mise, T.; Yamazaki, H. Eur. Pat. Appl. 0, 283, 739 A3. (b) Resconi, L.; Bossi, S.; Abis, L. *Macromolecules* **1990**, *23*, 4489.
- (36) Sinn, H.; Kaminsky, W. *Adv. Organomet. Chem.* **1980**, *18*, 99.
- (37) (a) Reichert, K. H.; Meyer, K. R. *Makromol. Chem.* **1973**, *169*, 163. (b) Long, W. P.; Breslow, D. S. *Liebigs Ann. Chem.* **1975**, 463.
- (38) Cam, D.; Albizzati, E.; Cinquina, P. *Makromol. Chem.* **1990**, *191*, 1641.
- (39) Chien, J. C. W.; Wang, B. P. *J. Polym. Sci. A, Polym. Chem.* **1988**, *26*, 3089.
- (40) Chien, J. C. W.; Sugimoto, R. *J. Polym. Sci. A, Polym. Chem.* **1991**, *29*, 459.
- (41) Sinn, H.; Kaminsky, W.; Vollmer, H. J.; Woldt, R. *Angew. Chem. Int. Ed. Engl.* **1980**, *19*, 390.

-
- (42) D'yachkovskii, F. S.; Shilova, A. K.; Shilov, A. Y. *J. Polym. Sci. C* **1967**, 2333.
- (43) Eish, J. J.; Piotrowski, A. M.; Brownstein, S. K.; Gabe, E. J.; Lee, F. L. *J. Am. Chem. Soc.* **1985**, 107, 7219.
- (44) Gassman, P. G.; Callstrom, M. R. *J. Am. Chem. Soc.* **1987**, 109, 7875.
- (45) Tritto, I.; Li, S.; Sacchi, M. C.; Zannoni, G. *Macromolecules* **1993**, 26, 7111 and references therein.
- (46) Sishta, C.; Hathorn, R.; Marks, T. J. *J. Am. Chem. Soc.* **1992**, 114, 1112.
- (47) Piers, W. E. *Chem. Eur. J.* **1998**, 4, 13.
- (48) Hlatky, G. G.; Turner, H. W.; Eckman, R. R. *J. Am. Chem. Soc.* **1989**, 111, 2728.
- (49) Bochmann, M.; Jaggar, A. J.; Nicholls, J. C. *Angew. Chem. Int. Ed. Engl.* **1990**, 29, 780.
- (50) Bochmann, M. *J. Chem. Soc. Dalton Trans.* **1996**, 255.
- (51) Chien, J. C. W.; Tsai, W. M.; Rausch, M. D. *J. Am. Chem. Soc.* **1991**, 113, 8570.
- (52) Bochmann, M.; Lancaster, S. J. *J. Organomet. Chem.* **1992**, 434, C1.
- (53) (a) Guram, A. G.; Jordan, R. F. in *Comprehensive Organometallic Chemistry*; Abel, E. W., Gordon, F., Stone, A., Wilkinson, G., Ed.; Elsevier Science Ltd: Oxford, 1995; Vol. 4, p. 538. (b) Jordan, R. F. *Adv. Organomet. Chem.* **1991**, 32, 325.
- (54) (a) Turner, H. W. Eur. Pat. Applic. 277004, 1988. (b) Turner, H. W. *Chem. Abstr.* **1989**, 110, 58290a. (c) Massey, A. G.; Park, A. *J. Organomet. Chem.* **1964**, 2, 245.
- (55) (a) Yang, X.; Stern, C. L.; Marks, T. J. *J. Am. Chem. Soc.* **1991**, 113, 3623. (b) Yang, X.; Stern, C. L.; Marks, T. J. *J. Am. Chem. Soc.* **1994**, 116, 10015.
- (56) Bochmann, M.; Lancaster S.J.; Hursthouse, M. B.; Malik, M. A. *Organometallics*, **1994**, 13, 2235.
- (57) Temme, B.; Erker, G; Karl, J; Luftmann, H.; Fröhlich, R.; Kotila, S. *Angew. Chem. Int. Ed. Engl.* **1995**, 34, 1755.
- (58) von H. Spence, R. E.; Piers, W. E. *Organometallics* **1995**, 14, 4617.

-
- (59) von H. Spence, R. E.; Parks, D. J.; Piers, W. E.; MacDonald, M.; Zaworotko, M. J.; Rettig, S. J. *Angew. Chem. Int. Ed. Engl.* **1995**, *34*, 1230.
- (60) Schock, L. E.; Brock, C. P.; Marks, T. J. *Organometallics* **1987**, *6*, 232.
- (61) Reetz, M. T.; Bruemmer, H.; Kessler, M.; Kuhnigk, J. *Chimia* **1995**, *49*, 501.
- (62) Sun, Y.; von H. Spence, R. E.; Piers, W. E.; Parvez, M.; Yap, G. P. A. *J. Am. Chem. Soc.* **1997**, *119*, 5132.
- (63) Henrici-Olivie, G.; Olivie, S. *Angew. Chem. Int. Ed. Engl.* **1971**, *10*, 105.
- (64) Möhring, P. C.; Coville, N. J. *J. Organomet. Chem.* **1994**, *479*, 1.
- (65) Woo, T. K.; Fan, L.; Ziegler, T. *Organometallics* **1994**, *13*, 432 and 2252.
- (66) Parsall, G. W. in *Homogeneous Catalysis*; Wiley-Interscience: New York, 1980.
- (67) For complexes **1**, **2**, and generally (N₄-macrocycle)MR₂ and (N₄-macrocycle)M(R)⁺; M = group IV) see : (a) Floriani, C.; Ciurli, S.; Chiesi-Villa, A.; Guastini, C. *Angew. Chem. Int. Ed. Engl.* **1987**, *26*, 70. (b) DeAngelis, S.; Solari, E.; Gallo, E.; Chiesi-Villa, A.; Floriani, C.; Rizzoli, C. *Inorg. Chem.* **1992**, *31*, 2520. (c) Uhrhammer, R.; Black, D. G.; Gardner, T. G.; Olsen, J. D.; Jordan, R. F. *J. Am. Chem. Soc.* **1993**, *115*, 8493. (d) Black, D. G.; Swenson, D. C.; Jordan, R. F.; Rogers, R. D. *Organometallics* **1995**, *14*, 3539.

For complex **3** and generally (N₄-porphyrin)MX₂; (M=group 4) see : (a) Arnold, J.; Hoffman, C. G. *J. Am. Chem. Soc.* **1990**, *112*, 8620. (b) Brand, H.; Arnold, J. *J. Am. Chem. Soc.* **1992**, *114*, 2266. (c) Brand, H.; Arnold, J. *Organometallics* **1993**, *12*, 3655. (d) Kim, H.-J.; Whang, D.; Kim, K.; Do, Y. *Inorg. Chem.* **1993**, *32*, 360. (e) Ryu, S.; Whang, D.; Kim, H.-J.; Yeo, W.; Kim, K. *J. Chem. Soc., Dalton Trans.* **1993**, 205.

For complex **4** and generally (RO)₂MX₂; (M=group 4) see : (a) Lubben, T. V.; Wolczanski, P. T.; Van Duyne, G. G. *Organometallics* **1984**, *3*, 977. (b) Lubben, T. V.; Wolczanski, P. T. *J. Am. Chem. Soc.* **1987**, *109*, 424. (c) Chesnut, R. W.; Durfee, L. D.; Fanwick, P. E.; Rothwell, I. P. *Polyhedron* **1987**, *6*, 2019.

For complex **5** and generally (NR₂)₂MX₂; (M=group 4) see : (a) Lappert, M. F.; Power, P.P.; Sanger, A. R.; Srivastava, R. C. in *Metal and Metalloid Amides*; Ellis Horwood Limited: Chichester, England, 1980; Chapter 8. (b) Andersen, R. A. *Inorg. Chem.* **1979**, *18*, 2928. (c) Tinkler, S.; Deeth, R. J.;

Duncalf, D. J.; McCamley, A. *J. Chem. Soc., Chem. Commun.* **1996**, 2623.

For complex **6** and generally for group IV metal Schiff base complexes, see : (a) Dell'Amico, G.; Marchetti, F.; Floriani, C. *J. Chem. Soc., Dalton Trans.* **1982**, 2197. (b) Floriani C. *Polyhedron* **1989**, *8*, 1717. (c) Floriani, C.; Solari, E.; Corazza, F.; Chiesi-Villa, A.; Guastini, C. *Angew. Chem. Int. Ed. Engl.* **1989**, *28*, 64. (d) Solari, E.; Floriani, C.; Chiesi-Villa, A.; Rizzoli, C. *J. Chem. Soc., Dalton Trans.* **1992**, 367. (e) Woodman, P.; Hitchcock, P. B.; Scott, P. *J. Chem. Soc., Chem. Commun.* **1996**, 2735. (f) Tjaden, E. B.; Swenson, D. C.; Jordan, R. F. *Organometallics* **1995**, *14*, 371.

- (68) (a) Zhang, W.; Loebach, J. L.; Wilson, S. R.; Jacobsen, E. N. *J. Am. Chem. Soc.* **1990**, *112*, 2801. (b) Jacobsen, E. N.; Zhang, W.; Guler, M. L. *J. Am. Chem. Soc.* **1991**, *113*, 6703. (c) Zhang, W.; Jacobsen, E. N. *J. Org. Chem.* **1991**, *56*, 2296.

CHAPTER 2

EXPERIMENTAL METHODS

A. Instrument Setups

1. Nuclear Magnetic Resonance

^1H (300 MHz) NMR and ^{13}C (75 MHz) NMR spectra were recorded in a Varian Gemini-300 or a VXR-300 NMR spectrometers. The chemical shifts were referenced to the residual solvent peaks.

2. Mass Spectroscopy

Low resolution mass spectra were obtained on a Trio-1 VG Masslab Ltd. mass spectrometer, by using powder specimens.

3. Single Crystal X-ray Structure Determination

***N*-(4-tolyl)-acetamide.** A crystal of the compound was attached to a glass fiber and mounted on the Siemens Smart system for data collection at 133(2) K. An initial set of cell constants was calculated from reflections harvested from three sets of 15 frames. These are oriented such that orthogonal wedges of reciprocal space were surveyed. This produces orientation matrices determined from 31 reflections. Final cell constants are calculated from a set of strong reflections from the actual data collection. Four major swaths of frames were collected with 0.30° steps in ω .

The space group $P2_1/c$ (#14) was determined based on systematic absences and intensity statistics¹. A successful direct-methods solution was calculated which provided most nonhydrogen atoms from the E-map. Several full-matrix least squares / difference Fourier cycles were performed which located the remainder of the nonhydrogen atoms. All nonhydrogen atoms were refined with anisotropic displacement parameters. All hydrogen atoms were placed in ideal positions and refined as riding atoms with group isotropic displacement parameters.

One crystallographically unique molecule of the titled compound was found in the unit cell. Structure solution and refinement proceeded without any complications.

$\{\mu\text{-O-[2-(2,4,6-trimethylphenylimino)-pentane-4-one]}\}_2\text{TiCl}_4 \cdot 0.5\text{C}_4\text{H}_8\text{O}$. A crystal of the compound was attached to a glass fiber and mounted on the Siemens Smart system for data collection at 133(2) K. An initial set of cell constants was calculated from reflections harvested from three sets of 15 frames. These are oriented such that orthogonal wedges of reciprocal space were surveyed. This produces orientation matrices determined from 25 reflections.

Final cell constants are calculated from a set of strong reflections from the actual data collection. Four major swaths of frames were collected with 0.30° steps in ω .

The centrosymmetric space group *C2/c* (#15) was determined based on systematic absences and intensity statistics¹. The structure was solved by direct-methods in the *C2/c* space group and this structure solution provided most nonhydrogen atoms from the E-map. Several full-matrix least squares / difference Fourier cycles were performed which located the remainder of the nonhydrogen atoms. All nonhydrogen atoms were refined with anisotropic displacement parameters. All hydrogen atoms were placed in ideal positions and refined as riding atoms with group isotropic displacement parameters.

Two crystallographically independent molecules were found in the unit cell along with a tetrahydrofuran solvent molecule. The solvent was disordered and was refined over two sites with a relative ratio 0.7:0.3.

$\{\mu^2\text{-O,N-[2-(4-methylphenylimino)-pentane-4-one]\}_2\text{TiCl}_2$. A crystal of the compound was attached to a glass fiber and mounted on the Siemens Smart system for data collection at 133(2) K. An initial set of cell constants was calculated from reflections harvested from three sets of 15 frames. These are oriented such that orthogonal wedges of reciprocal space were surveyed. This produces orientation matrices determined from 58 reflections. Final cell constants are calculated from a set of strong reflections from the actual data collection. Four major swaths of frames were collected with 0.30° steps in ω .

The space group *Pbca* (#61) was determined based on systematic absences and intensity statistics¹. A successful direct-methods solution was calculated which provided most nonhydrogen atoms from the E-map. Several full-matrix least squares / difference Fourier cycles were performed which located the remainder of the nonhydrogen atoms. All nonhydrogen atoms were refined with anisotropic displacement parameters. All hydrogen atoms were

placed in ideal positions and refined as riding atoms with group isotropic displacement parameters.

One crystallographically unique molecule of the titled compound was found in the unit cell. Structure solution and refinement proceeded without any complications.

$\{\mu^2\text{-O,N-[2-(2,4,6-trimethylphenylimino)-pentane-4-one]}\}_2\text{TiCl}_2\cdot\text{CH}_2\text{Cl}_2$. A crystal of the compound was attached to a glass fiber and mounted on the Siemens Smart system for data collection at 133(2) K. An initial set of cell constants was calculated from reflections harvested from three sets of 15 frames. These are oriented such that orthogonal wedges of reciprocal space were surveyed. This produces orientation matrices determined from 43 reflections. Final cell constants were calculated from a set of strong reflections from the actual data collection. Four major swaths of frames were collected with 0.30° steps in ω .

The space group $P\bar{1}$ (#2) was determined based on systematic absences and intensity statistics¹. A successful direct-methods solution was calculated which provided most nonhydrogen atoms from the E-map. Several full-matrix least squares / difference Fourier cycles were performed which located the remainder of the nonhydrogen atoms. All nonhydrogen atoms were refined with anisotropic displacement parameters. All hydrogen atoms were placed in ideal positions and refined as riding atoms with group isotropic displacement parameters.

One crystallographically unique molecule of the title compound was found in the unit cell, along with a molecule of dichloromethane per formula unit. The chlorine atoms of the latter were disordered and each one was refined over two closely spaced sites in a 0.70:0.10 ratio.

$\{\mu^2\text{-O,N-[2-(4-methylphenylimino)-pentane-4-one]\}_2\text{ZrCl}_2$. A crystal of the compound was attached to a glass fiber and mounted on the Siemens Smart system for data collection at 133(2) K. An initial set of cell constants was calculated from reflections harvested from three sets of 15 frames. These are oriented such that orthogonal wedges of reciprocal space were surveyed. This produces orientation matrices determined from 92 reflections. Final cell constants were calculated from a set of strong reflections from the actual data collection. Four major swaths of frames were collected with 0.30° steps in ω .

The chiral space group $P3_121$ (#152) was determined based on systematic absences and intensity statistics¹. A successful Patterson-methods solution was calculated which provided most nonhydrogen atoms from the E-map. Several full-matrix least squares / difference Fourier cycles were performed which located the remainder of the nonhydrogen atoms. All nonhydrogen atoms were refined with anisotropic displacement parameters. All hydrogen atoms were placed in ideal positions and refined as riding atoms with group isotropic displacement parameters.

Structure solution and refinement proceeded without any complications. Only half of the title molecule was crystallographically unique.

B. Materials and Synthesis

1. Synthesis of Ketimine-Type Free Ligands

Materials and General considerations. 2,4-pentanedione (acac) as well as 2,4,6-trimethylaniline, *p*-t-butylaniline and 2,6-diisopropyl aniline were distilled and *p*-toluidine was sublimed (0.1mm/30°C) prior to use. The free ligands were prepared by modification of literature² methods. The synthesis is described in detail for 2-(4-methylphenylimino)-pentane-4-one, while for the remaining derivatives only their spectroscopic data are reported.

Synthesis of 2-(4-methylphenylimino)-pentane-4-one (MPPOH). Method A:

In a 500 ml round bottom flask equipped with a magnetic stirring bar and a Dean-Stark equipment, were placed 28.29gr (264 mmoles) of *p*-toluidine, 27.2 ml (264 mmoles) acetylacetone and 1% *p*-toluenesulfonic acid monohydrate (0.5 gr, 2.64 mmoles) in 300 ml toluene. The solution was refluxed for 2 to 3 hours until all the theoretically expected amount of H₂O was collected in the Dean-Stark equipment. The volume of the amber solution was reduced in a rotorvap and *n*-hexane was added resulting to the precipitation of nice pale yellow crystals. The product was isolated by suction filtration and dried under vacuum. Repeated recrystallization afforded an overall yield of 69.4% (34.7gr). (Mp 68-70 °C); ¹H NMR (CDCl₃); δ ppm: 1.93 (s, 3 H), 2.07 (s, 3 H), 2.31 (s, 3 H), 5.14 (s, 1 H), 6.97 (d, ³J_{H-H} = 8.2 Hz, 2 H), 7.11 (d, ³J_{H-H} = 8.2 Hz, 2 H), 12.38 (s, br, 1 H); ¹³C {¹H} NMR (CDCl₃); δ ppm: 19.74, 20.87, 29.097, 97.15, 124.82, 129.61, 135.46, 136.02, 160.65, 195.86.

Method B: The reaction was performed as described in method A, without the presence of the catalyst (*p*-toluenesulfonic acid monohydrate) and required

significantly longer refluxing times. Hindered anilines were not driven to completion even after prolonged reaction times (2 to 3 days). The overall yield, after recrystallization, was 73%.

Synthesis of 2-(2,4,6-trimethylphenylimino)-pentane-4-one (TMPPOH).

This ligand was synthesized by method A, giving an overall yield, after recrystallization, of 71%. An attempt to synthesize the titled compound by method B did not lead to reaction completion even after 48h of refluxing. (Mp 66-68 °C); ^1H NMR (CDCl_3); δ ppm: 1.60 (s, 3 H), 2.08 (s, 3 H), 2.13 (s, 6 H), 2.26 (s, 3 H), 5.17 (s, 1 H), 6.88 (s, 2 H), 11.82 (s, br, 1 H). ^{13}C $\{^1\text{H}\}$ NMR (CDCl_3); δ ppm : 18.12, 18.85, 20.90, 29.03, 95.60, 128.84, 133.83, 135.68, 136.99, 163.08, 195.84.

Synthesis of 2-(2,6-diisopropylphenylimino)-pentane-4-one (DIPPOH).

Method A was used to synthesize this ligand resulting to pale yellow crystals and 55.80% yield. (Mp 48-50 °C); ^1H NMR (CDCl_3); δ ppm : 1.12 (d, $^3J_{\text{H-H}} = 6.8$ Hz, 6 H), 1.19 (d, $^3J_{\text{H-H}} = 6.8$ Hz, 6 H), 1.61 (s, 3 H), 2.10 (s, 3 H), 3.00 (heptet, $^3J_{\text{H-H}} = 6.8$ Hz, 1 H), 5.18 (s, 1 H), 7.15 (d, $^3J_{\text{H-H}} = 7.6$ Hz, 2 H), 7.27 (t, $^3J_{\text{H-H}} = 7.6$ Hz, 1 H), 12.03 (s, br, 1 H). ^{13}C $\{^1\text{H}\}$ NMR (CDCl_3); δ ppm : 19.10, 22.61, 24.54, 28.43, 29.00, 95.54, 123.49, 128.20, 133.44, 146.22, 163.25, 195.84.

Synthesis of 2-(4-*t*-butylphenylimino)-pentane-4-one (BPPOH).

The synthesis of this ligand was initially performed following method B, without completion even after 48h of refluxing. Addition of 1% *p*-toluenesulfonic acid monohydrate (method A) to the same reaction mixture gave after 2.5h of refluxing and isolation, a combined yield of 66.15%. ^1H NMR (CDCl_3); δ ppm : 1.28 (s, 9 H), 1.96 (s, 3 H), 2.06 (s, 3 H), 5.14 (s, 1 H), 7.01 (d, $^3J_{\text{H-H}} = 8.4$ Hz, 2 H), 7.32 (d, $^3J_{\text{H-H}} = 8.4$ Hz, 2 H), 12.42 (s, br, 1 H). ^{13}C $\{^1\text{H}\}$ NMR (CDCl_3); δ ppm : 19.79, 29.06, 31.26, 34.38, 97.18, 124.31, 125.88, 135.94, 148.54, 160.53, 195.79.

2. Synthesis of Ketimine-Type Ligand Salts

Materials and General Considerations. *n*-BuLi was purchased from Aldrich and used as received, while MeLi was synthesized according to literature methods³. NaH, KH were purchased from Fluka and washed with hexanes prior use. The synthesis is described in detail for the lithium salt of 2-(4-methylphenylimino)-pentane-4-one, while for the remaining derivatives only their spectroscopy characteristics are reported.

Synthesis of Lithium Salt of 2-(4-methylphenylimino)-pentane-4-one (MPPOLi). In a 250 ml round bottom schlenk flask equipped with a magnetic stirring bar, 10gr (52.8 mmoles) of 2-(4-methylphenylimino)-pentane-4-one were suspended in 60 ml of dry pentane. 36 ml of *n*-BuLi (57.6 mmoles, 1.6 M in hexanes) were quickly transferred via a glass syringe into a medium sized, degassed schlenk tube. It was then slowly (over a period of 10 min) cannulated into the stirred suspension. When approximately half of the *n*-BuLi solution has been added, a slightly yellow clear solution formed, which by the end of the *n*-BuLi addition turned afforded a white solid. The reaction mixture was under stirring at ambient temperature for 4 hours, before reduction of half of the pentane volume took place. The product was isolated as white powder by filtration under nitrogen, washed with 2 × 30 ml cold dry pentane, and dried under vacuum. The combined yellow filtrates were added to the mother liquor and a second amount of product was eventually isolated after reduction of the solution's volume and cooling at -80 °C for an hour. The overall yield was (9.84gr) 95.4%. (Mp 229-230 °C); ¹H NMR (CDCl₃); δ ppm : 1.34 (s, 3 H), 1.65 (s, 3 H), 2.25 (s, 3 H), 4.72 (s, 1 H), 6.59 (d, ³J_{H-H} = 7.9 Hz, 2 H), 6.99 (d, ³J_{H-H} = 7.9 Hz, 2 H). ¹³C {¹H} NMR (CDCl₃); δ ppm : 20.80, 22.05, 27.83, 98.70, 121.77, 129.16, 131.82, 149.34, 168.01, 175.59.

Alternatively the product was synthesized by the same procedure using MeLi (0.86M in ether) instead of *n*-BuLi affording approximately the same yield.

Synthesis of Lithium Salt of 2-(2,4,6-trimethylphenylimino)-pentane-4-one (TMPPOLi). This salt was synthesized by following the same procedure giving a yield of 91.30%. (Mp 252-254 °C); ¹H NMR (CDCl₃); δ ppm : 1.21 (s, 3 H), 1.45 (s, 3 H), 1.87 (s, 6 H), 2.18 (s, 3 H), 4.74 (s, 1 H), 6.74 (s, 2 H). ¹³C {¹H} NMR (CDCl₃); δ ppm : 17.72, 20.76, 21.64, 27.59, 98.21, 128.20, 128.61, 131.48, 146.61, 168.12, 175.41.

Synthesis of the Sodium salt of 2-(4-methylphenylimino)-pentane-4-one (MPPONa). In a medium sized, degassed schlenk tube, equipped with a magnetic stirring bar, 0.46gr (19.0 mmoles) of NaH (washed with hexanes prior to use) were suspended in 10ml dry THF. 3gr (15.8 mmoles) of 2-(4-methylphenylimino)-pentane-4-one were placed in a medium sized, degassed schlenk tube, and dissolved in the least necessary amount of dry THF (approximately 6ml). The yellow solution was then slowly added via cannula to the chilled, at -80 °C, gray suspension. Evolution of H₂ was immediately observed resulting in an almost clear yellow solution at the end of the addition. The mixture was stirred under nitrogen atmosphere at -80 °C for an additional 10 minutes and then allowed to warm to room temperature, where stirring continued for an additional 3 hours. The excess of NaH was removed by filtration via cannula and the filtrate was treated under vacuum to give a yellow-orange gel-like residue. Anhydrous pentane was subsequently used to dissolve the gel-like residue from which eventually nice pale yellow crystals were obtained after chilling at -80 °C overnight. Filtration under nitrogen atmosphere was the procedure used to isolate the crystalline product, which was then dried under vacuum. By the same process a second amount of product was isolated resulting to an overall yield after recrystallization of (2.60gr) 77.66%. (Mp 255-257 °C) ¹H

NMR (C_6D_6); δ ppm : 1.60 (s, br, 3 H), 2.05 (s, br, 3 H), 2.09 (s, br, 3 H), 4.76 (s, br, 1 H), 6.43 (s, br, 2 H), 6.85 (d, $^3J_{H-H} = 7.5$ Hz, 2 H).

An attempt to synthesize the product by a literature method⁴ using Na metal instead of NaH had no success according to NMR characterization.

3. Synthesis of 2-(dimethylamino)-4-(arylimino)-pent-2-ene Compounds

Synthesis of 2-(dimethylamino)-4-(4-methylphenylimino)-pent-2-ene. A medium sized, degassed schlenk tube, equipped with a magnetic stirring bar, was charged with 29.45 ml (\approx 0.66gr, 2.95 mmoles) of with tetrakis dimethylaminotitanium, $Ti[NMe_2]_4$, (standard solution 0.1 M in anhydrous toluene). 1.11gr (5.89 mmoles) of 2-(4-methylphenylimino)-pentane-4-one were added to a medium sized degassed schlenk tube, and then were dissolved in 3ml of dry toluene giving a slightly yellow clear solution which was subsequently transferred via cannula over a period of 10 minutes to the bright yellow $Ti(NMe_2)_4$ solution. A pronounced color change to bright red was immediately observed with the addition of the first drops of the ligand solution. The reaction mixture was then refluxed for 24 hours under nitrogen atmosphere. Formation of small amount of white slurry was observed, which was removed by filtration via cannula. The yellow filtrate was next evaporated to dryness under vacuum and the resulting orange solid was redissolved in 5 ml of dry hexanes, from which source nice needle orange crystals were grown after allowing the solution to stand at -80 °C for 48 hours. The product was finally isolated by filtration under nitrogen atmosphere, resulting to a yield after recrystallization of 89.5% (0.57gr). (Mp 35–36 °C); 1H NMR (C_6D_6); δ ppm : 1.92 (s, 3 H), 2.19 (s, 3 H), 2.29 (s, 6 H), 2.58 (s, 3 H), 4.76 (s, 1 H), 6.89 (d, $^3J_{H-H} = 7.9$ Hz, 2 H), 7.07 (d,

$^3J_{\text{H-H}} = 7.9$ Hz, 2 H). ^{13}C { ^1H } NMR (C_6D_6); δ ppm : 16.77, 20.90, 22.99, 39.12, 98.05, 120.74, 129.66, 130.58, 151.79, 154.58, 164.34. Elemental analysis; Calculated for $\text{C}_{14}\text{H}_{20}\text{N}_2$: C, 77.73; H, 9.32; N, 12.94. Found : C, 77.39; H, 9.37; N, 12.75.

Synthesis of 2-dimethylamino-4-(4-*t*-butylphenylimino)-2-pentane. The synthesis of this ligand was accomplished by the same method giving a crude ^1H NMR yield of 82% in the first 5 hours of refluxing; ^1H NMR (C_6D_6); δ ppm : 1.29 (s, 9 H), 1.92 (s, 3 H), 2.59 (s, 3 H), 4.77 (s, 1 H), 6.95 (d, $^3J_{\text{H-H}} = 8.7$ Hz, 2 H), 7.32 (d, $^3J_{\text{H-H}} = 8.7$ Hz, 2 H).

4. Synthesis of Titanium and Zirconium Starting Materials

Synthesis of Tetrachlorobis(tetrahydrofuran)titanium, $\text{TiCl}_4(\text{THF})_2$ ⁵. A 250 ml flamed dried schlenk flask equipped with a magnetic stirring bar was charged with 12.7gr (67 mmoles) TiCl_4 (distilled prior to use at 5 Torr, 30°C) dissolved in 100 ml dry CH_2Cl_2 . Anhydrous THF (19.32 gr, 268 mmoles) was added dropwise through an addition funnel, at room temperature and under nitrogen atmosphere. An exothermic reaction took place resulting in a clear yellow solution that was stirred at ambient temperature for approximately 30 min. During this time, formation of bright yellow solid was observed. 100 ml of dry pentane was added to the solution followed by subsequent chilling at -25°C (acetonitrile and liquid nitrogen bath) for 3 hours. The yellow precipitate was isolated by filtration under nitrogen atmosphere, washed with 3×60 ml dry pentane, and dried under vacuum. A second crop of the solid was isolated from the combined filtrates by the same procedure. The overall yield was 84.12% (19.66gr). (Mp $128\text{--}130^\circ\text{C}$).

Synthesis of Tetrachlorobis(tetrahydrofuran)zirconium, $\text{ZrCl}_4(\text{THF})_2$ ⁶. In a 250 ml flamed dried schlenk flask equipped with a magnetic stirring bar, 11.95gr

(51 mmoles) ZrCl_4 (sublimed⁷ prior to use at 130 °C under vacuum) were suspended in 150 ml dry CH_2Cl_2 . Anhydrous THF (7.56gr, 105 mmoles) was added dropwise to the mixture through an addition funnel, at room temperature and under nitrogen atmosphere. An exothermic reaction was observed resulting in a colorless solution at the end of the addition. If the solvent is not extensively dry, the color of the solution turns brown. In addition, if impure ZrCl_4 is used insoluble particles are suspended over the solution. To avoid this difficulty, the solution was filtered via cannula into a 500 ml flamed dried schlenk flask. 125 ml dry pentane was added to the solution, which is subsequently chilled at -80 °C for 3 hours. The white crystalline solid was isolated by filtration under nitrogen atmosphere, washed with 3×30 ml dry pentane, and dried under vacuum. The pentane washes were added to the mother liquor, and followed by subsequent volume reduction and cooling at -80 °C for 3 hours, resulted to a second crop of product. The combined yield was 84.98% (16.35gr). (Mp 170–171 °C (decomposition))

Synthesis of Tetrakisdimethylaminotitanium, $\text{Ti}[\text{NMe}_2]_4$ ⁸. In a 500 ml flamed dried schlenk flask, equipped with a magnetic stirring bar, 14.26gr (316.40 mmoles) dimethylamine were condensed and cooled to -80 °C. 127 ml (20.33gr, 317.50 mmoles) *n*-BuLi (2.5M in hexanes) were quickly transferred via a glass syringe into a schlenk tube, from where they were slowly cannulated to the cooled dimethylamine. The reaction mixture remained under stirring for 1 hour and during that time, the products were allowed to attain room temperature. 15gr (79.10 mmoles) of TiCl_4 (distilled prior to use at 5 Torr, 30°C) in 100 ml dry benzene were subsequently added at 0 °C to the lithium salt solution over a period of 30 minutes with vigorous stirring. A brown intermediate product was precipitated in the initial stages of the reaction and the mixture, following completion of the addition of the TiCl_4 , was refluxed for approximately 2 hours,

until the intermediate product disappeared and a dark red solution remained over a white–yellow precipitate of lithium salts. At this point the unwanted LiCl salt was removed by filtration under nitrogen atmosphere and washed twice with 20 ml dry benzene. The filtrates were collected and added to the mother liquor, and then the solvent was evaporated under reduced pressure to generate a viscous brown solution. Distillation of this brown solution at 50 °C / 0.05 mm Hg gave Ti(NMe₂)₄ as a viscous, intense orange liquid. The yield of the reaction after distillation was 83.20% (14.74gr). ¹H NMR (C₆D₆); δ ppm : 3.11 (s, 24 H). ¹³C {¹H} NMR (C₆D₆); δ ppm : 43.99 .

5. Synthesis of Non–chelated Titanium Complexes

Synthesis of $\{\mu\text{-O-[2-(4-methylphenylimino)-pentane-4-one]}\}_2\text{TiCl}_4$, (MPPOH)₂TiCl₄. In a medium sized, degassed schlenk tube, equipped with a magnetic stirring bar, 0.7gr (2.10 mmoles) of TiCl₄(THF)₂ were dissolved in the least necessary amount (≈25 ml) of anhydrous THF, giving a clear, bright yellow solution. 0.80gr (4.23 mmoles) of 2-(4-methylphenylimino)-pentane-4-one were added to a medium sized, degassed schlenk tube, and then were dissolved in 4 ml of dry THF, resulting to a slightly yellow (almost colorless) clear solution, which was subsequently transferred via cannula over a period of 10 minutes to the TiCl₄(THF)₂ solution. A conspicuous color change to bright red was immediately observed, resulting eventually in a dark red, clear solution at the end of the addition. The reaction mixture was then stirred for 2 hours under nitrogen atmosphere, although precipitation of the product as dark red-purple solid was observed after the first 30 minutes of stirring. The solid was then filtrated via cannula, washed twice with 7 ml of dry pentane and finally dried under vacuum. The filtrates were added to the red-orange mother liquor, the volume was

reduced to half, and the resulting solution was placed at $-80\text{ }^{\circ}\text{C}$ for 24 hours. A second amount of product was eventually isolated by filtration under nitrogen atmosphere. The combined yield was 89.5% (0.57gr). (Mp $155\text{ }^{\circ}\text{C}$ (decomposition)); ^1H NMR (CDCl_3); δ ppm : 2.13 (s, 3 H), 2.33 (s, 3 H), 2.69 (s, 3 H), 5.35 (s, 1 H), 7.13 (d, $^3J_{\text{H-H}}=8.8\text{ Hz}$, 2 H), 7.20 (d, $^3J_{\text{H-H}}=8.8\text{ Hz}$, 2 H), 12.62 (s, 1 H).

Synthesis of $\{\mu\text{-O-[2-(2,4,6-trimethylphenylimino)-pentane-4-one]\}_2\text{TiCl}_4$, (TMPPOH) $_2\text{TiCl}_4$. The synthesis of this complex was accomplished by following the same procedure resulting in an overall yield of 91.76%. (Mp $130\text{ }^{\circ}\text{C}$ (decomposition)); ^1H NMR (CDCl_3); δ ppm : 1.84 (s, 3 H), 2.19 (s, 6 H), 2.24 (s, 3 H), 2.65 (s, 3 H), 5.33 (s, 1 H), 6.85 (s, 2 H), 12.12 (s, 1 H). ^{13}C $\{^1\text{H}\}$ NMR (CDCl_3); δ ppm : 18.36, 20.44, 20.98, 26.00, 97.83, 129.28, 132.26, 134.50, 138.72, 172.18, 191.24.

Synthesis of $\{\mu\text{-O-[2-(4-}t\text{-butylphenylimino)-pentane-4-one]\}_2\text{TiCl}_4$, (BPPOH) $_2\text{TiCl}_4$. This complex was prepared by the same procedure giving an overall yield of 88.94%. (Mp $160\text{ }^{\circ}\text{C}$ (decomposition)); ^1H NMR (CDCl_3); δ ppm : 1.28 (s, 9 H), 2.14 (s, 3 H), 2.70 (s, 3 H), 5.35 (s, 1 H), 7.26 (d, $^3J_{\text{H-H}}=8.7\text{ Hz}$, 2 H), 7.37 (d, $^3J_{\text{H-H}}=8.7\text{ Hz}$, 2 H), 12.60 (s, 1 H).

6. Synthesis of Chelated Titanium and Zirconium Complexes by Reaction with the β -Ketimine Lithium Salts

Synthesis of $\{\mu^2\text{-O,N-[2-(4-methylphenylimino)-pentane-4-one]\}_2\text{TiCl}_2$, (MPPO) $_2\text{TiCl}_2$. In a medium sized, flamed dry, degassed schlenk tube, equipped with a magnetic stirring bar, 0.50gr (1.49 mmoles) of $\text{TiCl}_4(\text{THF})_2$ were dissolved in the least necessary amount ($\cong 20\text{ ml}$) of anhydrous CH_2Cl_2 (dried over basic alumina prior use) — alternatively this synthesis can be also successfully

accomplished in dry THF or toluene — giving a clear, bright yellow solution. 0.58gr (2.99 mmoles) of the lithium salt of 2-(4-methylphenylimino)-pentane-4-one were added to a medium sized, flamed dry, degassed schlenk tube, and then were dissolved in 5 ml of dry CH₂Cl₂, resulting to a colorless solution, which was subsequently transferred via cannula over a period of 10 minutes to the TiCl₄(THF)₂ solution. A conspicuous color change to bright red was immediately occurred, resulting eventually in a dark red, clear solution at the end of the addition. The reaction mixture was then stirred for an additional 2 hours under nitrogen atmosphere. The LiCl salt was removed by filtration via cannula, and washed with 5ml of dry pentane (dried over basic alumina prior to use). The volume of the filtrate was reduced to one third and the remaining solution was layered with dry pentane. Red crystals were grown by allowing the solution to stand at -80 °C for 24 hours. The product was isolated by filtration. The filtrate was recollected and by following the same procedure a second amount of the crystalline product was recovered. The combined yield was (0.59gr) 79.7%. (Mp 163–165 °C(decomposition)); ¹H NMR (CDCl₃); δ ppm : 1.33 (s, 3 H), 1.66 (s, 3 H), 2.31 (s, 3 H), 5.31 (s, 1 H), 6.48 (d, ³J_{H-H} =8.1 Hz, 1 H), 7.02 (d, ³J_{H-H} =7.5 Hz, 1 H), 7.17 (two d, ³J_{H-H} =7.5 Hz, 2 H). ¹³C {¹H} NMR (CDCl₃); δ ppm : 20.82, 22.04, 24.41, 109.51, 121.78, 125.70, 128.55, 129.40, 135.07, 148.79, 169.76, 175.42.

Alternatively the title complex was successfully synthesized using the corresponding sodium salt in good yields as indicated by NMR characterization.

Another synthetic approach includes the reaction between the corresponding non-chelate complex with freshly distilled triethylamine (distilled twice over CaH₂ and LiAlH₄) utilized in 10% excess. The product was identified to be the chelate complex by NMR spectroscopy.

Sy

on

the

128

H).

1 H

128

amb

form

by i

utiliz

spe

Syn

(MP

givin

^oC(d

3 H)

20.8

173.

ambi

form

treat

in 10^o

Synth

one}}

Synthesis of $\{\mu^2\text{-O,N-[2-(2,4,6-trimethylphenylimino)-pentane-4-one]}\}_2\text{TiCl}_2$, (TMPPO) $_2\text{TiCl}_2$. The synthesis of this complex was accomplished by the same method as described above giving a combined yield of 70.27%. (Mp 125–126 °C(decomposition)); ^1H NMR (CDCl_3); δ ppm : 1.69 (s, 3 H), 1.85 (s, 3 H), 2.06 (s, 3 H), 2.24 (s, 3 H), 2.27 (s, 3 H), 5.80 (s, 1 H), 6.77 (s, 1 H), 6.86 (s, 1 H). ^{13}C $\{^1\text{H}\}$ NMR (CDCl_3); δ ppm : 18.67, 19.73, 20.94, 22.61, 23.44, 109.65, 128.15, 128.98, 129.77, 132.40, 135.42, 146.51, 172.16, 176.57.

A different synthetic route to the title complex involves the reaction at ambient temperature of the starting metal reagent, $\text{TiCl}_4(\text{THF})_2$, with the anionic form of the free ligand, 2-(2,4,6-trimethylphenylimino)-pentane-4-one, formed by its treatment with freshly distilled Et_3N (distilled twice over CaH_2 and LiAlH_4) utilized in 10% excess. The identity of the product was confirmed by NMR spectroscopy.

Synthesis of $\{\mu^2\text{-O,N-[2-(4-methylphenylimino)-pentane-4-one]}\}_2\text{ZrCl}_2$, (MPPO) $_2\text{ZrCl}_2$. This complex was synthesized by using the same procedure giving nice pale yellow crystals in a 78.5 % yield. (Mp 205–207 °C(decomposition)); ^1H NMR (CDCl_3); δ ppm : 1.33 (s, 3 H), 1.69 (s, 3 H), 2.32 (s, 3 H), 5.22 (s, 1 H), 6.51 (br, 1 H), 7.12 (br, 3 H). ^{13}C $\{^1\text{H}\}$ NMR (CDCl_3); δ ppm : 20.84, 22.78, 24.52, 106.28, 122.84, 125.49, 129.40, 129.92, 135.16, 145.82, 173.09, 174.85.

A different synthetic route of the title complex involves the reaction at ambient temperature of the starting metal reagent, $\text{ZrCl}_4(\text{THF})_2$, with the anionic form of the free ligand, 2-(4-methylphenylimino)-pentane-4-one, formed by its treatment with freshly distilled Et_3N (distilled twice over CaH_2 and LiAlH_4) utilized in 10% excess. The identity of the product was confirmed by NMR spectroscopy.

Synthesis of $\{\mu^2\text{-O,N-[2-(2,4,6-trimethylphenylimino)-pentane-4-one]}\}_2\text{ZrCl}_2$, (TMPPO) $_2\text{ZrCl}_2$. The synthesis of this complex was accomplished

by utilizing the same general method giving a white powder as a product in 78.54% yield. (Mp 195–198 °C(decomposition)). ¹H NMR (CDCl₃); δ ppm : 1.68 (s, 3 H), 1.93 (s, 3 H), 2.19 (s, 6 H), 2.24 (s, 3 H), 5.58 (s, 1 H), 6.85 (br, 2 H). ¹³C {¹H} NMR (CDCl₃); δ ppm : 18.10, 18.89, 20.90, 23.55, 106.39, 129.34, 134.30, 135.50, 143.59, 174.88, 175.41.

LIST OF REFERENCES

- (1) SHELXTL-PLUS V5.0, Siemens Industrial Automation, Inc., Madison, WI.
- (2) (a) Everett, G. W.; Holm, R. H. *J. Am. Chem. Soc.* **1965**, *87*, 2117. (b) Martin, D. F.; Janusonis, G. A.; Martin, B. B. *J. Chem. Soc.* **1961**, *83*, 73.
- (3) (a) Bergbreiter, D. E.; Pendergrass, E. *J. Org. Chem.* **1981**, *46*, 219. (b) Furniss, B. S.; Hannaford, A. J.; Smith, P. W. G.; Tatchell, A. R. in *Vogel's Textbook of Practical Organic Chemistry*; Longman Group UK Limited 1989, p.444.
- (4) Thiele, K. H.; Scholz, A.; Scholz, J.; Böhme, U.; Kempe, R.; Sieler J. *Z.Naturforsch.* **1993**, *48b*, 1753.
- (5) Manzer, L. E. *Inorg.Syntheses* **1982**, *21*, 135.
- (6) Manzer, L. E. *Inorg.Syntheses* **1982**, *21*, 136.
- (7) Hummers, W. S.; Tyree, S. Y. Jr; Yolles, S. *Inorg.Syntheses* **1953**, *4*, 121.
- (8) Bradley, D. C.; Thomas, I. M. *J. Chem. Soc.* **1960**, 3857.

CHAPTER 3

SYNTHESIS AND CHARACTERIZATION OF METAL DICHLORIDES STABILIZED BY β -KETIMINE LIGANDS

A. Introduction

Cationic d^0 $Cp_2M(R^+)$ complexes, with M a group IV metal, have been utilized in a variety of catalytic processes, including Ziegler–Natta olefin polymerization¹. Their success in olefin activation is attributed to a variety of factors, including the high degree of electrophilicity displayed by the metals, the reactivity of the M — C bonds and the bent metallocene structure. All these characteristics are derived from the synergistic interplay of structural and electronic properties. Hence, ideal catalytic systems should comprise from

flexible subunits that enable tuning of both these parameters via facile chemical sequences.

Traditionally, the design of new catalytic systems targets organometallic complexes with various non-group IV metals or non-Cp ligand environments. Apart from the limited success that lanthanides² had in olefin polymerization, group IV metals continued to provide the most successful class of Ziegler–Natta catalysts! Hence, the design of new ligands surrounding group IV metal centers, seems the most attractive approach for the synthesis of improved catalytic systems.

The general synthetic sequence of such systems initially involves the generation of neutral metal dichlorides, which are subsequently transformed to the corresponding dialkyl derivatives and finally combined with strong boron-based Lewis acid co-catalysts. This process results in the generation of catalytically active cationic alkyl species. The supporting ligands utilized in initial attempts were mainly N₄-macrocycles³ and Schiff base type ligands⁴. The former class of compounds results in metal complexes where the labile groups possess the desirable *cis* orientation, which places the olefin substrate in close contact with the inserting alkyl group. This effect is attributed to the large size of the metal ions, which do not fit inside the macrocycle pocket and adopt an out of plane arrangement. The displacement of the metal from the macrocycle plane is the drawback of this design since the steric environment of the ligand would be a non-factor in the catalytic process.

Tetradentate Schiff base ligands, synthesized by the condensation of 2,4-pentanedione derivatives and diamines, provided a promising alternative because they could be easily synthesized and modified sterically and electronically⁵. However, the resulting complexes possessed coordination geometries with the labile ligands mainly *trans* to each other, rendering these

systems catalytically inactive. In addition the rigid core of the ligand, imposed by the interconnection of the 2,4-pentanedione units by the diamine, enforces its almost planar arrangement in the basal coordination plane of the metal, and therefore its steric environment would have limited impact to the approaching substrates.

Our strategy to overcome these obstacles targets the synthesis of chelate group IV metal complexes with ancillary ligands of the β -ketimine type. An infinite number of such ligands are easily available by the facile condensation reaction of 2,4-pentanedione with various amines and anilines. We have chosen to attach aryl units to the imino group of the chelates, since they enable facile electronic and stereochemical tuning by the aromatic π -cloud and by the use of bulky substituents in the aryl core respectively.

In the proceeding sections, the synthesis and structural characterization of a number of such complexes is described. Our initial results indicate that indeed the desired chelate complexes can be synthesized via a variety of routes and that such compounds possess, in addition to the advantages of Schiff bases, the benefits of more flexible chelate cores that create reaction centers within tunable stereochemical environments.

B. Results and Discussion

1. Synthesis and Characterization of β -ketimine Free Ligands

The condensation reaction of 2,4-pentanedione with primary anilines in refluxing toluene, as shown in *Figure 1*, was the effective synthetic route to the desired β -ketimine ligands⁶. The reaction proceeded via nucleophilic attack of the aniline on the diketone substrate with the simultaneous release of an equimolar amount of H₂O. The latter was azeotropically removed from the reaction medium with the aid of a Dean-Stark trap in order to prevent product hydrolysis. Apart from toluidene which reacted with the diketone without any problems, *ortho* and *para* substituted anilines (*Figure 1*) required the presence of an acid catalyst for successful completion of the reaction. Small amounts of *p*-toluenesulfonic acid monohydrate (typically 1%) and reaction times ranging from two to four hours were the optimum conditions for large yields of the desired ketoimines. Heating the reaction mixture for prolonged times in the presence of the acid catalyst, irrespective of the aniline utilized, resulted in large quantities of byproducts along with the desired β -ketimine ligands. These were identified as the amide and allene of the corresponding substituted anilines, and were characterized by NMR, MS spectroscopy, and in one case (*N*-(4-tolyl)-acetamide) by single crystal X-ray studies. The latter byproduct, as well as the corresponding β -ketoimine, were isolated in pure form from the reaction mixture. *N*-(4-tolyl)-acetamide precipitated first as an off-white powder from a concentrated toluene solution layered with hexane, followed by the crystallization of the 2-(4-methylphenylimino)-pentane-4-one from the same solution. The ¹H NMR spectra of the *N*-(4-tolyl)-acetamide, displayed two lines at 2.10 and 2.27 ppm assigned to the keto and the tolyl methyl groups respectively, two doublets

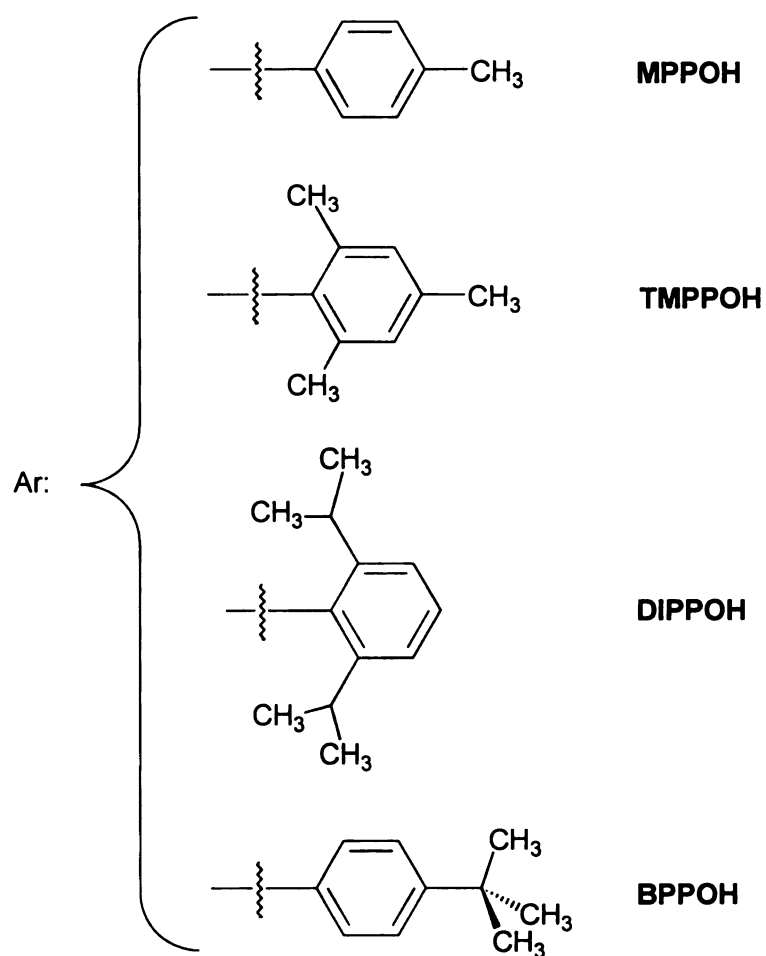
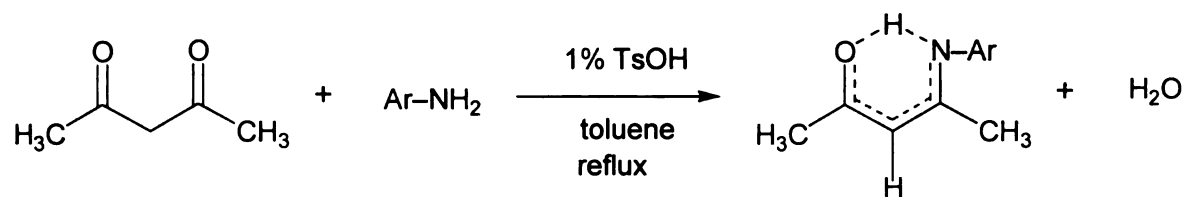


Figure 1. General synthetic scheme of β -ketimine ligands.

in the aromatic region at 7.07 and 7.36 ppm, and a broad peak at 7.81 ppm due to the characteristic –NH group. The ^{13}C NMR was as expected, displaying two peaks in the 20 — 24 ppm region for the methyl groups, four lines assigned to the aromatic carbons between 120 and 135 ppm and the carbonyl resonance at 168 ppm. Colorless crystals of the compound were grown from a diethylether solution and a single crystal X–ray analysis was undertaken. The detailed crystallographic data are summarized in Table 1, and an ORTEP representation of the compound is shown in *Figure 2*. Inspection of Table 2, where selected bond distances and angles are gathered, indicates that the compound possesses metric parameters typical of those displayed by other amides⁷.

The second byproduct was not isolated, but its formation was postulated by mass and ^1H NMR spectroscopies. Mass spectroscopy gave a molecular ion with a mass of 278, corresponding to the molecular formula $\text{C}_{19}\text{H}_{22}\text{N}_2$. The proton NMR spectra assignments were performed in the spectrum of the crude reaction mixture, where the $\text{C}_{19}\text{H}_{22}\text{N}_2$ byproduct was present along with the amide and the β –ketimine. The spectra of the later two compounds were known since both have been isolated in pure form, and therefore the remaining peaks — two singlets at 1.25 and 2.24 ppm and two doublets at 6.96 ($^3J_{\text{H-H}} = 8.3$ Hz) and 6.60 ($^3J_{\text{H-H}} = 8.3$ Hz) with a relative ratio of 3:3:2:2 respectively— were attributed to the former. Initially this byproduct was thought to be the corresponding β –diimine. The ^1H –NMR spectra of this compound however, which has been synthesized in a pure form by an alternative synthetic methodology, does not agree with the peaks attributed to the $\text{C}_{19}\text{H}_{22}\text{N}_2$ product. An alternative structure is the corresponding allene, since both the ^1H –NMR and the mass spectroscopy data (*Figure 3*) were satisfied by such formulation. The formation, however, of an allene byproduct seems unlikely due to thermodynamic reasons. *Figure 4* depicts a proposed mechanism of the reaction that accounts for the isolation and detection of the β –

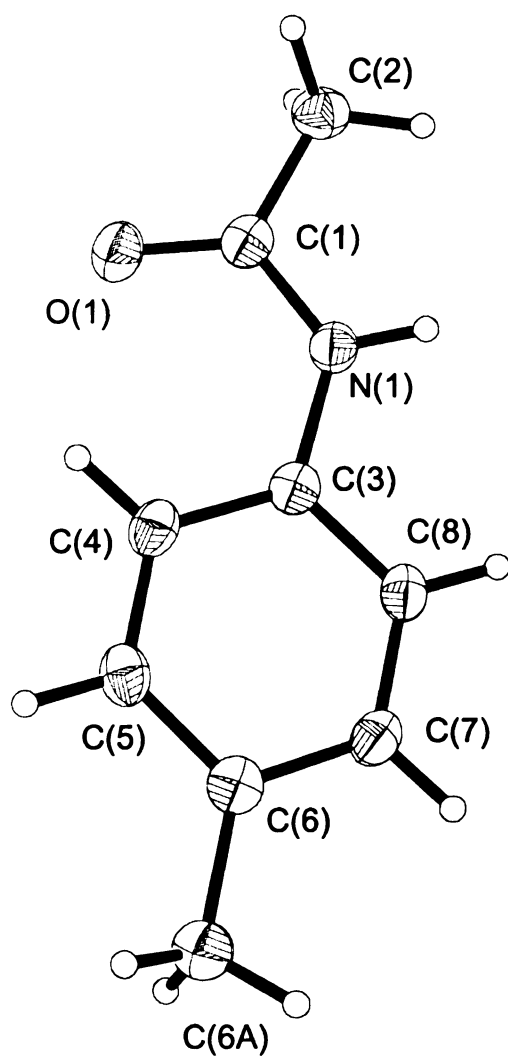


Figure 2. ORTEP representation (at 50% probability) of *N*-(4-tolyl)acetamide.

Table 1. Crystallographic Data for *N*-tolylmethanamide, and (TMPPOH)₂TiCl₄.

	<i>N</i> -(4-tolyl)-acetamide	(TMPPOH) ₂ TiCl ₄
	(A) Crystal Parameters	
formula	C ₁₈ H ₂₂ N ₂ O ₂	C ₃₂ H ₄₆ Cl ₄ N ₂ O ₃ Ti ₂
crystal habit, color	block, white	plate, orange
FW	298.38	696.41
crystal size (mm ³)	0.50 × 0.34 × 0.23	0.55 × 0.31 × 0.04
crystal system	monoclinic	monoclinic
space group	<i>P</i> 2 ₁ / <i>c</i>	<i>C</i> 2/ <i>c</i>
<i>a</i> (Å)	11.738(2)	15.260(3)
<i>b</i> (Å)	9.556(2)	16.724(3)
<i>c</i> (Å)	7.473(1)	27.774(6)
α (deg)	90	90
β (deg)	106.44(3)	90.46(3)
γ (deg)	90	90
<i>V</i> (Å ³)	804.0(3)	7088(3)
<i>Z</i>	2	4
<i>d</i> _{calc} (Mg/m ³)	1.232	1.305
<i>F</i> (000)	320	2928
μ(Mo Kα), mm ⁻¹	0.081	0.576
	(B) Data Collection	
2θ _{max} (deg)	50.0	50.0
	-13 ≤ <i>h</i> ≤ 13	-19 ≤ <i>h</i> ≤ 19
index ranges	-11 ≤ <i>k</i> ≤ 11	-21 ≤ <i>k</i> ≤ 19
	-8 ≤ <i>l</i> ≤ 8	-35 ≤ <i>l</i> ≤ 35
temperature / K	133(2)	133(2)
reflections collected	7418	18779
independent reflections	1417	6162
R(int) (%)	4.46	9.1
	(C) Refinement	
Refinement method	Full-matrix least-squares on <i>F</i> ²	Full-matrix least-squares on <i>F</i> ²
R indices (<i>I</i> > 2σ(<i>I</i>))	R1 = 0.0398 WR2 = 0.1048	R1 = 0.0788 WR2 = 0.1083
R indices all data	R1 = 0.0463 WR2 = 0.1087	R1 = 0.1636 WR2 = 0.1313
Δρ (e ⁻ /Å ³)	0.212	0.300
GOF	1.034	1.052

Table 2. Selected Bond Distances and Angles of Compound *N*-(4-tolyl)-acetamide.

<i>Atom 1</i>	<i>Atom 2</i>		<i>Distance / Å</i>
O(1)	C(1)		1.238(2)
C(1)	N(1)		1.358(2)
C(1)	C(2)		1.506(2)
N(1)	C(3)		1.421(2)
C(3)	C(4)		1.403(2)
C(4)	C(5)		1.392(2)
C(5)	C(6)		1.399(2)
C(6)	C(7)		1.398(2)
C(7)	C(8)		1.390(2)
C(8)	C(3)		1.398(2)
C(6)	C(6A)		1.513(2)

<i>Atom 1</i>	<i>Atom 2</i>	<i>Atom 3</i>	<i>Angle / °</i>
O(1)	C(1)	N(1)	123.0(1)
O(1)	C(1)	C(2)	121.7(1)
N(1)	C(1)	C(2)	115.3(1)
C(1)	N(1)	C(3)	128.2(1)
C(7)	C(6)	C(6A)	120.9(1)

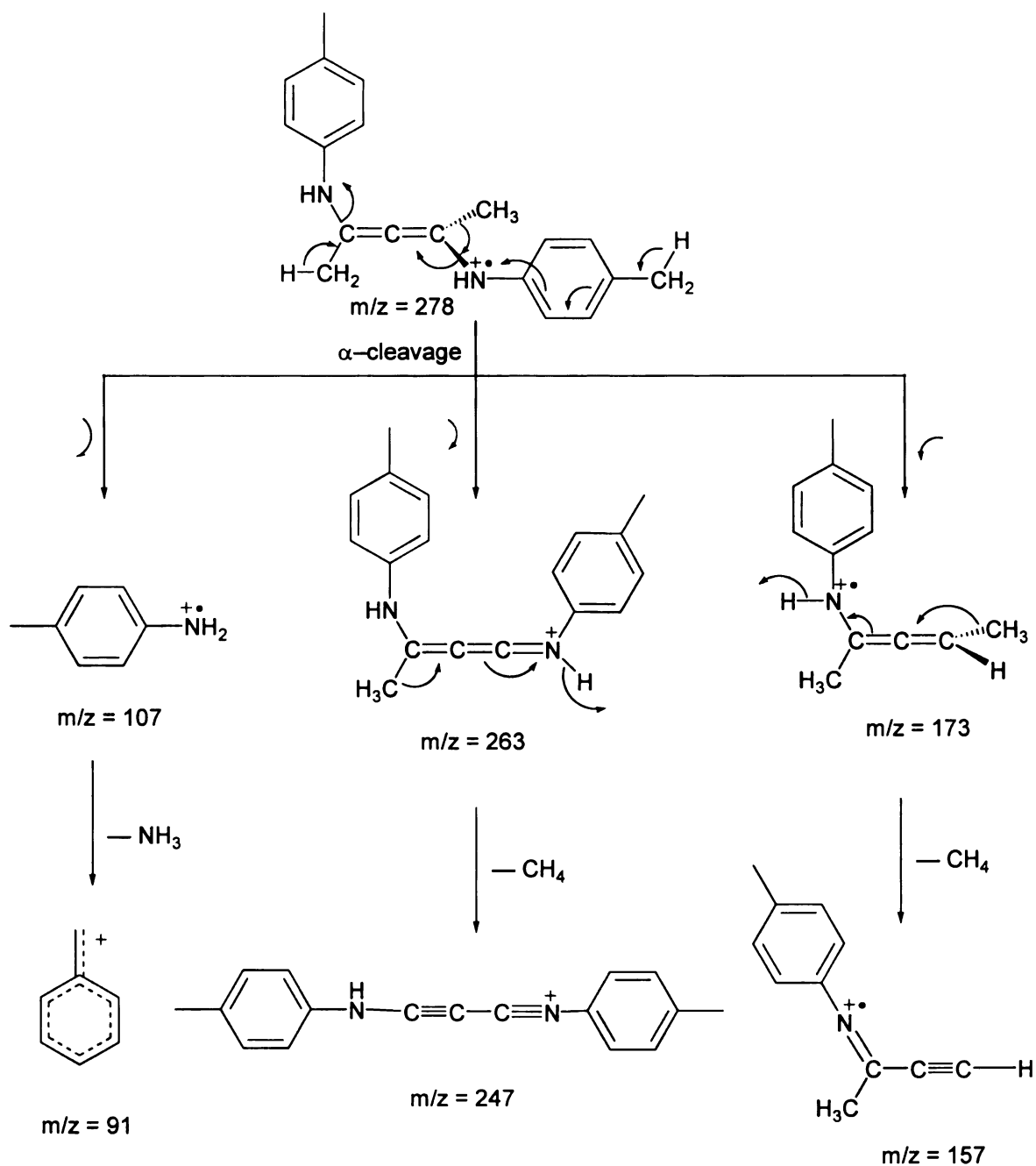


Figure 3. Fragmentation mechanism and assignment of the main MS peaks of the allene.

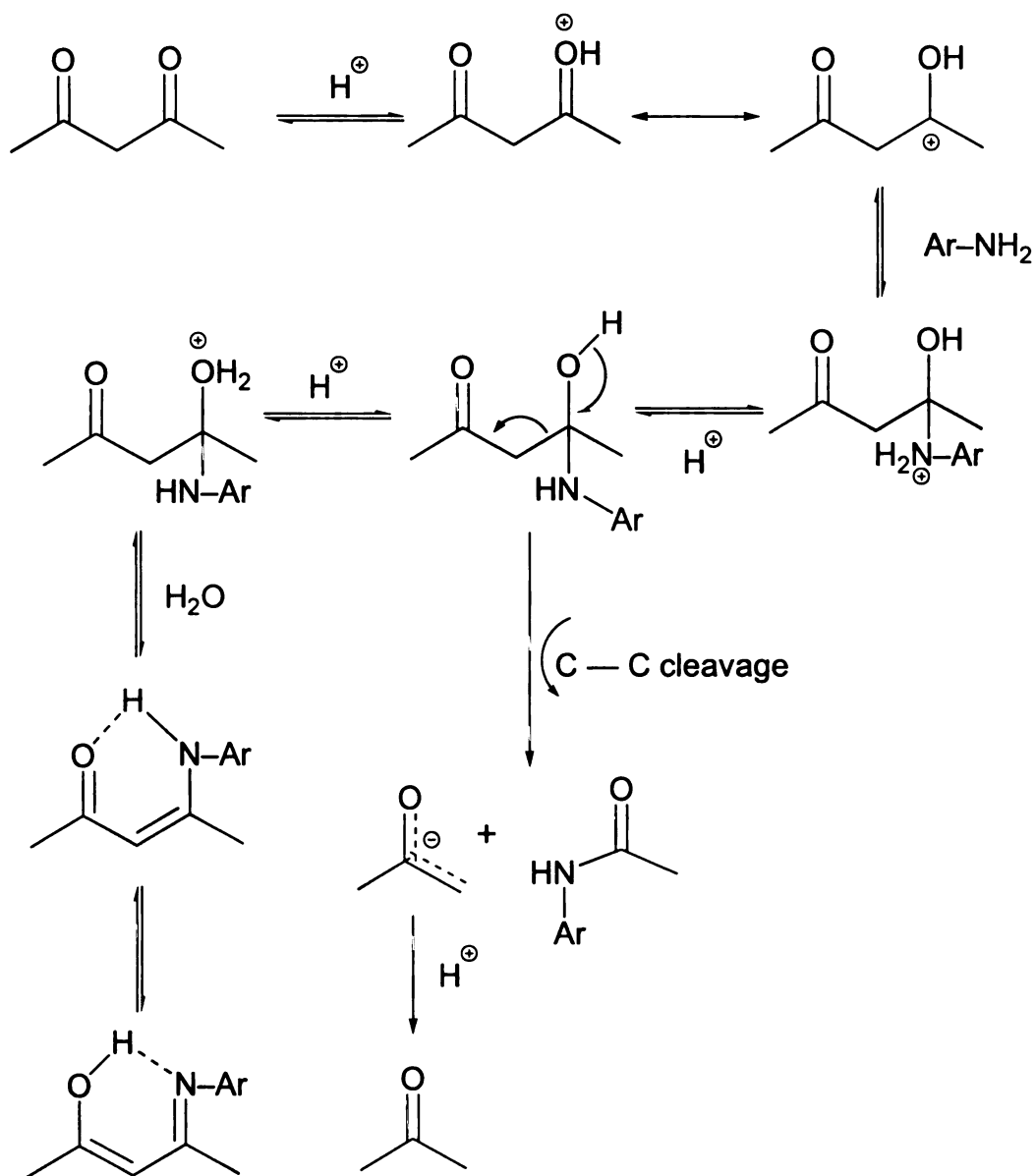
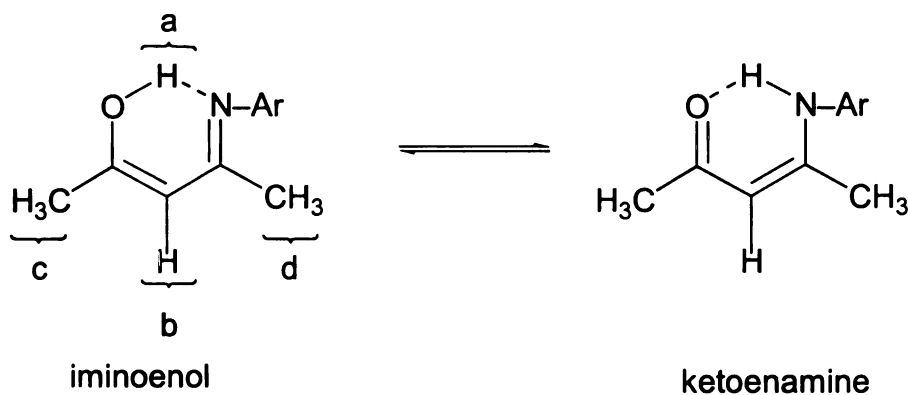


Figure 4. Proposed mechanism accounting for the formation of the amide and β -ketimine products, in the condensation reaction of substituted anilines with 2,4-pentanedione.

ketimine and the amide products. Under the acidic reaction conditions, protonation of the 2,4-pentanedione promotes the nucleophilic attack by the aniline. Dehydration of the intermediate results in the desired β -ketimine ligand, while C — C bond cleavage, facilitated by the presence of a good leaving group, gives the corresponding amide and acetone.

Formation of the byproducts can however be avoided, by carefully controlling the reaction time. Refluxing for two to four hours affords the desired β -ketimine ligands in good yields. Four such ligands — namely 2-(4-methylphenylimino)-pentane-4-one (MPPOH), 2-(2,4,6-trimethylphenylimino)-pentane-4-one (TMPPOH), 2-(2,6-diisopropylphenylimino)-pentane-4-one (DIPPOH), and 2-(4-*t*-butylphenylimino)-pentane-4-one (BPPOH) — were synthesized and characterized by NMR spectroscopy. These neutral compounds are found in two tautomeric forms,⁶ namely as iminoenols and ketoenamines (Scheme 1).



Scheme 1

Tables 3 and 4 display the ^1H and ^{13}C chemical shifts respectively of the four β -ketimine ligands synthesized in this work. The two characteristic proton resonance peaks that these materials exhibit are those attributed to the

Table 3. ^1H NMR Data of the β -Ketimine Free Ligands.

Compound	H _{methyl}	H _{vinyl}	H _{aromatics}	H _{tautomeric}
MPPOH (1)	1.93 (s, 3H)			
	2.07 (s, 3H)	5.14 (s, 1H)	6.97 (d, 2H)	12.38 (s, 1H)
	2.31 (s, 3H)		7.11 (d, 2H)	
TMPPOH (2)	1.60 (s, 3H)			
	2.08 (s, 3H)			
	2.13 (s, 6H)	5.17 (s, 1H)	6.88 (s, 2H)	11.82 (s, 1H)
	2.26 (s, 3H)			
DIPPOH (3)	1.12 (d, 6H)			
	1.19 (d, 6H)			
	1.61 (s, 3H)	5.18 (s, 1H)	7.15 (d, 2H)	12.03 (s, 1H)
	2.10 (s, 3H)		7.27 (d, 2H)	
BPPOH (4)	1.28 (s, 9H)			
	1.96 (s, 3H)	5.14 (s, 1H)	7.01 (d, 2H)	12.42 (s, 1H)
	2.06 (s, 3H)		7.32 (d, 2H)	

Table 4. ^{13}C NMR Data of the β -Ketimine Free Ligands.

Compound	C _{methyl}	C _{vinyl}	C _{aromatics}	C _{imine}	C _{keto}
MPPOH (1)	19.74		124.82		
	20.87	97.15	129.61	160.65	195.86
	29.10		135.46		
			136.02		
			128.84		
TMPPOH (2)	18.85		133.83		
	20.90	95.60	135.68	163.08	195.84
	29.03		136.99		
	19.10		123.49		
	22.61		128.20		
DIPPOH (3)	24.54	95.54	133.44	163.25	195.84
	29.00		146.22		
			124.31		
	19.79		125.88		
BPPOH (4)	29.06	97.18	135.94	160.53	195.79
	31.26		148.54		

tautomeric proton *a* (11.82 to 12.42 ppm) and to the vinyl proton *b* (5.14 to 5.18 ppm). The resonance position of the latter is not influenced by the substitution pattern of the aniline moiety. The same was observed for the ^1H and ^{13}C chemical shifts of methyl hydrogens *c* and the carbonyl carbon, which resonated at approximately the same position (~ 2.08 and 195.8 ppm respectively) for all four compounds. The other methyl group of the ketoimine moiety (*d*) does show however some variation in chemical shift along the series. In the *para* substituted derivatives MPPOH and BPPOH this resonance appears at ~ 1.94 ppm, while in compounds TMPPOH and DIPPOH where *ortho* substitution of the phenyl rings occurs, a shift towards high fields is observed (1.60 ppm). A similar trend is seen in the ^{13}C spectra of the ligands, where the imine and the vinyl carbon resonate at higher and lower fields respectively (~ 160.6 and ~ 97.16 ppm) for MPPOH and BPPOH than those of TMPPOH and DIPPOH (~ 163.1 and 95.57 ppm). These effects are attributed to two factors. First, the relative twist between the aromatic groups and the ketoimine backbone is presumably larger when *ortho* substituents are present in the aromatic ring due to unfavorable steric interactions. Second, the diamagnetic anisotropy of these ligands' aryl rings is responsible for the shielding of the imino methyl protons *d* and the vinyl carbon, and the deshielding of the imine carbon. In MPPOH and BPPOH electron delocalization is larger resulting in decreased shielding of the methyl protons *d* and the vinyl carbon, and decreased deshielding for the imine carbon, in accordance with the experimental observations.

2. Reactivity of Free Ligands towards Titanium Complexes

Initially the free neutral β -ketimine ligands were reacted with tetrakis dimethylaminotitanium ($\text{Ti}[\text{NMe}_2]_4$) in an effort to synthesize the corresponding

titanium chelate complexes. Specifically, the reaction was tried first by MPPOH in a ratio 2:1 with the metal starting reagent. The addition of the β -ketimine ligand to the standard toluene solution of $\text{Ti}[\text{NMe}_2]_4$ (0.1M) occurred slowly at room temperature and under argon atmosphere. Although a pronounced color change to bright red was observed from the mixing of the two yellow solutions, ^1H NMR spectra taken immediately after the end of the addition and after overnight stirring at ambient temperature showed just the starting reagents. Heating of the reaction mixture at 60 °C overnight gave a satisfactory 78% NMR yield of a product. When the reaction was repeated in refluxing toluene the isolated yield after recrystallization from hexanes was 89.5%.

Chemical analysis indicated the complete absence of titanium metal from the product and pointed to the chemical formula $\text{C}_{14}\text{H}_{20}\text{N}_2$. The compound, which was characterized by using MS and NMR, was identified as 2-(dimethylamino)-4-(4-methylphenylimino)pent-2-ene. *Figure 5* displays the structure of the molecular ion ($m/z = 216$) and its fragmentation course, where all the main fragments have been recognized. The ^1H NMR spectrum of the compound taken in deuterated benzene, displayed four peaks for the methyl groups from 1.92 to 2.58 ppm, one vinyl peak at 4.76 ppm and two doublets in the aromatic region at 6.89 and 7.07 ppm. The ^{13}C NMR spectra on the other hand exhibited three methyl peaks from 16.77 ppm to 22.99 ppm and one at 39.12 assigned to the two methyl groups attached on the nitrogen. In addition to the expected four aromatic peaks, which resonate from 120.74 to 151.79 ppm, two more lines were observed at low fields corresponding to the amino (154.58 ppm) and the imino (164.34 ppm) carbons. The latter carbon resonates in a similar range with the corresponding carbons of the β -ketimine ligands, indicating that these are more of the iminoenol rather than the ketoenamino type (see Scheme 1).

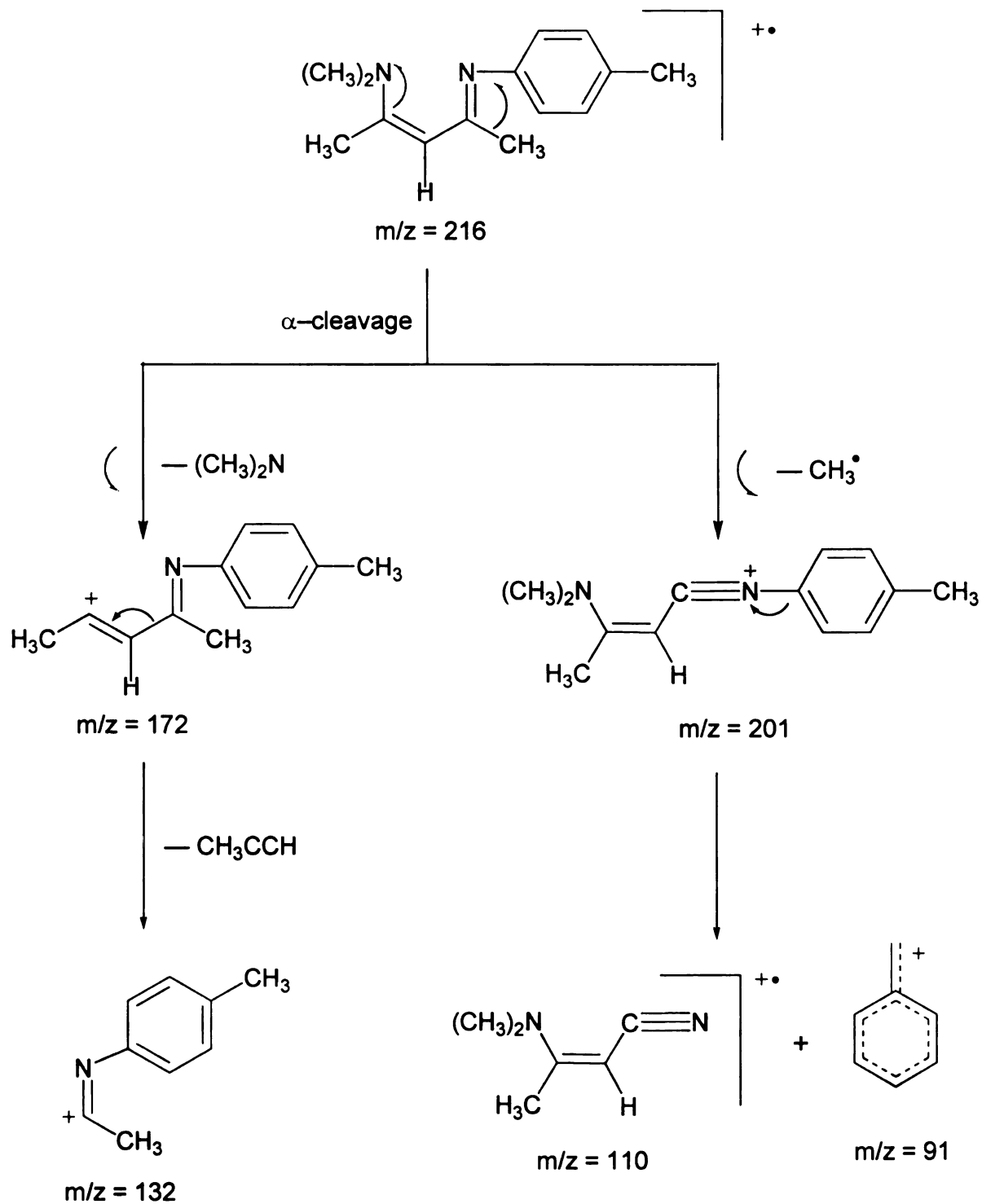


Figure 5. Fragmentation mechanism and assignment of the main MS peaks of the 2-(dimethylamino)-4-(4-methylphenylimino)-pent-2-ene.

When BPPOH was reacted under the same conditions with $\text{Ti}[\text{NMe}_2]_4$ a similar product, namely 2-(dimethylamino)-4-(4-*t*-butylphenylimino)-pent-2-ene, was isolated giving a crude NMR yield of 82%.

The target product of these reactions were the corresponding titanium chelate complexes of the β -ketimine ligands. The dimethylamino group was expected to perform the dual duty of a leaving group and of a base, which would abstract the acidic O — H proton of the neutral ligands. Instead, a purely organic product was obtained, where C — O bond cleavage followed by C — N bond formation occurred. The great affinity of titanium for oxygen and the strong nucleophilic character of the dimethylamino ligands should be considered as the driving forces for such reactivity. Although the details of the exact mechanism are not known, the initial formation of a non-chelate titanium-ligand complex is anticipated. The concentration of such a complex probably remained low during the reaction course since it could not be detected by NMR spectroscopy. The next step is thought to be proton abstraction and subsequent nucleophilic attack in the activated C — O bond by the metal ligands, resulting in 2-(dimethylamino)-4-(arylimino)-pent-2-ene and TiO_2 . The presence of the latter was indicated by the formation of a white precipitate at the end of the reaction and is strengthened by literature reports where titanium complexes have been used for C — O bond activation⁸.

The same targets, namely β -ketiminato titanium complexes were approached by a different synthetic procedure. Specifically, the use of tetrachlorobis(tetrahydrofuran)titanium, $\text{TiCl}_4(\text{THF})_2$, was tried instead of the tetrakis dimethylaminotitanium. The choice of the former reagent was grounded in the mild nucleophilic character of the chloride ligand relative to the dimethylamino group, which is considered as the main reason for the formation of the deoxygenated organic product. Mixing of THF solutions of $\text{TiCl}_4(\text{THF})_2$ and

free TMPPOH at room temperature under a nitrogen atmosphere gave a clear red solution from which product precipitated after stirring for two hours. Eventually an additional crop of product was obtained from the mother liquor as nice orange-red plate-like crystals by layering the THF solution with heptane in a 1:1 ratio.

An orange plate-like crystal was mounted for X-ray structure determination on a Siemens Smart system. Although the crystal diffracted poorly and a weak data set was collected a satisfactory solution of the structure was obtained. The product was found to be the non-chelate titanium complex of the 2-(2,4,6-trimethylphenylimino)-pentane-4-one ketimine ligand, $(\text{TMPPOH})_2\text{TiCl}_4$. Two crystallographically independent complexes crystallized within the unit cell along with one molecule of THF solvent (crystallographic data are gathered in Table 1). The ORTEP diagrams for one of the two complexes is shown in *Figure 6*, while the metric parameters of both complexes are found in Table 5.

The coordination environment around the titanium metal is that of a distorted octahedron, with four chloride ions located in the equatorial plane and two β -ketimine ligands occupying the axial positions. The latter are bound to the metal through the oxygen atom of the β -ketimine backbone, while there is no chemical bond between the nitrogen atoms and the titanium centers, as indicated by their large separation (mean value 3.97 Å). This is attributed to the greater affinity of titanium for oxygen. The two crystallographically independent complexes have very small differences concerning bond distance and angles as indicated in Table 5. The axial bonds within each organometallic complex vary slightly in length while small deviations are also observed among the Ti — Cl bonds. The four ketimine backbones, which consist of acac-type units with CC(O)CC(N)C connectivity, are found to have almost identical metric

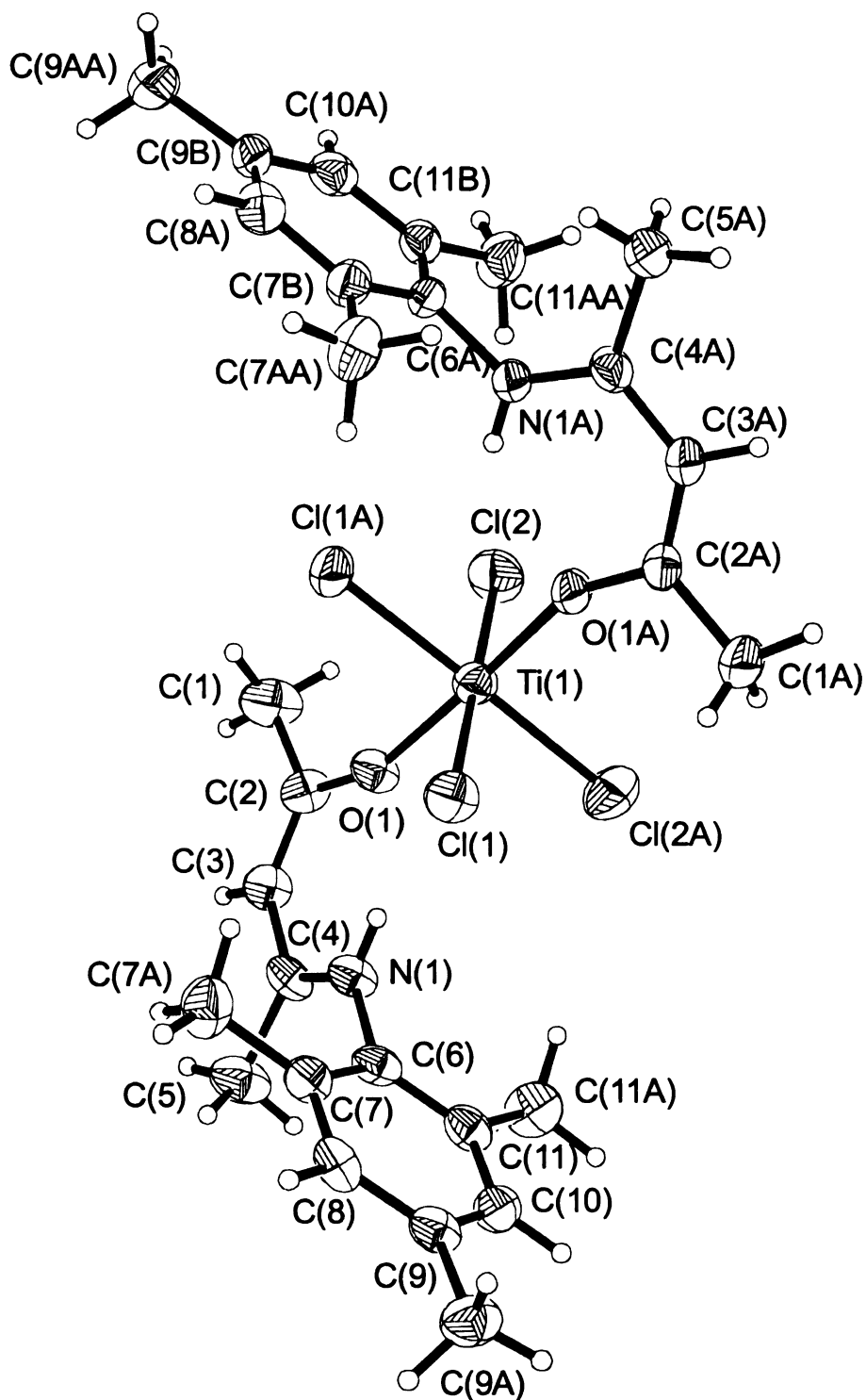


Figure 6. ORTEP diagram (at 50% probability) of the non-chelate $\{\mu\text{-O-[2-(2,4,6-trimethylphenylimino)-pentane-4-one]}\}_2\text{TiCl}_4 \cdot 0.5\text{C}_4\text{H}_8\text{O}$, displaying one of the two crystallographically independent organometallic complexes.

Table 5. Selected Bond Distances and Angles of (TMPPOH)₂TiCl₄.

<i>Atom 1</i>	<i>Atom 2</i>	<i>Distance</i>	<i>Atom 1</i>	<i>Atom 2</i>	<i>Distance</i>
Ti(1)	O(1)	1.915(3)	Ti(2)	O(2)	1.904(3)
Ti(1)	N(1)	3.982(5)	Ti(2)	N(2)	3.964(5)
Ti(1)	Cl(1)	2.353(2)	Ti(2)	Cl(3)	2.358(1)
Ti(1)	Cl(2)	2.321(2)	Ti(2)	Cl(4)	2.325(2)
C(2)	O(1)	1.298(6)	C(13)	O(2)	1.303(6)
C(4)	N(1)	1.316(6)	C(15)	N(2)	1.315(6)
C(1)	C(2)	1.501(7)	C(12)	C(13)	1.499(7)
C(2)	C(3)	1.362(7)	C(13)	C(14)	1.367(7)
C(3)	C(4)	1.418(7)	C(14)	C(15)	1.413(7)
C(4)	C(5)	1.500(7)	C(15)	C(16)	1.490(6)

<i>Atom 1</i>	<i>Atom 2</i>	<i>Atom 3</i>	<i>Angle / °</i>	<i>Atom 1</i>	<i>Atom 2</i>	<i>Atom 3</i>	<i>Angle / °</i>
O(1)	Ti(1)	O(1A)	175.5(2)	O(2)	Ti(2)	O(2A)	180
Cl(1)	Ti(1)	Cl(2)	178.9(1)	Cl(3)	Ti(2)	Cl(4)	90.5(1)
Cl(1)	Ti(1)	Cl(1A)	89.6(1)	Cl(3)	Ti(2)	Cl(3A)	180
Cl(2)	Ti(1)	Cl(2A)	91.3(1)	Cl(4)	Ti(2)	Cl(4A)	180

parameters. The average C — O and C — N bonds are 1.301 and 1.315 Å respectively. The former value is much larger than the typical carbonyl bonds and the latter is shorter from the value observed for *N*-(4-tolyl)-acetamide suggesting extended delocalization within the ligand chelate core. The local symmetry around the metal can be approximated as D_{4h} taking into account only the Cl_4O_2 coordination sphere. The symmetry point group drops to C_{2h} if one considers the relative *anti* orientation of the β -ketimine ligands, which have their chelate acac-backbones parallel by symmetry. The aromatic units are almost orthogonal to the acac-backbones with angles of $83.4(3)^\circ$ and $87.2(3)^\circ$ for the two crystallographically independent molecules, minimizing steric interactions with the keto and imino methyl groups.

Reaction of the free ligands MPPOH and BPPOH with $TiCl_4(THF)_2$ afforded the corresponding non-chelate complexes $(MPPOH)_2TiCl_4$ and $(BPPOH)_2TiCl_4$. Since suitable single crystals for X-ray structure determination were not available for these derivatives, their characterization was based on 1H NMR spectroscopy, by utilizing as a reference the corresponding spectrum of the structurally characterized $(TMPPOH)_2TiCl_4$ derivative. The 1H chemical shifts of the three compounds are collected in Table 6, along with the ^{13}C shifts of $(TMPPOH)_2TiCl_4$. Carbon NMR spectra of the other two derivatives were not available due to solubility problems. The 1H NMR spectra of $(MPPOH)_2TiCl_4$ and $(BPPOH)_2TiCl_4$ were different from those of the corresponding free ligands and in addition displayed the characteristic N — H resonance for the tautomeric proton (12.12 to 12.62 ppm) precluding the formation of a metal chelate complex. The resonance of the vinyl proton appears at 5.35 ppm for both complexes, a value almost identical with the corresponding one (5.33 ppm) for the structurally characterized $(TMPPOH)_2TiCl_4$. Comparison of the methyl group chemical shifts among the three compounds offer additional insights to the structure of

Table 6. $^1\text{H}^{\text{a}}$ and $^{13}\text{C}^{\text{b}}$ NMR Data for the Non-chelate $(\beta\text{-ketimine})_2\text{TiCl}_4$ Complexes.

Compound ^a	H _{methyl}	H _{vinyl}	H _{aromatics}	H _{hydroxyl}
(MPPOH)₂TiCl₄	2.13 (s, 3H)		7.13 (d, 2H)	
	2.33 (s, 3H)	5.35 (s, 1H)		12.62 (s, 1H)
	2.69 (s, 3H)		7.20 (d, 2H)	
(BPPOH)₂TiCl₄	1.28 (s, 9H)		7.26 (d, 2H)	
	2.14 (s, 3H)	5.35 (s, 1H)		12.60 (s, 1H)
	2.70 (s, 3H)		7.37 (d, 2H)	
(TMPPOH)₂TiCl₄	1.84 (s, 3H)			
	2.19 (s, 3H)			
	2.24 (s, 6H)	5.33 (s, 1H)	6.85 (s, 2H)	12.12 (s, 1H)
	2.65 (s, 3H)			

Compound ^b	C _{methyl}	C _{vinyl}	C _{aromatics}	C _{imine}	C _{keto}
(TMPPOH)₂TiCl₄	18.36		129.28		
	20.44		132.26		
	20.98	97.83	134.50	172.18	191.24
	26.00		138.72		

(MPPOH)₂TiCl₄ and (BPPOH)₂TiCl₄ complexes. The *t*-butyl lines of (BPPOH)₂TiCl₄ appeared at 1.28 ppm, a value identical to the corresponding one in the free ligand. The remaining peaks at 2.14 and 2.70 ppm are assigned to the protons of the imino and keto methyl groups respectively, since oxygen coordination to the electropositive titanium(4+) center is expected to reduce electron density around the keto-group of the molecule. In (MPPOH)₂TiCl₄ the line at 2.33 ppm is assigned to the tolyl group (2.31 ppm in MPPOH) and the peaks at 2.13 and 2.69 ppm to the protons of the imino and keto methyl groups respectively. In (TMPPOH)₂TiCl₄ the lines at 2.19 and 2.24 ppm belong to the three aromatic methyl groups, while the corresponding values for the protons of the imino and keto methyl groups are 1.84 and 2.65 ppm. Hence, coordination to the metal shifts the keto methyl group from 2.08 ppm (mean value in free ligands) to a mean value of 2.68 ppm in the non-chelate complexes. The corresponding chemical shifts of the imino methyl group in the free ligands were dependent on the relative orientation of the aromatic group and the ketoimine backbone, with shifts towards high fields as these groups approached orthogonality. In (TMPPOH)₂TiCl₄, where indeed X-ray structure determination confirms the orthogonal arrangement of the two units, the protons of the imino methyl group resonate at 1.84 ppm. In the other two derivatives, where the aromatic rings are *para* substituted, the shift towards low fields — 2.13 ppm for (MPPOH)₂TiCl₄ and 2.14 ppm for (BPPOH)₂TiCl₄ — indicates a more coplanar arrangement that permits electron delocalization.

3. Synthesis of Group IV Chelate Complexes

Direct reaction of the free ligands with $\text{TiCl}_4(\text{THF})_2$ failed to give the desired chelate products. The choice of the starting metal reagent, i.e. $\text{TiCl}_4(\text{THF})_2$, was successful in terms of the nucleophilic potential of the chloride ligands, since it did not cause any nucleophilic attack at the activated C — O bond as $\text{Ti}[\text{NMe}_2]_4$ did. On the other hand the chlorides were not basic enough in order to promote proton abstraction from the free β -ketimine ligand, and hence enforce the formation of the desired chelate ring upon complexation to titanium. To overcome this obstacle, the salts of the ligands were synthesized and subsequently allowed to directly react with $\text{TiCl}_4(\text{THF})_2$.

The general synthetic procedure is shown in *Figure 7*. The reaction involves mixing, under nitrogen atmosphere, of the β -ketimine ligands dissolved or suspended in dry pentane with the appropriate amount of *n*-BuLi solution at ambient temperature. Signs of reactivity were visible when the ligands were suspended in pentane, since the starting suspension transforms to a clear solution upon addition of approximately 0.5 equivalents of *n*-BuLi, which finally results in precipitation of the white product upon total consumption of *n*-BuLi. The lithium salts of MPPOH and TMPPOH (MPPOLi and TMPPOLi) were synthesized in excellent yields of 95% and 91%, respectively. These salts possess moderate solubility in the reaction solvent which enabled a facile isolation process by simply removing the solvent from the chilled ($-80\text{ }^\circ\text{C}$) solutions. The same reaction performed in dry THF, where the products are highly soluble, gave satisfactory yields but not so high as the corresponding ones obtained from pentane.

The product identity was confirmed by ^1H and ^{13}C NMR spectroscopy. Chemical shifts for MPPOLi and TMPPOLi are gathered in Table 7. The

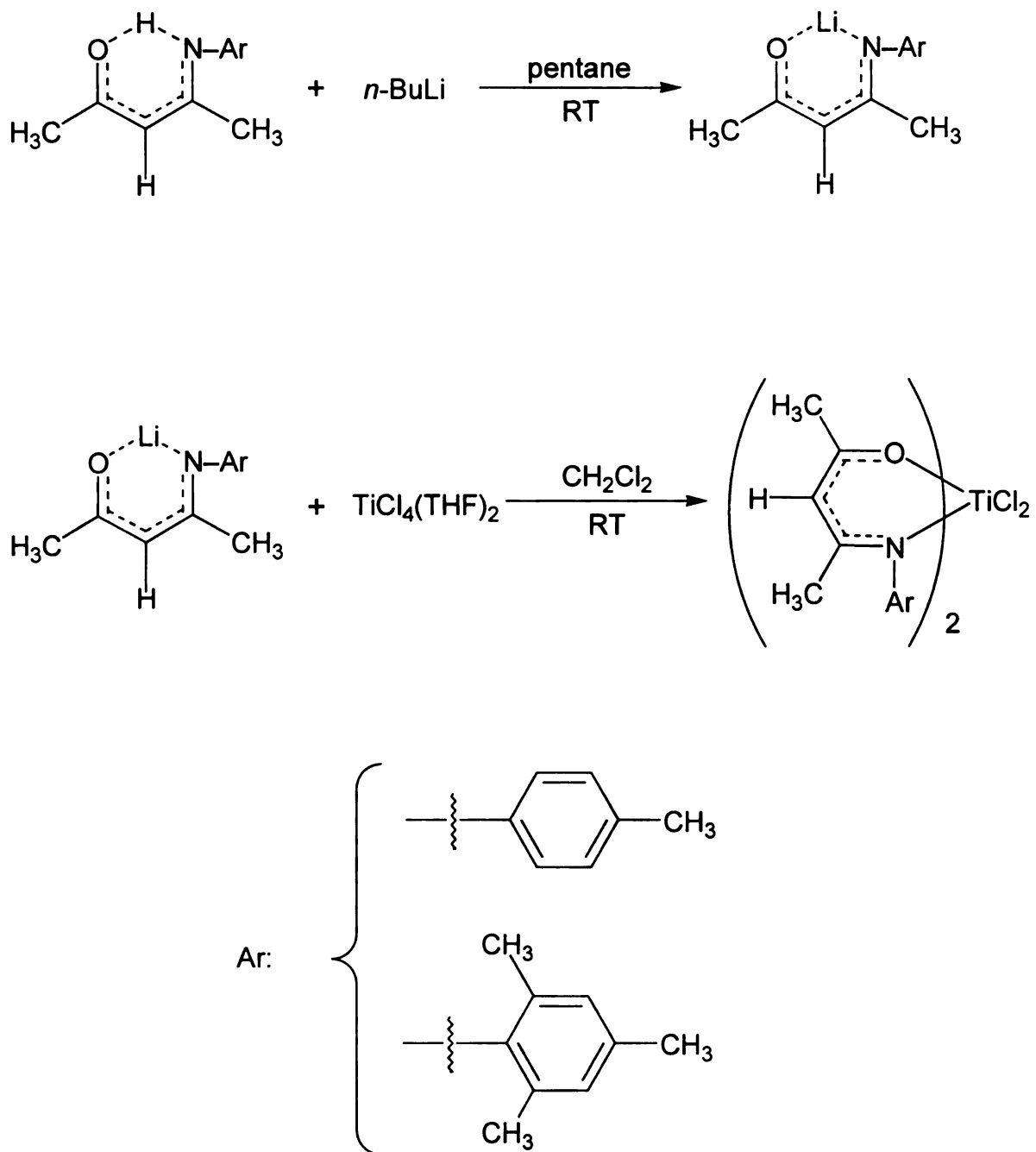


Figure 7. General synthetic scheme for the synthesis of Titanium chelate complexes.

Table 7. $^1\text{H}^{\text{a}}$ and $^{13}\text{C}^{\text{b}}$ NMR Data for the Lithium Salts of β -Ketimine Ligands.

Compound ^a	H _{methyl}	H _{vinyl}	H _{aromatics}	H _{hydroxyl}
MPPOLI	1.34 (s, 3H)		6.59 (d, 2H)	—
	1.65 (s, 3H)	4.72 (s, 1H)	6.99 (d, 2H)	
	2.25 (s, 3H)			
TMPOLI	1.21 (s, 3H)			
	1.45 (s, 3H)			
	1.87 (s, 6H)	4.74 (s, 1H)	6.74 (s, 2H)	—
	2.18 (s, 3H)			

Compound ^b	C _{methyl}	C _{vinyl}	C _{aromatics}	C _{imine}	C _{keto}
MPPOLI			121.77		
	20.80		129.16		
	22.05	98.70	131.82	168.01	175.59
	27.83		149.34		
	17.72		128.20		
TMPOLI	20.76		128.61		
	21.64	98.21	131.48	168.12	175.41
	27.59		146.61		

characteristic peak of the tautomeric proton that the corresponding free β -ketoimine ligands exhibit around 12 ppm has disappeared verifying the lithium salt formation. Proton abstraction increases the electron density within the chelate ring, producing high field shifts of the remaining protons. Hence, the vinyl hydrogen for both salts has been shifted 0.4 ppm upfield in comparison with the corresponding free ligands, while significant upfield shifts are observed for the keto and imino methyl protons. The ^{13}C NMR spectra show the expected number of peaks, ten for the MPPOLi and eleven for TMPPOLi. The most interesting features of the spectra concerns the large upfield shift of the carbonyl carbon (195.85 versus 175.50 ppm) and the downfield shift of the imino carbon (161.86 versus 168.06 ppm). These effects are attributed to the increased electron density and the diamagnetic anisotropy of the chelate ring.

Lithium was not the only alkali metal used for the preparation of the salts. Sodium and potassium were tried in the form of sodium hydrate and potassium hydrate respectively. Hydrogen evolution was observed upon treatment of the hydrides with the corresponding ligands, resulting in white powder precipitates. The ^1H NMR of the sodium salt consisted of relatively broad peaks, which corresponded to the suggested compound. The potassium derivative could not be characterized since it was insoluble in all the common NMR solvents. Since the lithium salts exhibited nice NMR spectra with sharp and well separated peaks, they were the compounds of choice for the preparation of the chelate group IV complexes.

The synthesis of the target compounds was accomplished successfully in high yields by the reaction of the $\text{MCl}_4(\text{THF})_2$ ($\text{M} = \text{Ti}, \text{Zr}$) with the lithium salts of the β -ketimine ligands in methylene chloride, under nitrogen atmosphere at ambient temperature (*Figure 7*). The optimum reaction conditions required the absolute absence of moisture. In several unsuccessful reactions, the failure to

obtain the desired complexes was due to the presence of moisture either in the starting metal reagents, the solvent, or the inert nitrogen atmosphere. Therefore, a number of precautions were taken in order to overcome the problem. The titanium starting metal reagent, $\text{TiCl}_4(\text{THF})_2$, was recrystallized from methylene chloride/pentane, and the zirconium tetrachloride, ZrCl_4 , utilized for the synthesis of tetrachlorobis(tetrahydrofuran)zirconium, $\text{ZrCl}_4(\text{THF})_2$, was sublimed at 130 °C under vacuum. The lithium salts of the β -ketimine ligands were all recrystallized prior to their use. The reaction solvents as well as the solvents used for recrystallization of the products, not only were freshly distilled over sodium/benzophenone ketyl but also were saturated with nitrogen and were stirred with dry basic alumina at least for an hour before use. The vacuum line was renovated and nitrogen gas passed through two drying columns.

The reaction was performed in methylene chloride, since its pairing with pentane proved to be the best solvent system for the recrystallization of the products. However, dry THF and toluene were also effective solvents for the reaction. Simple mixing of $\text{TiCl}_4(\text{THF})_2$ with the corresponding lithium salts resulted in the formation of a deep red solution, which was stirred at ambient temperature for two hours. Layering the solvent with *n*-pentane and allowing the mixture to stand undisturbed at ambient temperature for a few hours resulted in the precipitation of large well formed red crystals (the color is probably due to a ligand to metal charge transfer transition). Generally, the conditions of the reaction are mild since no heat is necessary for the formation of the product and short reaction times are sufficient for generation of the products in high yields.

The complexes $(\text{MPPO})_2\text{TiCl}_2$ and $(\text{TMPPO})_2\text{TiCl}_2$ were synthesized in the manner described above. $(\text{MPPO})_2\text{TiCl}_2$ forms red rectangular-like crystals upon diffusion of pentane into a concentrated methylene chloride solution (ratio 3:1) at room temperature. A single crystal X-ray study was undertaken revealing the

chelate nature of the complex (crystallographic data and selected bond distances and angles are summarized in Tables 8 and 9 respectively). The local coordination environment of titanium metal, which consists of two MPPO ligands and two chlorine atoms, is that of a distorted octahedron with roughly D_{2h} symmetry (Figure 8). The two chlorine atoms are positioned in a *cis* orientation ($\text{Cl}(1) - \text{Ti}(1) - \text{Cl}(2) = 98.46(3)^\circ$), with an average displacement from the metal of 2.324(1) Å. Similarly, the two nitrogen atoms are also *cis* to each other forming a $\text{N}(1) - \text{Ti}(1) - \text{N}(2)$ angle of $85.59(8)^\circ$ with a mean Ti — N bond distance of 2.171(2) Å. The remaining axial sites are occupied by the oxygen atoms of the β -ketiminato ligands, which are located at an average distance of 1.892(2) Å from the titanium metal. The two six-membered chelate rings (defined by Ti(OC)C(CN) atoms) are planar and almost orthogonal to each other, as indicated by their dihedral angle of 86.15° . The average C — N bond distance is 1.325 Å, a value identical with that observed in the non-chelate $(\text{TMPPO})_2\text{TiCl}_4$ complex, while the corresponding carbonyl groups are slightly longer (mean C — O = 1.323 Å). The tolyl groups are almost orthogonal to the plane of the six-membered chelate ring to which they are bound via a C — N bond, with angles of 87.49° and 84.3° . Furthermore, they possess a parallel arrangement with respect to the other chelate ring. The relative orientation of the aromatic groups is imposed by the stereochemical and packing requirements of the β -ketiminato and chloride ligands, producing a tight molecular structure with minimized steric repulsions between the constituent units.

Single red rectangular-like crystals, suitable for X-ray structure determination, were also grown for $(\text{TMPPO})_2\text{TiCl}_2$ by layering a concentrate methylene chloride solution with pentane, in a 1:3 ratio. The crystallographic data are presented in Table 8, while selected bond distances and angles are gathered in Table 9. The synthesis of the desired chelate complex was confirmed and

Table 8. Crystallographic Data of (MPPO)₂TiCl₂, (TMPPO)₂TiCl₂, and (MPPO)₂ZrCl₂.

	(MPPO) ₂ TiCl ₂	(TMPPO) ₂ TiCl ₂
(A) Crystal Parameters		
formula	C ₂₄ H ₂₈ Cl ₂ N ₂ O ₂ Ti	C ₂₉ H ₃₈ Cl ₄ N ₂ O ₂ Ti
crystal habit, color	plate, red	block, red
FW	495.28	636.31
crystal size (mm ³)	0.75 × 0.19 × 0.08	0.80 × 0.39 × 0.39
crystal system	orthorhombic	triclinic
space group	<i>Pbca</i>	<i>P</i> $\bar{1}$
a (Å)	11.5548(2)	8.1662(1)
b (Å)	20.0716(3)	14.8386(2)
c (Å)	21.5875(1)	14.9441(2)
α (deg)	90	67.182(1)
β (deg)	90	83.706(1)
γ (deg)	90	77.764(1)
V (Å ³)	5006.7(1)	1630.5(1)
Z	8	2
d _{calc} (Mg/m ³)	1.314	1.296
F(000)	2064	664
μ(Mo Kα), mm ⁻¹	0.577	0.617
(B) Data Collection		
2θ _{max} (deg)	50.0	56.5
	-13 ≤ h ≤ 13	-10 ≤ h ≤ 10
index ranges	-23 ≤ k ≤ 23	-19 ≤ k ≤ 19
	-25 ≤ l ≤ 25	-19 ≤ l ≤ 19
temperature / K	133(2)	133(2)
reflections collected	43366	18904
independent reflections	4409	7554
R(int) (%)	8.57	2.60
(C) Refinement		
Refinement method	Full-matrix least-squares on F ²	Full-matrix least-squares on F ²
R indices (<i>I</i> > 2σ(<i>I</i>))	R1 = 0.0493 WR2 = 0.0847	R1 = 0.0308 WR2 = 0.0863
R indices all data	R1 = 0.0754 WR2 = 0.0927	R1 = 0.0394 WR2 = 0.0892
Δ(ρ) (e ⁻ /Å ³)	0.315	0.356
GOF	1.096	1.057

Table 8. (con't)

(MPPO)₂ZrCl₂	
(A) Crystal Parameters	
formula	C ₂₄ H ₂₈ Cl ₂ N ₂ O ₂ Zr
crystal habit, color	block, colorless
FW	1377.36
crystal size (mm ³)	0.52 × 0.30 × 0.26
crystal system	hexagonal
space group	<i>P</i> 3 ₁ 21
a (Å)	8.6167(1)
b (Å)	8.6154(1)
c (Å)	28.5731(1)
α (deg)	90
β (deg)	90
γ (deg)	120
V (Å ³)	1837.0(1)
Z	3
d _{calc} (Mg/m ³)	1.461
F(000)	828
μ(Mo Kα), mm ⁻¹	0.690
(B) Data Collection	
2θ _{max} (deg)	56.5
	-10 ≤ h ≤ 11
index ranges	-11 ≤ k ≤ 10
	-26 ≤ l ≤ 37
temperature / K	133(2)
reflections collected	11625
independent reflections	2967
R(int) (%)	1.99
(C) Refinement	
Refinement method	Full-matrix
	least-squares on F ²
R indices (<i>I</i> > 2σ(<i>I</i>))	R1 = 0.0172
	WR2 = 0.0446
R indices all data	R1 = 0.0177
	WR2 = 0.0447
Δ(ρ) (e ⁻ /Å ³)	0.282
GOF	1.168

Table 9. Selected Bond Distances and Angles of Compound (MPPO)₂TiCl₂ and (TMPPO)₂TiCl₂.

(MPPO) ₂ TiCl ₂			(TMPPO) ₂ TiCl ₂				
<i>Atom 1</i>	<i>Atom 2</i>	<i>Distance</i>	<i>Atom 1</i>	<i>Atom 2</i>	<i>Distance</i>		
Ti(1)	O(1)	1.892(2)	Ti(1)	O(1)	1.890(1)		
Ti(1)	O(2)	1.893(2)	Ti(1)	O(2)	1.887(1)		
Ti(1)	N(1)	2.172(2)	Ti(1)	N(1)	2.174(1)		
Ti(1)	N(2)	2.170(2)	Ti(1)	N(2)	2.176(1)		
Ti(1)	Cl(1)	2.322(1)	Ti(1)	Cl(1)	2.340(1)		
Ti(1)	Cl(2)	2.326(1)	Ti(1)	Cl(2)	2.376(1)		
O(1)	C(2)	1.325(3)	O(1)	C(2)	1.331(2)		
O(2)	C(13)	1.320(3)	O(2)	C(13)	1.327(2)		
N(1)	C(4)	1.322(3)	N(1)	C(4)	1.321(2)		
N(2)	C(15)	1.328(3)	N(2)	C(15)	1.327(2)		
<i>Atom 1</i>	<i>Atom 2</i>	<i>Atom 3</i>	<i>Angle / °</i>	<i>Atom 1</i>	<i>Atom 2</i>	<i>Atom 3</i>	<i>Angle / °</i>
O(1)	Ti(1)	O(2)	170.72(8)	O(1)	Ti(1)	O(2)	94.51(5)
N(1)	Ti(1)	N(2)	85.59(8)	N(1)	Ti(1)	N(2)	172.95(5)
Cl(1)	Ti(1)	Cl(2)	98.46(3)	Cl(1)	Ti(1)	Cl(2)	89.01(1)
O(2)	Ti(1)	Cl(1)	91.16(6)	O(2)	Ti(1)	Cl(1)	174.59(3)
O(1)	Ti(1)	N(1)	82.92(8)	O(1)	Ti(1)	N(1)	82.52(5)

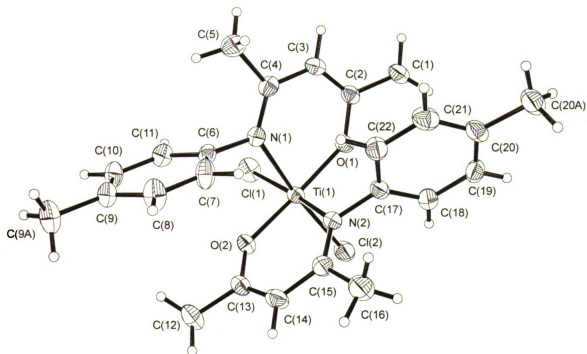


Figure 8. ORTEP representation (50% probability) of $\{\mu^2\text{-O,N-[2-(4-methylphenylimino)pentane-4-one]}\}_2\text{TiCl}_2$.

although the distorted octahedron metal environment has a local symmetry of D_{2h} its structure (*Figure 9*) is not quite the same as that of $(MPPO)_2TiCl_2$. The most pronounced difference concerns the *trans* and the *cis* arrangements of the nitrogen ($N(1) - Ti(1) - N(2)$ angle of $172.95(5)^\circ$) and oxygen ($O(1) - Ti(1) - O(2)$ angle of $94.51(5)^\circ$) atoms respectively in antithesis with what was observed in $(MPPO)_2TiCl_2$. This discrepancy is attributed to steric reasons and can be understood by examining the structure of $(MPPO)_2TiCl_2$, where close hydrogen – hydrogen contacts of just 2.560 \AA were observed between the *ortho* hydrogen atoms of the aromatic rings. By substituting MPPO by TMPPO, these hydrogen atoms are replaced by bulky methyl groups, which cannot be accommodated in the *trans*–oxygen arrangement, due to the close contact of the *ortho* positions. In the *trans*–nitrogen coordination environment the aryl groups point away from each other with no other close contacts encountered, while they retain their almost orthogonal arrangement (76.06°) with the corresponding chelate ring.

The metric data between the two complexes remain essentially the same, as can be seen by inspection of Table 9. The average Ti – N and Ti – O bond distances are of the same order, while the two chlorine atoms retain their *cis* arrangement, although the $Cl(1) - Ti(1) - Cl(2)$ angle is significantly smaller ($89.00(1)^\circ$ versus $98.46(3)^\circ$). Another noteworthy discrepancy between the two complexes concerns the deviation from planarity of the six–membered chelate rings. The planar chelates in $(MPPO)_2TiCl_2$ have been replaced by envelope–type rings in $(TMPPO)_2TiCl_2$ with the titanium metal being displaced by $0.740(2) \text{ \AA}$ from the plane.

The chelate complexes were also characterized by mass spectroscopy (the NMR characterization of these complexes is discussed below along with the corresponding data of Zirconium chelates). Hence, apart from the molecular ions (M^{+}) of $(MPPO)_2TiCl_2$ ($m/z = 494$) and $(TMPPO)_2TiCl_2$ ($m/z = 550$), the major

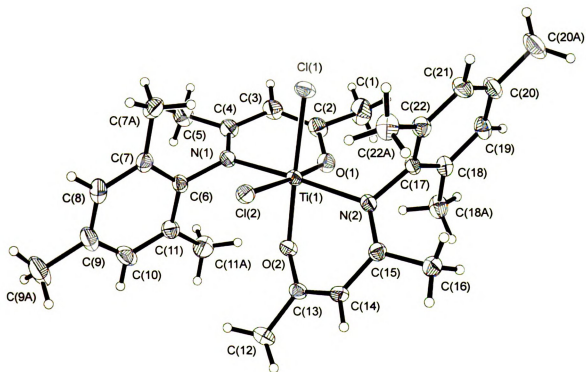


Figure 9. ORTEP representation (50% probability) of $\{\mu^2\text{-O,N-[2-(2,4,6-trimethylphenylimino)-pentane-4-one]}_2\text{TiCl}_2 \cdot \text{CH}_2\text{Cl}_2$.

fragments $[M^{**} - Cl]$ ($m/z = 459$ and 515), $[M^{**} - 2Cl]$ ($m/z = 424$ and 480), $[M^{**} - (T)MPPO]$ ($m/z = 306$ and 334), $[M^{**} - (T)MPPO - Cl]$ ($m/z = 271$ and 299), $[M^{**} - (T)MPPO - 2Cl]$ ($m/z = 236$ and 264), and $[(T)MPPOH]^{**}$ ($m/z = 189$ and 217) were located in the spectra and identified.

Reaction of MPPOLi and TMPPOLi with $ZrCl_4(THF)_2$ or $ZrCl_4$ under similar conditions to those utilized in the synthesis of titanium chelates generated the corresponding zirconium complexes, $(MPPO)_2ZrCl_2$ and $(TMPPO)_2ZrCl_2$, which were isolated in high yields. The latter compound was obtained as white powder and it was characterized by NMR and MS spectroscopies.

$(MPPO)_2ZrCl_2$ on the other hand, afforded large transparent crystals upon layering the reaction solution with pentane. Hence, it was structurally characterized by single crystal X-ray studies and its crystallographic data are listed in Table 8. The structure of this complex (selected bond distances and angles are collected in Table 10) is analogous to that of the corresponding titanium chelate, $(MPPO)_2TiCl_2$, as shown in *Figure 10*. The local symmetry in this case is also D_{2h} with the zirconium coordination environment being that of a distorted octahedron. The two β -ketiminato ligands MPPO, which occupy four of the six coordination sites around the metal, form two six-membered chelate rings, which are orthogonal to each other ($89.84(2)^\circ$) and have the zirconium metal as the common atom. The remaining two coordination sites are occupied by two chlorine atoms, which are *cis* to each other ($Cl - Zr - Cl = 91.24(2)^\circ$), and have an average bond distance to zirconium of $2.456(1)$ Å. The average $Zr - N$ bond distance is $2.337(1)$ Å. This is longer than the corresponding distance of the titanium chelate ($Ti - N = 2.171(2)$ Å), which is reasonable since Zr has a larger atomic radius than Ti. The two oxygen atoms occupy the axial positions of the octahedron ($O - Zr - O = 157.28(6)^\circ$) and their average displacement from

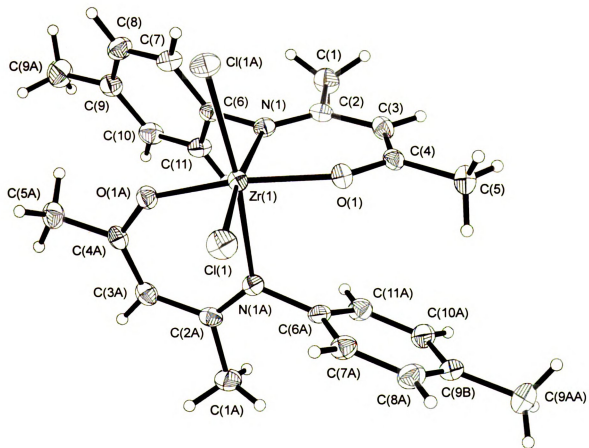


Figure 10. ORTEP representation (50% probability) of $\{\mu^2\text{-O,N-[2-(4-methylphenylimino)pentane-4-one]}\}_2\text{ZrCl}_2$. Only half of the molecule is crystallographically unique.

Table 10. Selected Bond Distances and Angles of (MPPO)₂ZrCl₂.

<i>Atom 1</i>	<i>Atom 2</i>		<i>Distance / Å</i>
Zr(1)	O(1)		2.012(1)
Zr(1)	N(1)		2.338(1)
Zr(1)	Cl(1)		2.456(1)
O(1)	C(4)		1.318(2)
N(1)	C(2)		1.322(2)
C(1)	C(2)		1.516(2)
C(2)	C(3)		1.436(2)
C(3)	C(4)		1.358(2)
C(4)	C(5)		1.496(2)
N(1)	C(6)		1.449(2)

<i>Atom 1</i>	<i>Atom 2</i>	<i>Atom 3</i>	<i>Angle / °</i>
O(1)	Zr(1)	O(1)*	157.28(6)
N(1)	Zr(1)	N(1)*	90.96(6)
Cl(1)	Zr(1)	Cl(1)*	91.24(2)
O(1)	Zr(1)	N(1)	77.92(4)
O(1)	Zr(1)	Cl(1)	95.14(3)

the metal is 2.012 (1) Å. The two aryl groups are tilted from the corresponding six-membered chelate ring by an angle of 73.17(4)°.

(TMPPO)₂ZrCl₂ was characterized by ¹H and ¹³C NMR spectroscopies. Comparison of its ¹H and ¹³C chemical shifts with the corresponding ones of the titanium (Table 11) and the zirconium chelates (Table 12), reveals significant similarities, indicating that indeed (TMPPO)₂ZrCl₂ is a chelate complex. The resemblance is apparent in the ¹³C chemical shifts of the vinyl carbon, which appears in the same region with those of the other three compounds, and of the imino carbon, which is like that of the (MPPO)₂ZrCl₂ derivative. More specifically, upon complexation of the MPPOLi and TMPPOLi to Ti⁴⁺ or Zr⁴⁺ a downfield shift of approximately 11 and 8 ppm respectively was observed for the vinyl carbon ¹³C peak, accompanied by a downfield shift of the vinyl proton resonance. The corresponding lines of the keto carbons remain unchanged, while those of the imino carbons shift approximately –6 ppm for the zirconium derivatives.

Inspection of the aromatic region in the carbon NMR shows six resonances for the (MPPO)₂TiCl₂, (TMPPO)₂TiCl₂, and (MPPO)₂ZrCl₂ complexes indicating that the carbon atoms of the aromatic rings are magnetically inequivalent. The proton spectra of the chelates also display one peak per aromatic proton (except for one set of protons in (MPPO)₂TiCl₂ and (MPPO)₂ZrCl₂ which have rather broad peaks due to accidental overlap degeneracy. In addition, the *ortho* methyl protons of (TMPPO)₂TiCl₂ also appear at different chemical shifts. The NMR data conclusively show that the solid state structure is maintained in solution and rotation about the aryl C — N bond is slow at the NMR time-scale.

Two alternative synthetic methods were utilized for the generation of titanium and zirconium chelate complexes (*Figure 11*). The first method involves the *in situ* generation of the β-ketiminato compound by simply adding

Table 11. $^1\text{H}^{\text{a}}$ and $^{13}\text{C}^{\text{b}}$ NMR Data $(\text{MPPO})_2\text{TiCl}_2$ and $(\text{TMPPO})_2\text{TiCl}_2$.

Compound ^a	H _{methyl}	H _{vinyl}	H _{aromatics}	H _{hydroxyl}	
(MPPO)₂TiCl₂	1.33 (s, 3H)		6.48 (d, 1H)		
	1.66 (s, 3H)	5.31 (s, 1H)	7.02 (d, 1H)	—	
	2.31 (s, 3H)		7.17 (b.d, 2H)		

(TMPPO)₂TiCl₂	1.69 (s, 3H)				
	1.85 (s, 3H)				
	2.06 (s, 3H)	5.80 (s, 1H)	6.77 (s, 1H)	—	
	2.24 (s, 3H)		6.86 (s, 1H)		
	2.27 (s, 3H)				
Compound ^b	C _{methyl}	C _{vinyl}	C _{aromatics}	C _{imine}	C _{keto}
(MPPO)₂TiCl₂			121.78		
			125.70		
	20.82		128.55		
	22.04	109.51	129.40	169.76	175.42
	24.41		135.07		
			148.79		

(TMPPO)₂TiCl₂			128.15		
			128.98		
	20.94	109.65	129.77	168.12	175.41
	22.61		132.40		
	23.44		135.42		
		146.51			

Table 12. $^1\text{H}^{\text{a}}$ and $^{13}\text{C}^{\text{b}}$ NMR Data $(\text{MPPO})_2\text{ZrCl}_2$ and $(\text{TMPPO})_2\text{ZrCl}_2$.

Compound ^a	H _{methyl}	H _{vinyl}	H _{aromatics}	H _{hydroxyl}	
(MPPO)₂ZrCl₂	1.33 (s, 3H)		6.51 (d, 1H)	—	
	1.69 (s, 3H)	5.22 (s, 1H)	7.12 (b.s,		
	2.32 (s, 3H)				
(TMPPO)₂ZrCl₂	1.68 (s, 3H)				
	1.93 (s, 3H)				
	2.19 (s, 6H)	5.58 (s, 1H)	6.85 (s, 2H)	—	
	2.24 (s, 3H)				
Compound ^b	C _{methyl}	C _{vinyl}	C _{aromatics}	C _{imine}	C _{keto}
(MPPO)₂ZrCl₂			122.84		
			125.49		
	20.84		129.40		
	22.78	106.28	129.92	173.09	174.85
	24.52		135.16		
			145.82		
(TMPPO)₂ZrCl₂	18.10		129.34		
	18.89		134.30		
	20.90	106.39	135.50	174.88	175.41
	23.55		143.59		

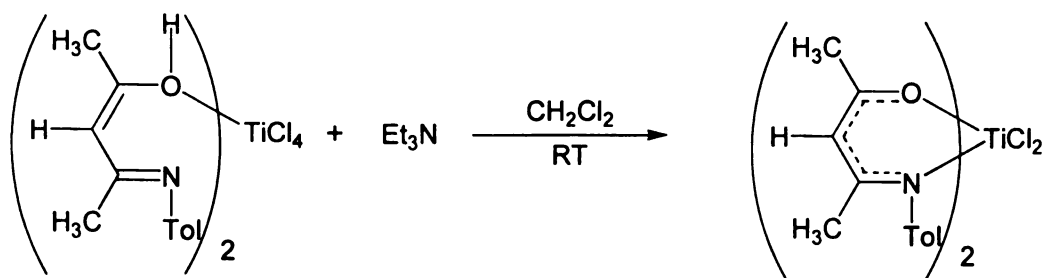
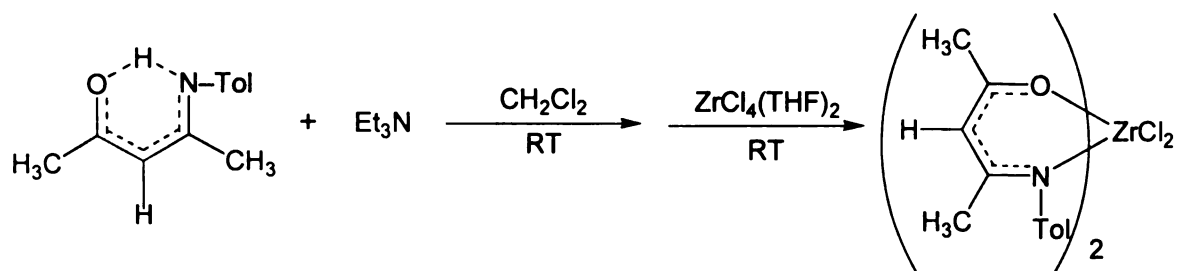


Figure 11. Synthesis of Zirconium and Titanium chelates by *in situ* generation of the β -ketoimine salt with triethylamine (top), and from the corresponding non-chelate complex by action of triethylamine (bottom).

triethylamine to dichloromethane solutions of β -ketimine ligands. The resulting mixture was allowed to stir at ambient temperature for thirty minutes and then transferred to a solution of the desired metal chloride. The reaction was tested for the MPPOH and TMPPOH ligands, which were further reacted with $ZrCl_4(THF)_2$ and $TiCl_4(THF)_2$ respectively. The products of these reactions were characterized by NMR spectroscopy. The data were identical to those for the corresponding chelate complexes $(MPPO)_2ZrCl_2$ and $(TMPPO)_2TiCl_2$ synthesized by the lithium salts route. However, thoroughly dried triethylamine and utilization of the base in 10% excess were essential factors for the preparation of pure products.

The corresponding chelate complex was also obtained by treatment of the non-chelate compound $(MPPOH)_2TiCl_4$ with triethylamine. Stirring at ambient temperature for an hour, was sufficient to transform the suspended in dichloromethane powder of the $(MPPOH)_2TiCl_4$ to the corresponding chelate. The identity of the product was verified by 1H NMR spectroscopy, which also indicated the high efficiency of the process.

CONCLUSIONS

Our choice of β -ketiminato ligands for the synthesis of group IV chelate complexes was based on the advantages offered by the facile and general preparation of these compounds. The condensation of 2,4-pentanedione with various anilines, substituted in *ortho* and *para* positions, generated ligands of modulated steric properties. Initial attempts to synthesize group IV chelates by direct interaction of the free ligands with the corresponding metal dimethylamino or chloro derivatives were unsuccessful, producing either organic products or the corresponding non-chelate complexes. The facile synthesis of the desired chelates was finally accomplished by utilizing various routes. More specifically, the combination of metal chlorides with lithium salts, afforded both titanium and zirconium chelates in high yields. In addition, we demonstrated the irreversible conversion of a non-chelate analog to the corresponding chelate by simply treating the former with a mild base.

Structural characterization of three of the β -ketiminato chelate complexes, indicated that these possessed the labile chloride groups in a *cis* orientation. Such topology is a requirement for the generation of active catalytic species, since the olefin substrate and the inserting alkyl group are proximal enabling facile insertion. The ancillary ligands also provide a rigid stereochemical environment around the metal center. The substitution pattern of the auxiliary aromatic units and their relative orientations were responsible for *trans*-nitrogen coordination of the TMPPO derivatives whereas *cis*-nitrogen geometries were observed in the MPPO analogs. ^1H and ^{13}C NMR data also indicate rigid stereochemical environments about the metal in solution.

The future goals of this project involve the synthesis of metal alkyl complexes, which are the crucial synthons for generating cationic alkyl species. These compounds can generally be prepared by treating the chelate metal

halides with appropriate lithium or magnesium alkyl reagents. Generation of the corresponding cationic alkyl species can then be accomplished by treatment with various non-coordinating anions⁹. The chemistry of the latter compounds with α -olefins will then be explored, introducing at the same time selective variations in the electronic and stereochemical environment of the metal by utilizing β -ketoimines as ancillary ligands.

LIST OF REFERENCES

- (1) (a) Jordan, R. F. *Adv. Organomet. Chem.* **1991**, *32*, 325. (b) Bochmann, M. *J. Chem. Soc., Dalton Trans.* **1996**, 255. (c) Piers, W. E. *Chem. Eur. J.* **1998**, *4*, 13.
- (2) Watson, P. L.; Parshall, G. W. *Acc. Chem. Res.* **1985**, *18*, 51.
- (3) Black, D. G.; Swenson, D. C.; Jordan, R. F. *Organometallics* **1995**, *14*, 3539.
- (4) Tjaden, E. B.; Swenson, D. C.; Jordan, R. F. *Organometallics* **1995**, *14*, 371.
- (5) a) Dell'Amico, G.; Marchetti, F.; Floriani, C. *J. Chem. Soc. Dalton Trans.* **1982**, 2197. b) Floriani, C.; Solari, E.; Corazza, F.; Chiesi-Villa, A.; Guastini, C. *Angew. Chem. Int. Ed. Engl.* **1989**, *28*, 64. c) Floriani, C. *Polyhedron* **1989**, *8*, 1717.
- (6) Martin, D. F.; Janusonis, G. A.; Martin, B. B. *J. Chem. Soc.* **1961**, *83*, 73.
- (7) (a) Leiserowitz, L.; Schmidt, G. M. J. *J. Chem. Soc. A* **1969**, 2372. (b) Lewis, F. D.; Yang, J.-S.; Stern, C. *J. Am. Chem. Soc.* **1996**, *118*, 2772. (c) Lewis, F. D.; Yang, J.-S.; Stern, C. *J. Am. Chem. Soc.* **1996**, *118*, 12029.
- (8) Weingarten, H.; Chupp, J. P.; White, W. A. *J. Chem. Soc.* **1967**, *32*, 3246.
- (9) (a) Hlatky, G. G.; Turner, H. W.; Eckman, R. R. *J. Am. Chem. Soc.* **1989**, *111*, 2728. (b) Brookhart, M.; Grant, B.; Volpe, A. F., Jr. *Organometallics* **1992**, *11*, 3920. (c) Jia, I.; Yang, X.; Stern, C. L.; Marks, T. J. *Organometallics* **1997**, *16*, 842.

APPENDIX

Table 1. Atomic Coordinates ($\times 10^4$) and Equivalent Isotropic Thermal Parameters ($\text{\AA}^2 \times 10^2$) for *N*-(4-tolyl)-acetamide.

Atom	x	y	z	U_{eq}	Occupancy
O(1)	9759(1)	2666(1)	1499(1)	31(1)	1
C(1)	9677(1)	1447(1)	2006(2)	23(1)	1
C(2)	8543(1)	892(1)	2315(2)	29(1)	1
N(1)	10587(1)	514(1)	2326(1)	23(1)	1
C(3)	11756(1)	734(1)	2185(2)	21(1)	1
C(4)	12079(1)	1840(1)	1193(2)	24(1)	1
C(5)	13249(1)	1947(1)	1119(2)	25(1)	1
C(6)	14124(1)	981(1)	1995(2)	24(1)	1
C(6A)	15397(1)	1119(2)	1934(2)	31(1)	1
C(7)	13781(1)	-122(1)	2960(2)	26(1)	1
C(8)	12618(1)	-248(1)	3056(2)	24(1)	1

Table 2. Anisotropic Thermal Parameters ($\text{\AA}^2 \times 10^3$) for *N*-(4-tolyl)-acetamide.

Atom	U ₁₁	U ₂₂	U ₃₃	U ₂₃	U ₁₃	U ₁₂
O(1)	33(1)	24(1)	35(1)	3(1)	10(1)	5(1)
C(1)	26(1)	24(1)	17(1)	-4(1)	3(1)	1(1)
C(2)	25(1)	31(1)	30(1)	-4(1)	6(1)	-1(1)
N(1)	23(1)	21(1)	24(1)	0(1)	5(1)	0(1)
C(3)	24(1)	22(1)	16(1)	-3(1)	3(1)	0(1)
C(4)	28(1)	23(1)	20(1)	3(1)	3(1)	3(1)
C(5)	31(1)	24(1)	20(1)	2(1)	7(1)	-2(1)
C(6)	26(1)	25(1)	21(1)	-4(1)	6(1)	-1(1)
C(6A)	27(1)	31(1)	35(1)	0(1)	9(1)	0(1)
C(7)	26(1)	22(1)	27(1)	0(1)	3(1)	3(1)
C(8)	28(1)	20(1)	24(1)	2(1)	5(1)	-1(1)

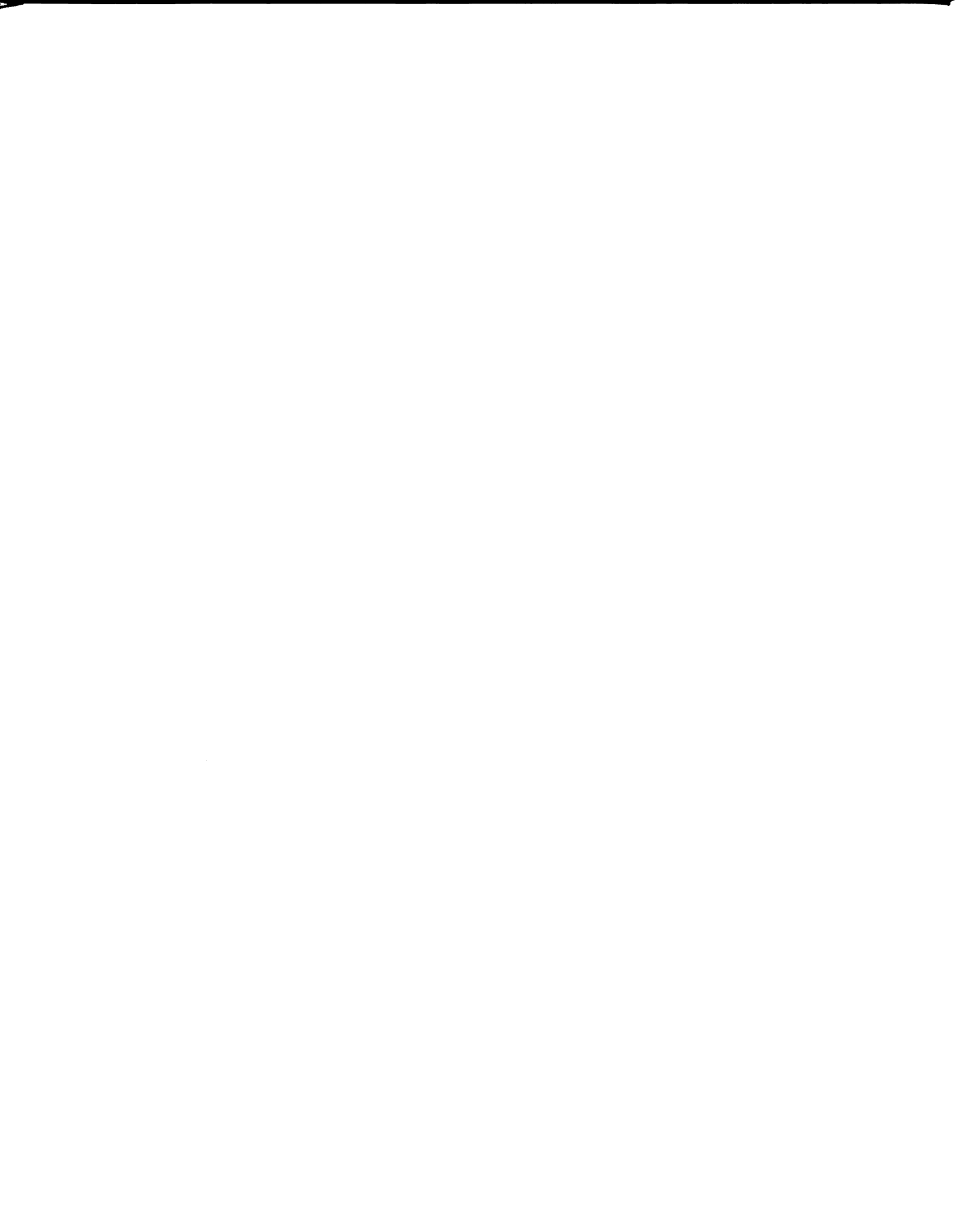
Table 3. Atomic Coordinates ($\times 10^4$) and Equivalent Isotropic Thermal Parameters ($\text{\AA}^2 \times 10^2$) for $\{\mu\text{-O-[2-(2,4,6-trimethylphenylimino)-pentane-4-one]}\}_2\text{TiCl}_4 \cdot 0.5\text{C}_4\text{H}_8\text{O}$.

Atom	x	y	z	U_{eq}	Occupancy
Ti(1)	0	4493(1)	2500	34(1)	1
Cl(1)	895(1)	5491(1)	2165(1)	42(1)	1
Cl(2)	-907(1)	3522(1)	2826(1)	52(1)	1
O(1)	732(2)	4538(2)	3062(1)	35(1)	1
C(1)	171(4)	4247(4)	3840(2)	53(2)	1
C(2)	919(3)	4464(3)	3517(2)	35(1)	1
C(3)	1744(3)	4584(3)	3692(2)	35(1)	1
C(4)	2472(3)	4852(3)	3423(2)	32(1)	1
C(5)	3342(3)	4965(4)	3668(2)	50(2)	1
N(1)	2410(3)	5020(3)	2960(2)	32(1)	1
C(6)	3072(3)	5365(3)	2655(2)	30(1)	1
C(7)	3115(3)	6196(3)	2628(2)	34(1)	1
C(7A)	2540(4)	6730(3)	2926(2)	48(2)	1
C(8)	3706(3)	6524(3)	2302(2)	38(1)	1
C(9)	4218(3)	6048(3)	2006(2)	34(1)	1
C(9A)	4800(3)	6433(4)	1636(2)	46(2)	1
C(10)	4156(3)	5225(3)	2054(2)	37(1)	1
C(11)	3592(3)	4866(3)	2380(2)	33(1)	1
C(11A)	3527(4)	3974(3)	2422(2)	49(2)	1
Ti(2)	2500	7500(0)	0	30(1)	1
Cl(3)	3299(1)	6449(1)	-354(1)	41(1)	1
Cl(4)	1189(1)	6875(1)	-207(1)	57(1)	1
O(2)	2523(2)	6910(2)	586(1)	38(1)	1
C(12)	2405(4)	7507(3)	1365(2)	46(2)	1
C(13)	2430(3)	6785(3)	1046(2)	32(1)	1
C(14)	2372(3)	6025(3)	1225(2)	30(1)	1
C(15)	2472(3)	5300(3)	971(2)	29(1)	1
C(16)	2409(3)	4527(3)	1235(2)	37(1)	1
N(2)	2655(3)	5290(3)	509(2)	35(1)	1
C(17)	2888(3)	4596(3)	230(2)	32(1)	1
C(18)	3763(4)	4365(3)	237(2)	34(1)	1
C(18A)	4436(4)	4822(4)	528(2)	53(2)	1
C(19)	3995(4)	3709(3)	-44(2)	41(2)	1
C(20)	3402(4)	3304(3)	-322(2)	38(2)	1
C(20A)	3675(4)	2599(3)	-633(2)	53(2)	1

C(21)	2536(4)	3568(3)	-322(2)	39(2)	1
C(22)	2263(3)	4212(3)	-49(2)	35(1)	1
C(22A)	1316(3)	4484(4)	-51(2)	51(2)	1
O(1S)	93(7)	1940(5)	6610(3)	74(3)	0.7
C(1S)	-20(7)	2741(5)	6776(3)	63(3)	0.7
C(2S)	-237(9)	3266(6)	6361(5)	75(4)	0.7
C(3S)	-313(14)	2712(9)	5959(5)	144(9)	0.7
C(4S)	-324(10)	1909(8)	6164(6)	84(5)	0.7
O(1S')	251(14)	2145(19)	6409(19)	252(24)	0.3
C(1S')	164(16)	2880(20)	6148(16)	146(21)	0.3
C(2S')	-756(16)	3147(12)	6254(10)	65(8)	0.3
C(3S')	-1207(13)	2379(14)	6222(11)	103(10)	0.3
C(4S')	-602(18)	1805(14)	6436(14)	87(12)	0.3

Table 4. Anisotropic Thermal Parameters ($\text{\AA}^2 \times 10^3$) for $\{\mu\text{-O-[2-(2,4,6-trimethylphenylimino)-pentane-4-one]\}_2\text{TiCl}_4 \cdot 0.5\text{C}_4\text{H}_8\text{O}$.

Atom	U ₁₁	U ₂₂	U ₃₃	U ₂₃	U ₁₃	U ₁₂
Ti(1)	29(1)	43(1)	29(1)	0(0)	1(1)	0(0)
Cl(1)	42(1)	53(1)	29(1)	8(1)	3(1)	-5(1)
Cl(2)	49(1)	50(1)	56(1)	0(1)	6(1)	-15(1)
O(1)	33(2)	49(2)	23(2)	6(2)	-3(2)	-8(2)
C(1)	42(3)	85(5)	33(4)	19(4)	2(3)	-7(3)
C(2)	34(3)	39(4)	31(3)	12(3)	4(3)	4(3)
C(3)	37(3)	43(4)	26(3)	9(3)	-1(3)	-2(3)
C(4)	34(3)	32(3)	31(3)	4(3)	-1(3)	-6(3)
C(5)	40(3)	76(5)	35(4)	14(3)	-8(3)	-13(3)
N(1)	30(3)	39(3)	28(3)	9(2)	-5(2)	-7(2)
C(6)	27(3)	38(4)	27(3)	9(3)	-2(2)	-9(3)
C(7)	34(3)	37(4)	30(3)	2(3)	-1(3)	-6(3)
C(7A)	61(4)	44(4)	41(4)	0(3)	1(3)	-6(3)
C(8)	45(4)	33(3)	35(3)	-2(3)	-8(3)	-8(3)
C(9)	33(3)	44(4)	26(3)	8(3)	-5(3)	-8(3)
C(9A)	38(3)	58(4)	41(4)	7(3)	5(3)	-3(3)
C(10)	33(3)	50(4)	28(3)	-2(3)	-2(3)	4(3)
C(11)	35(3)	35(3)	30(3)	5(3)	-7(3)	-7(3)
C(11A)	53(4)	36(4)	58(4)	8(3)	8(3)	-1(3)
Ti(2)	43(1)	26(1)	20(1)	-1(1)	3(1)	6(1)
Cl(3)	61(1)	34(1)	27(1)	0(1)	11(1)	15(1)
Cl(4)	50(1)	55(1)	67(1)	-14(1)	-5(1)	-5(1)
O(2)	69(3)	28(2)	18(2)	1(2)	6(2)	1(2)
C(12)	79(4)	30(3)	31(4)	-5(3)	4(3)	12(3)
C(13)	37(3)	36(4)	25(3)	1(3)	5(3)	7(3)
C(14)	38(3)	33(3)	19(3)	6(3)	9(2)	5(3)
C(15)	26(3)	33(3)	29(3)	3(3)	1(2)	0(2)
C(16)	47(3)	34(3)	31(3)	7(3)	2(3)	-7(3)
N(2)	59(3)	22(3)	25(3)	4(2)	8(2)	0(2)
C(17)	46(3)	24(3)	26(3)	-2(3)	9(3)	-3(3)
C(18)	43(3)	34(3)	27(3)	3(3)	9(3)	-5(3)
C(18A)	47(4)	61(4)	51(4)	-8(3)	1(3)	-3(3)
C(19)	44(4)	42(4)	38(4)	6(3)	13(3)	2(3)
C(20)	59(4)	26(3)	29(3)	0(3)	9(3)	0(3)
C(20A)	66(4)	38(4)	56(4)	-7(3)	21(4)	-1(3)



C(21)	47(4)	39(4)	32(3)	-6(3)	5(3)	-12(3)
C(22)	46(4)	29(3)	30(3)	4(3)	7(3)	4(3)
C(22A)	52(4)	56(4)	43(4)	-11(3)	-3(3)	1(3)
O(1S)	98(8)	46(5)	79(6)	-3(4)	1(5)	-33(5)
C(1S)	76(8)	57(6)	55(6)	-26(5)	14(5)	2(6)
C(2S)	67(10)	66(7)	93(9)	-11(6)	-1(8)	-4(7)
C(3S)	231(24)	94(10)	106(10)	-29(7)	-96(15)	58(14)
C(4S)	65(9)	84(8)	101(11)	-44(8)	-17(9)	-14(8)
O(1S')	99(16)	187(30)	472(61)	211(33)	89(28)	39(18)
C(1S')	111(21)	125(32)	205(50)	89(34)	130(28)	7(17)
C(2S')	106(21)	48(12)	40(17)	-18(12)	29(16)	7(11)
C(3S')	106(16)	70(17)	134(29)	26(17)	34(19)	-17(14)
C(4S')	133(25)	66(16)	62(23)	20(17)	29(24)	-21(15)

Table 5. Atomic Coordinates ($\times 10^4$) and Equivalent Isotropic Thermal Parameters ($\text{\AA}^2 \times 10^2$) for $\{\mu^2\text{-O,N-[2-(4-methylphenylimino)-pentane-4-one]}\}_2\text{TiCl}_2$.

Atom	x	y	z	U_{eq}	Occupancy
Ti(1)	5022(1)	1587(1)	6196(1)	22(1)	1
Cl(1)	3366(1)	2241(1)	6158(1)	37(1)	1
Cl(2)	4151(1)	570(1)	6418(1)	36(1)	1
O(1)	5046(2)	1406(1)	5335(1)	25(1)	1
C(1)	5146(3)	1295(2)	4236(1)	35(1)	1
C(2)	5365(2)	1699(1)	4812(1)	25(1)	1
C(3)	5872(3)	2306(1)	4809(1)	29(1)	1
C(4)	6203(2)	2677(1)	5350(1)	28(1)	1
C(5)	6833(3)	3326(2)	5230(2)	40(1)	1
N(1)	5996(2)	2463(1)	5919(1)	23(1)	1
C(6)	6400(2)	2872(1)	6430(1)	24(1)	1
C(7)	7496(3)	2773(2)	6678(1)	35(1)	1
C(8)	7859(3)	3144(2)	7186(2)	39(1)	1
C(9)	7148(3)	3625(1)	7454(1)	30(1)	1
C(9A)	7560(3)	4033(2)	8001(2)	46(1)	1
C(10)	6049(3)	3715(2)	7201(1)	32(1)	1
C(11)	5673(2)	3342(1)	6695(1)	30(1)	1
O(2)	5253(2)	1804(1)	7040(1)	26(1)	1
C(12)	5590(3)	1904(2)	8121(1)	40(1)	1
C(13)	5913(2)	1610(1)	7506(1)	28(1)	1
C(14)	6823(3)	1189(2)	7420(1)	34(1)	1
C(15)	7217(2)	955(1)	6831(1)	28(1)	1
C(16)	8279(3)	512(2)	6840(1)	43(1)	1
N(2)	6696(2)	1112(1)	6303(1)	23(1)	1
C(17)	7231(2)	861(1)	5738(1)	25(1)	1
C(18)	6877(3)	253(2)	5497(1)	33(1)	1
C(19)	7415(3)	-5(2)	4974(1)	35(1)	1
C(20)	8318(3)	332(2)	4682(1)	33(1)	1
C(20A)	8968(3)	16(2)	4145(1)	48(1)	1
C(21)	8618(3)	959(2)	4913(1)	37(1)	1
C(22)	8084(3)	1226(2)	5438(1)	32(1)	1

Table 6. Anisotropic Thermal Parameters ($\text{\AA}^2 \times 10^3$) for $\{\mu^2\text{-O,N-[2-(4-methylphenylimino)-pentane-4-one]}\}_2\text{TiCl}_2$.

Atom	U ₁₁	U ₂₂	U ₃₃	U ₂₃	U ₁₃	U ₁₂
Ti(1)	22(1)	25(1)	20(1)	0(1)	0(1)	-2(1)
Cl(1)	22(1)	48(1)	42(1)	-4(1)	-3(1)	6(1)
Cl(2)	45(1)	34(1)	30(1)	-2(1)	8(1)	-14(1)
O(1)	28(1)	28(1)	20(1)	0(1)	0(1)	-4(1)
C(1)	44(2)	39(2)	22(2)	-2(1)	2(1)	-2(2)
C(2)	23(2)	31(2)	22(2)	-1(1)	2(1)	6(1)
C(3)	34(2)	32(2)	21(2)	3(1)	2(1)	-1(1)
C(4)	23(2)	25(2)	35(2)	1(1)	5(1)	-2(1)
C(5)	43(2)	36(2)	40(2)	3(2)	6(2)	-13(2)
N(1)	20(1)	24(1)	26(1)	-2(1)	-2(1)	-1(1)
C(6)	24(2)	20(2)	28(2)	-2(1)	2(1)	-5(1)
C(7)	24(2)	33(2)	48(2)	-15(2)	-2(2)	5(1)
C(8)	24(2)	44(2)	49(2)	-16(2)	-11(2)	5(2)
C(9)	29(2)	27(2)	35(2)	-7(1)	-2(1)	-1(1)
C(9A)	41(2)	46(2)	49(2)	-21(2)	-7(2)	1(2)
C(10)	28(2)	28(2)	39(2)	-10(1)	4(1)	3(1)
C(11)	23(2)	28(2)	37(2)	-1(1)	-2(1)	2(1)
O(2)	27(1)	31(1)	22(1)	-4(1)	-2(1)	0(1)
C(12)	40(2)	54(2)	27(2)	-10(2)	-2(2)	7(2)
C(13)	28(2)	32(2)	22(1)	-3(1)	-1(1)	-3(1)
C(14)	40(2)	41(2)	22(2)	2(1)	-4(1)	9(2)
C(15)	30(2)	28(2)	27(2)	1(1)	-1(1)	4(1)
C(16)	45(2)	51(2)	34(2)	-1(2)	-4(2)	19(2)
N(2)	25(1)	24(1)	20(1)	0(1)	0(1)	1(1)
C(17)	26(2)	28(2)	21(1)	0(1)	0(1)	5(1)
C(18)	40(2)	28(2)	30(2)	-2(1)	5(1)	0(1)
C(19)	48(2)	26(2)	31(2)	-4(1)	-8(2)	11(2)
C(20)	35(2)	44(2)	21(2)	2(1)	-2(1)	18(2)
C(20A)	58(2)	58(2)	28(2)	0(2)	3(2)	28(2)
C(21)	32(2)	45(2)	35(2)	5(2)	7(1)	1(2)
C(22)	32(2)	32(2)	32(2)	-2(1)	2(1)	-2(1)

Table 7. Atomic Coordinates ($\times 10^4$) and Equivalent Isotropic Thermal Parameters ($\text{\AA}^2 \times 10^2$) for $\{\mu^2\text{-O,N-[2-(2,4,6-trimethylphenylimino)-pentane-4-one]}\}_2\text{TiCl}_2\cdot\text{CH}_2\text{Cl}_2$.

Atom	x	y	z	U_{eq}	Occupancy
Ti(1)	4752(1)	2494(1)	2432(1)	18(1)	1
Cl(1)	6936(1)	3326(1)	1619(1)	26(1)	1
Cl(2)	5995(1)	2120(1)	3930(1)	23(1)	1
O(1)	3739(1)	2888(1)	1228(1)	26(1)	1
C(1)	3502(3)	3747(2)	-490(1)	49(1)	1
C(2)	3409(2)	3775(1)	511(1)	29(1)	1
C(3)	2986(2)	4629(1)	691(1)	31(1)	1
C(4)	2704(2)	4655(1)	1646(1)	27(1)	1
C(5)	1745(3)	5634(1)	1702(1)	40(1)	1
N(1)	3192(2)	3876(1)	2440(1)	21(1)	1
C(6)	2611(2)	3927(1)	3376(1)	21(1)	1
C(7)	3598(2)	4234(1)	3881(1)	25(1)	1
C(7A)	5192(2)	4615(1)	3424(1)	34(1)	1
C(8)	3059(2)	4189(1)	4818(1)	32(1)	1
C(9)	1595(2)	3847(1)	5261(1)	36(1)	1
C(9A)	1054(3)	3768(2)	6291(1)	53(1)	1
C(10)	626(2)	3577(1)	4725(1)	34(1)	1
C(11)	1081(2)	3621(1)	3781(1)	27(1)	1
C(11A)	-69(2)	3392(1)	3204(1)	37(1)	1
O(2)	3147(1)	1722(1)	3154(1)	22(1)	1
C(12)	1921(2)	651(1)	4598(1)	30(1)	1
C(13)	3311(2)	814(1)	3836(1)	22(1)	1
C(14)	4643(2)	85(1)	3814(1)	24(1)	1
C(15)	5875(2)	201(1)	3032(1)	22(1)	1
C(16)	6955(2)	-750(1)	2985(1)	31(1)	1
N(2)	6043(2)	1082(1)	2361(1)	20(1)	1
C(17)	7132(2)	1103(1)	1516(1)	20(1)	1
C(18)	6439(2)	1075(1)	703(1)	24(1)	1
C(18A)	4666(2)	895(1)	744(1)	32(1)	1
C(19)	7447(2)	1189(1)	-139(1)	29(1)	1
C(20)	9110(2)	1317(1)	-192(1)	31(1)	1
C(20A)	10167(3)	1455(2)	-1122(1)	47(1)	1
C(21)	9770(2)	1300(1)	636(1)	30(1)	1
C(22)	8820(2)	1186(1)	1503(1)	24(1)	1
C(22A)	9619(2)	1141(1)	2390(1)	32(1)	1

C(1S)	6487(3)	2461(2)	6172(2)	63(1)	1
CI(1A)	8286(3)	1508(2)	6294(3)	57(1)	0.68
CI(1B)	8113(16)	1491(6)	6580(18)	111(3)	0.32
CI(2A)	5551(3)	2501(2)	7285(1)	64(1)	0.7
CI(2B)	5733(13)	2713(7)	7235(6)	160(4)	0.3

Table 8. Anisotropic Thermal Parameters ($\text{\AA}^2 \times 10^3$) for $\{\mu^2\text{-O,N-[2-(2,4,6-trimethylphenylimino)-pentane-4-one]\}_2\text{TiCl}_2 \cdot \text{CH}_2\text{Cl}_2$.

Atom	U_{11}	U_{22}	U_{33}	U_{23}	U_{13}	U_{12}
Ti(1)	21(1)	18(1)	14(1)	5(1)	1(1)	-4(1)
Cl(1)	26(1)	24(1)	23(1)	3(1)	5(1)	-7(1)
Cl(2)	30(1)	23(1)	17(1)	6(1)	-2(1)	-7(1)
O(1)	33(1)	26(1)	18(1)	7(1)	-3(1)	-3(1)
C(1)	81(2)	42(1)	20(1)	10(1)	-8(1)	-3(1)
C(2)	34(1)	31(1)	17(1)	5(1)	-3(1)	-2(1)
C(3)	39(1)	26(1)	20(1)	1(1)	-2(1)	0(1)
C(4)	28(1)	25(1)	25(1)	7(1)	1(1)	-2(1)
C(5)	50(1)	26(1)	34(1)	7(1)	1(1)	7(1)
N(1)	21(1)	22(1)	19(1)	8(1)	2(1)	-4(1)
C(6)	24(1)	19(1)	20(1)	8(1)	1(1)	0(1)
C(7)	27(1)	22(1)	27(1)	12(1)	0(1)	-2(1)
C(7A)	34(1)	31(1)	43(1)	20(1)	2(1)	-12(1)
C(8)	40(1)	29(1)	28(1)	16(1)	-4(1)	2(1)
C(9)	46(1)	31(1)	24(1)	11(1)	5(1)	4(1)
C(9A)	68(1)	54(1)	28(1)	18(1)	12(1)	4(1)
C(10)	31(1)	33(1)	33(1)	11(1)	12(1)	-3(1)
C(11)	23(1)	25(1)	31(1)	12(1)	4(1)	-2(1)
C(11A)	22(1)	41(1)	52(1)	24(1)	2(1)	-6(1)
O(2)	22(1)	23(1)	19(1)	6(1)	3(1)	-5(1)
C(12)	27(1)	36(1)	22(1)	7(1)	5(1)	-10(1)
C(13)	25(1)	26(1)	17(1)	8(1)	1(1)	-10(1)
C(14)	30(1)	21(1)	18(1)	5(1)	2(1)	-9(1)
C(15)	25(1)	22(1)	20(1)	9(1)	-1(1)	-5(1)
C(16)	39(1)	22(1)	30(1)	10(1)	4(1)	-3(1)
N(2)	20(1)	23(1)	17(1)	9(1)	1(1)	-4(1)
C(17)	21(1)	21(1)	18(1)	9(1)	3(1)	-2(1)
C(18)	24(1)	27(1)	23(1)	13(1)	-1(1)	-2(1)
C(18A)	27(1)	43(1)	36(1)	24(1)	-3(1)	-7(1)
C(19)	34(1)	33(1)	20(1)	13(1)	0(1)	-1(1)
C(20)	33(1)	31(1)	25(1)	10(1)	10(1)	-2(1)
C(20A)	49(1)	51(1)	31(1)	14(1)	18(1)	-6(1)
C(21)	20(1)	33(1)	34(1)	13(1)	6(1)	-4(1)
C(22)	20(1)	25(1)	26(1)	11(1)	-1(1)	-2(1)
C(22A)	26(1)	37(1)	36(1)	18(1)	-8(1)	-1(1)

C(1S)	49(1)	59(2)	64(2)	5(1)	-16(1)	-5(1)
CI(1A)	50(1)	41(1)	76(1)	16(1)	-20(1)	-1(1)
CI(1B)	107(4)	103(4)	131(7)	61(3)	-60(4)	28(3)
CI(2A)	97(1)	48(1)	52(1)	20(1)	-14(1)	-13(1)
CI(2B)	241(8)	63(3)	207(7)	89(3)	-155(7)	60(4)

Table 9. Atomic Coordinates ($\times 10^4$) and Equivalent Isotropic Thermal Parameters ($\text{\AA}^2 \times 10^2$) for $\{\mu^2\text{-O,N-[2-(4-methylphenylimino)-pentane-4-one]}\}_2\text{ZrCl}_2$.

Atom	x	y	z	U_{eq}	Occupancy
Zr(1)	3097(1)	10000	8333.0	16(1)	1
Cl(1)	5096(1)	10012	7719.0	28(1)	1
O(1)	3956(1)	12638	8289.0	21(1)	1
C(1)	196(2)	11865	9423.0	30(1)	1
C(2)	1378(2)	11847	9032.0	21(1)	1
C(3)	2453(2)	13542	8804.0	23(1)	1
C(4)	3617(2)	13877	8447.0	20(1)	1
C(5)	4586(2)	15658	8207.0	27(1)	1
N(1)	1379(2)	10369	8909.0	19(1)	1
C(6)	135(2)	8750.0	9156.0	20(1)	1
C(7)	755(2)	7997.0	9488.0	25(1)	1
C(8)	-464(2)	6426.0	9719.0	28(1)	1
C(9)	-2284(2)	5574.0	9627.0	26(1)	1
C(9A)	-3579(3)	3836.0	9868.0	38(1)	1
C(10)	-2886(2)	6344.0	9293.0	27(1)	1
C(11)	-1694(2)	7914.0	9059.0	24(1)	1

Table 10. Anisotropic Thermal Parameters ($\text{\AA}^2 \times 10^3$) for $\{\mu^2\text{-O,N-[2-(4-methylphenylimino)-pentane-4-one]}\}_2\text{ZrCl}_2$.

Atom	U ₁₁	U ₂₂	U ₃₃	U ₂₃	U ₁₃	U ₁₂
Zr(1)	15(1)	16(1)	18(1)	-1(1)	-1(1)	8(1)
Cl(1)	27(1)	36(1)	27(1)	0(1)	6(1)	20(1)
O(1)	21(1)	18(1)	24(1)	-1(1)	1(1)	9(1)
C(1)	35(1)	33(1)	26(1)	-3(1)	7(1)	19(1)
C(2)	19(1)	26(1)	17(1)	-4(1)	-2(1)	12(1)
C(3)	23(1)	21(1)	27(1)	-5(1)	-2(1)	12(1)
C(4)	19(1)	18(1)	23(1)	-3(1)	-6(1)	8(1)
C(5)	28(1)	20(1)	33(1)	1(1)	1(1)	11(1)
N(1)	17(1)	21(1)	18(1)	0(1)	-1(1)	10(1)
C(6)	22(1)	23(1)	14(1)	0(1)	2(1)	11(1)
C(7)	24(1)	31(1)	21(1)	1(1)	-1(1)	14(1)
C(8)	34(1)	31(1)	22(1)	4(1)	1(1)	18(1)
C(9)	32(1)	25(1)	19(1)	1(1)	6(1)	12(1)
C(9A)	42(1)	30(1)	35(1)	9(1)	9(1)	11(1)
C(10)	22(1)	28(1)	25(1)	-1(1)	0(1)	7(1)
C(11)	23(1)	28(1)	21(1)	1(1)	-2(1)	12(1)

MICHIGAN STATE UNIV. LIBRARIES



31293018017412